# TERMINAL DNA SEQUENCES OF VARICELLA-ZOSTER AND MAREK'S DISEASE VIRUS: ROLES IN GENOME REPLICATION, INTEGRATION, AND REACTIVATION

A Dissertation

Presented to the Faculty of the Graduate School

of Cornell University

In Partial Fulfillment of the Requirements for the Degree of

Doctor of Philosophy

by

Benedikt Bertold Kaufer

May 2010

# TERMINAL DNA SEQUENCES OF VARICELLA-ZOSTER AND MAREK'S DISEASE VIRUS: ROLES IN GENOME REPLICATION, INTEGRATION, AND REACTIVATION

Benedikt Bertold Kaufer, Ph. D.

Cornell University 2010

One of the major obstacles in varicella-zoster virus (VZV) research has been the lack of an efficient genetic system. To overcome this problem, we generated a full-length, infectious bacterial artificial chromosome (BAC) system of the P-Oka strain (pP-Oka), which facilitates generation of mutant viruses and allowed light to be shed on the role in VZV replication of the *ORF9* gene product, a major tegument protein, and *ORFS/L* (*ORF0*), a gene with no known function and no direct orthologue in other alphaherpesviruses. Mutation of the *ORF9* start codon in pP-Oka, abrogated pORF9 expression and severely impaired virus replication. Delivery of ORF9 in *trans* via baculovirus-mediated gene transfer partially restored virus replication of ORF9 deficient viruses, confirming that *ORF9* function is essential for VZV replication *in vitro*. Next we targeted *ORFS/L* and could prove that the *ORFS/L* gene product is important for efficient VZV replication *in vitro*. Furthermore, we identified a 5' region of *ORFS/L* that is essential for replication and plays a role in cleavage and packaging of viral DNA.

To elucidate the mechanisms of Marek's disease virus (MDV) integration and tumorigenesis, we investigated two sequence elements of the MDV genome: vTR, a virus encoded telomerase RNA, and telomeric repeats present at the termini of the virus genome. We demonstrate that vTR serves two distinct functions in MDV-induced tumor formation. The first is dependent on an increase of telomerase activity

mediated by vTR, which contributes to the survival of rapidly dividing transformed cells and is crucial for rapid onset of lymphoma formation in infected animals. The second function of vTR is independent of telomerase action and is required for tumor formation and metastasis. This function is likely mediated by vTR interaction with RPL22, a cellular factor involved in T-cell development and virus-induced transformation. Finally, our studies on herpesvirus telomeric repeats provide the first conclusive evidence that herpesvirus telomeric repeats mediate integration into host telomeres, are critical for efficient tumor formation, and support efficient reactivation of latent virus.

# BIOGRAPHICAL SKETCH

Benedikt Bertold Kaufer was born in Dachau, Bavaria, Germany on November 4th 1981. He grew up in Markt Indersdorf near Munich and attended high school at the Luisengymnasium Munich, graduating in 2001. As part of his German civil service, Benedikt attended the German Red Cross School in Jettingen-Scheppach, where he attained the Emergency medical technician (EMT) degree in 2001. He worked as an EMT at the regional chapter of the German Red Cross Dachau for almost five years, obtained a license as instructor for automated external defibrillators (AED) and served as a shift coordinator.

Benedikt attended the Technical University Munich (TUM) where he attained a bachelor's degree in molecular biotechnology in 2005. At the same time, he worked as a technical assistant at the biotechnology company EpiLogic & EpiGene GmbH on resistance development of plant pathogens to fungicides from 2002 until 2005. At EpiLogic he also met his wife Susanne Möβmer in 2002 and they married in October 2009. As part of his bachelor degree he did an internship in the Osterrieder lab at Cornell University, where he worked on a genetic system for Varicella-zoster virus, in 2004. Benedikt performed his bachelor thesis research in the laboratory of Arne Skerra at the TUM on the "expression, characterization and crystallization of the carbohydrate recognition domain of the C-type lectin Langerin".

In August 2005, he came to the United States with his future wife to Ithaca and started his Ph.D. work in the Field of Comparative Biomedical Science. After his rotations, Benedikt worked in the lab of Nikolaus Osterrieder in April 2006. He served as chair of the Graduate Advisory Council, organized the virology journal club and obtained travel grants from various sources. Upon completion of his Ph.D., Benedikt will be appointed as an Assistant Professor at the Free University Berlin, Germany.

Dedicated to my wife Susanne,

My parents Elisabeth & Enrique Ernesto

And my brother Michael

# ACKNOWLEDGMENTS

After almost 5 years, there are many people who I must thank and acknowledge for their support and help during these years. Firstly, I thank my advisor Dr. Nikolaus Osterrieder who provided intellectual stimulation and financial support, but especially has been an inspiration for many years. Secondly, I would like to express my gratitude to Drs. Joel Baines, Ted Clark and John Parker for serving as members of my special committee and far beyond that. I would also like to thank the members of the Virology Journal Club, especially Drs. Volker Vogt, Colin Parrish and John Parker for weekly inspiring discussions.

I thank all the people who supported me over the years, especially Drs. Donna Cassidy-Hanley and Ted Clark for providing me the pulsed field gel electrophoresis system, Drs. Barbara Butcher and Eric Denkers for supplying HFF cells and Dr Gary Whittaker for letting me use the LAS imaging system. Many thanks to Walt Iddings, a genius, who can literally repair any broken lab equipment you could think of, and has helped me out many, many times. Also thanks to the office team, Sachiko, Mary, Gwen and Karen who made work in the department so much easier. I would like to thank Casey Isham and Janna Lamey for the past and present graduate student support and the collaborations with the Graduate Advisory Council. Keep up the good work!

All the past and present members of the Osterrieder lab deserve my gratitude for personal and scientific advice as well as encouragement they have offered me throughout the years. In particular, I want to thank Keith Jarosinski, Karsten Tischer, Cristina Rosas, Jens von Einem, Neil Margulis, Gerlinde van de Walle and Sascha Trapp. Especially Keith was a tremendous help and deserves more gratitude than words can say. Intriguing discussions with him and others contributed immensely to the success of my work. Further more, I would like to thank the interns that worked

with me over the years, such as Annemarie Egerer, Sina Arndt, Jessica Privett and Cun Zhang, for their hard work and enthusiasm for research. Also special thanks to the short term Osterrieder lab member and office mate Michele Bialecki that kept me company through all these years and was always there for cheerful conversations when needed. All in all, I would also like to thank the entire department of Microbiology and Immunology, for providing an extremely open, friendly, helpful and inspiring work environment. It really felt like home and the years just flew by.

I would like to thank my parents for all they have done for me. From the cradle to our wonderful wedding, they have given me more than life and showed me what is important. Also special thanks to my brother Michael. Even though I had some rough fights with my older, 2 meter (6 foot 6) tall brother, you have always been an inspiration and our time together as paramedics has been (one of ) the best time of my life. I also want to thank my family in law, who is just wonderful. It is good to have a family, but it is even better to have two. Finally I would like to thank my wife Susanne for her love, support and patience. I could not have done it without her and I'm looking forward to our future together.

TABLE OF CONTENTS

LIST OF FIGURES

LIST OF TABLES

# CHAPTER ONE

## Introduction and literature review

## 1.1. *Herpesviridae*

The *Herpesviridae* family within the newly established order *Herpesvirales* is classified in three subfamilies, *Alphaherpesvirinae*, *Betaherpesvirinae* and *Gammaherpesvirinae*, based on their biological properties such as clinical manifestation, host range, preferential establishment of latency in certain cell types, and, more recently, genome structure and sequence (17, 84). Herpesviruses are abundant in nature, with one or frequently several distinct viruses found in most animal species. So far, more than 200 herpesviruses have been discovered and the number is steadily increasing (81). To date, eight human herpesviruses (HHV) have been identified. Among those are representatives from each subfamily, the *Alphaherpesvirinae* represented by herpes simplex virus 1 (HSV-1; HHV-1) herpes simplex virus 2 (HSV-2; HHV-2) and Varicella-zoster virus (VZV; HHV-3), the *Betaherpesvirinae* with human cytomegalovirus (HCMV; HHV-5), human herpesvirus 6 (HHV-6) and 7 (HHV-7), and the *Gammaherpesvirinae* with Epstein-Barr virus (EBV; HHV-3) and Kaposi's sarcoma-associated herpesvirus (KHSV; HHV-8).

Herpesviruses contain a large linear, non-segmented, double stranded DNA. Genome sizes of herpesvirus species vary from 124 to 230 kbp in length. Based on the presence of direct and inverted repeats within their genome, herpesviruses are categorized into six genome classes, designated by the letters A through F. They encode between 60 and more than 230 genes that are mainly transcribed by host cell polymerase II and the cell's transcription apparatus (81). In mature virions, the linear, non-segmented genome is encased in an icosahedral capsid that consists of 162 capsomers and is 120 nm in diameter. The capsid is surrounded by a proteinaceous matrix termed tegument and then by an envelope composed of a large number of glycoproteins embedded in a lipid bilayer (Fig. 1.1). The size of the herpes virion

varies from approximately 150 nm to as much as 260 nm, which is partially dependent on the thickness of the tegument (81).

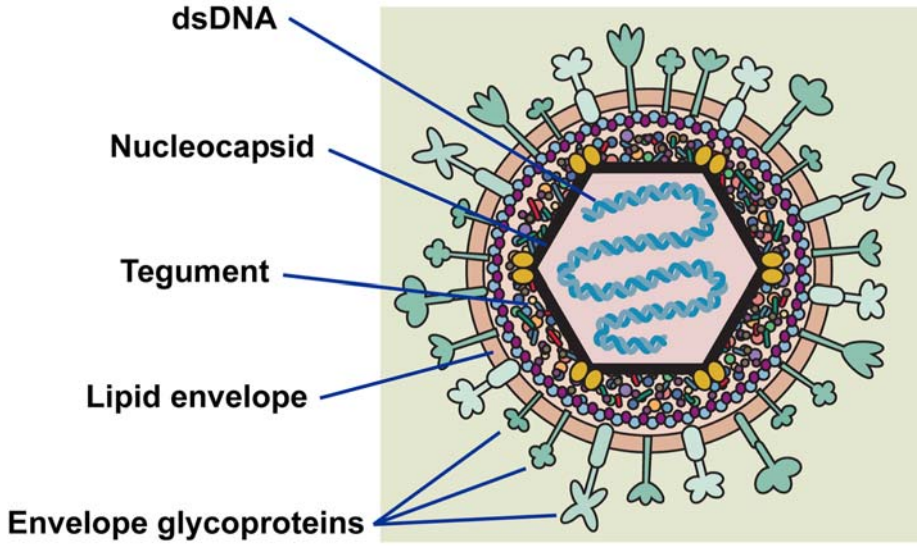


**Figure 1.1.** Schematic representation of the herpesvirus virion. The linear, double stranded DNA (dsDNA) genome in enclosed in an icosahedral nucleocapsid, which is surrounded by the tegument, a proteinaceous matrix, and the lipid envelope containing several viral glycoproteins. Modified from "Field's Virology"(81).

### 1.2. *Alphaherpesvirinae*

The alphaherpesvirus subfamily, which diverged from the beta- and gammaherpesvirus lineages about 180-220 million years ago, contains numerous mammalian and avian viruses (64). Generally, members of the *Alphaherpesvirinae* are biologically characterized by relatively short replication cycles, a variable host range *in vitro* and the ability to establish latency in sensory neurons. Alphaherpesviruses are further classified in four genera. Members of the genus *Simplexvirus* and *Varicellovirus* harbor viruses that infect mammalian hosts, while members of the

*Mardivirus* and *Iltovirus* genus infect avian species(81). Human VZV and Marek's disease virus (MDV) are two members of the *Alphaherpesvirinae* that will be discussed further in this dissertation.

### 1.3. Alphaherpesvirus life cycle

Alphaherpesvirus infection is initiated by the attachment of the virion to the host cell. This process is mediated by viral glycoproteins that are able to bind receptor molecules on the surface of the host cell (Fig. 1.2). The contact initiates fusion of the viral envelope with the plasma membrane, which results in the release of the nucleocapsid as well as tegument components into the cytosol (28, 40). Once in the cytosol, the capsid binds to microtubule-associated motors and is transported to the nucleus, where it docks to a nuclear pore through which the viral genome is released into the nucleus. Tegument proteins, such as VP16, are translocated into the nucleus, where they interact with the cellular transcription machinery and stimulate the expression of immediate early proteins (α proteins). Immediate early proteins are subsequently transported into the nucleus were they induce the transcription and expression of early (β) genes (43). Several β proteins are also translocated into the nucleus, where they facilitate the replication of the viral genome. Genome replication is initiated at the viral origins of replication and leads to the synthesis of concatemeric DNA likely through a rolling circle replication mechanism. During the replication process, transcription of late genes (γ proteins) is initiated. Late proteins are mainly involved in the process of assembly and/or are structural proteins of the virion (43). Components of the nucleocapsid are transported into the nucleus where capsid assembly occurs (66). Packaging sites, *pac1* and *pac2*, within concatemeric DNA are recognized by the viral cleavage and packaging machinery, whereupon replicated DNA is cleaved into unit length genomes and packaged into preformed nucleocapsids

(65). DNA-containing viral capsids associate with several tegument proteins and bud through the nuclear envelope into the cytoplasm, where additional tegumentation occurs. Subsequently, capsids are transported to the *trans*-Golgi network, in which they bud into and obtain their final envelope (66). After budding into those vesicles, mature virions are transported to the plasma membrane where they are released via fusion of the vesicle with the plasma membrane. In addition, virions can be specifically redirected to cell junctions that results in spread of infectivity to neighboring cells by a not fully understood mechanism (46). Some herpesviruses, such as VZV and MDV, almost exclusively utilize cell-to-cell transfer of virus for viral spread *in vitro* and *in vivo*, while cell free VZV and MDV virions are only produced in differentiated epithelial cells of hair and feather follicles, respectively (80).

### 1.4. Herpesvirus latency

Latency is one of the most intriguing features of the herpesvirus life cycle. It ensures the maintenance of the viral genome in the host for extended periods of time in the absence of productive lytic replication. This latent state can be maintained throughout the life of the host allowing continued persistence, while sporadic reactivation events ensure the dissemination to naïve individuals. Establishment of latency is cell-type dependent and can occur in several lymphoid and neuronal cells. Members of the *Alphaherpesvirinae* subfamily predominantly establish latency in sensory neurons of the peripheral nervous system (48). One exception is Marek's disease virus (MDV) which maintains latency exclusively in the peripheral blood mononuclear compartment (PBMC) compartment, predominantly in infected CD4+ T-cells (10, 94).

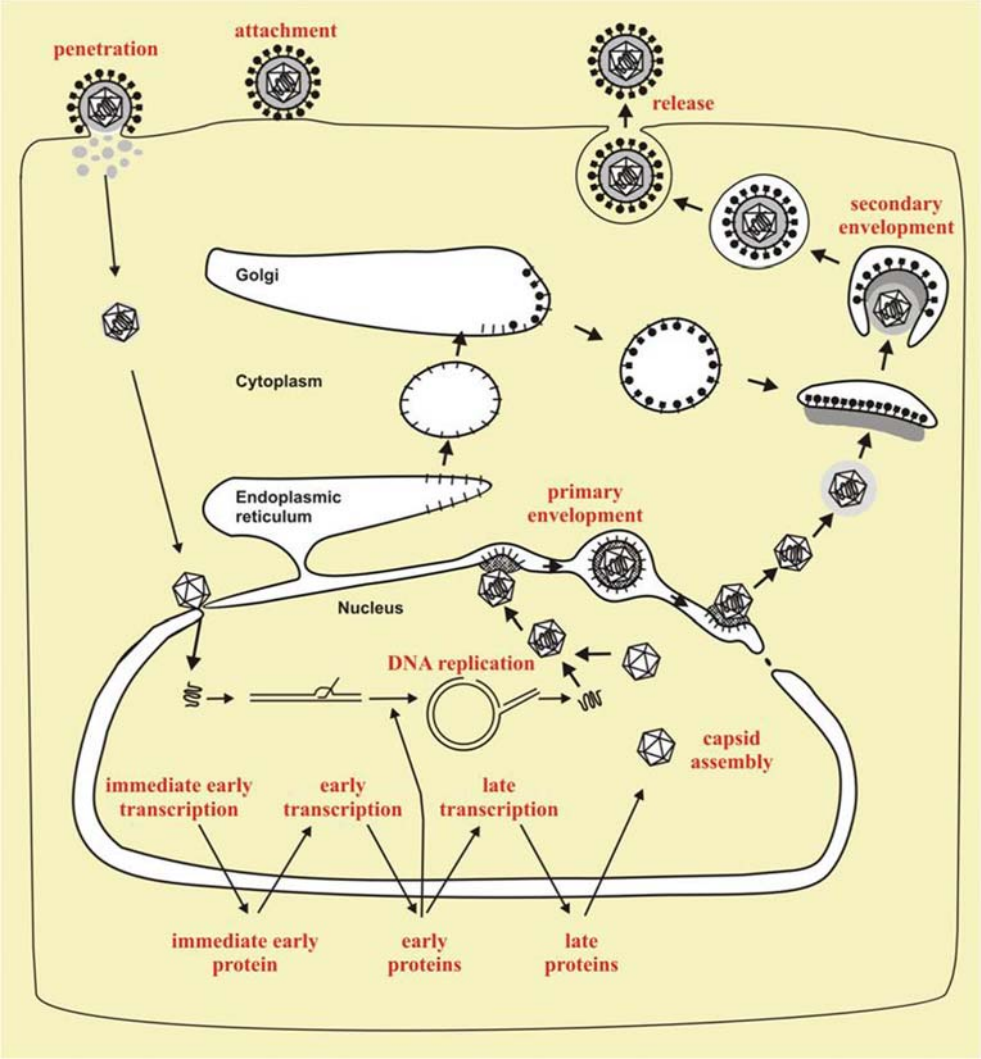


**Figure 1.2.** Model of the alphaherpesvirus replication cycle. The first step of the herpesvirus life cycle is the attachment to the target cell, which is mediated by viral glycoproteins. Subsequently, the viral envelope fuses with the plasma membrane, which results in the release of the capsid into the cytosol. The capsid is transported to the nucleus, where it docks to a nuclear pore and releases the linear viral genome into the nucleus. In the nucleus, a cascade of viral transcripts is initiated, with immediate early genes (α proteins) at first, then early (β proteins) and late genes (γ proteins). β proteins provide the components for DNA replication, while γ proteins contribute structural components. Rolling circle replication of the viral genome results in concatemeric viral DNA, which is cleaved into unit length genomes and packaged into preformed capsids. DNA-containing capsids bud through the nuclear membrane and are released into the cytosol, where they obtains most tegument components. Subsequently, capsids bud into the Golgi compartment and thereby obtain their final envelope. The mature virus particles bud into vesicles that transport the virions to the plasma membrane where they are released by exocytosis. Modified from Mettenleiter et al. 2002 (66)

The virus genome can have three different states in the host nucleus: i) As an episome as observed in the case of HSV-1 and VZV; ii) tethered to host chromosomes as was shown for EBV (90), and iii) integrated into the host genome, which represents a unique mechanism utilized by some herpesviruses and which is discussed in detail in CHAPTER 5.

### 1.5. *Varicella-zoster virus*

Varicella-zoster virus (VZV), a highly cell-associated alphaherpesvirus, also known as human herpesvirus 3 (HHV-3), is one of the eight known human herpesviruses. It belongs to the genus Varicellovirus, which includes several mammalian viruses such as pseudorabies virus (PRV), equine herpesvirus 1 (EHV-1), bovine herpesvirus 1 (BoHV-1), and the closest relative of VZV, simian varicella virus (SVV) (17). Primary infection with VZV usually occurs early in life and results in varicella, also known as chicken pox, which is associated with fever and a generalized rash. During primary infection VZV is able to infect neurons of sensory ganglia, where it establishes latency. Reactivation of VZV from the latent state results in the development of herpes zoster, also known as shingles, in the form of a localized, mostly very painful vesicular rash that can lead to postherpetic neuralgia (13). VZV is highly transmissible via airborne vesicular droplet infection and direct contact (35, 86). In contrast to HSV that is labile under dry conditions (99), dehydrated VZV is stable in the environment for at least 2 years at various temperatures (27, 58), ensuring efficient transmission and persistence of the virus in the population.

In recent years, novel VZV research tools have light on molecular mechanisms involved in VZV pathogenesis. First, the development of an animal model for VZV, a severe combined immunodeficiency (SCID) mouse model with human tissue xenografts, with histopathology comparable to the disease in humans, allowed new

insights in VZV pathogenesis *in vivo* (55, 70). Secondly, a genetic system for VZV, consisting of four overlapping cosmids harboring the entire VZV genome, was developed. This cosmid-based approach allowed the generation of VZV mutants in *E.coli*, while virus could be reconstituted by cotransfection of all four cosmids into cells susceptible to VZV infection (14, 75). The only drawback of the system is that reconstitution of the virus is dependent on the recombination of cosmids in mammalian cells, which can result in genetic rearrangements and has low efficiency. To overcome this obstacle, we generated a bacterial artificial chromosome (BAC) system, as described in CHAPTER 2.

### 1.6. Varicella-zoster virus genome structure

The VZV genome, the smallest among the human herpesviruses, is approximately 125 kbp in size and encodes at least 70 unique open reading frames (ORFs) (2). The organization of the VZV genome is similar to that of HSV-1 and over 90% of the VZV ORFs have counterparts (orthologues) in the HSV-1 genome (2, 49). As has been reported for all alphaherpesviruses, the VZV genome consists of two unique regions, the unique long ($U_L$) and unique short ($U_S$) segment, each flanked by inverted repeat regions ($TR_L$, $IR_L$, $TR_S$, $IR_S$) (Fig. 1.3) (18). In contrast to HSV-1, the prototype alphaherpesvirus, VZV contains only very short repeats (88 bp) on either end of the $U_L$(16). During alphaherpesvirus replication, four isomers of viral DNA are generated, which can be distinguished by the orientation of $U_L$ and $U_S$ relative to each other. While all four possible isomers of HSV-1 DNA are represented in the virion in equimolar amounts, virions produced by VZV and other members of the genus *Varicellovirus*, such as EHV-1, predominantly contain only two isomeric forms of the genome (16, 26, 36, 54, 96). Southern blot analysis of VZV virion DNA demonstrated that inversion of the $U_L$ region is rare amounting to only approximately 5% (16) and

could also be attributed to a rare circular configuration of the genome within the virion (50). A previous report on EHV-1 suggested that inversion of the $U_L$ region in infected cells is common, but that packaging occurs in a directional manner (96). For both VZV and EHV-1, the reason for the preferential orientation of the $U_L$ has remained unknown and will be further discussed in CHAPTER 3.

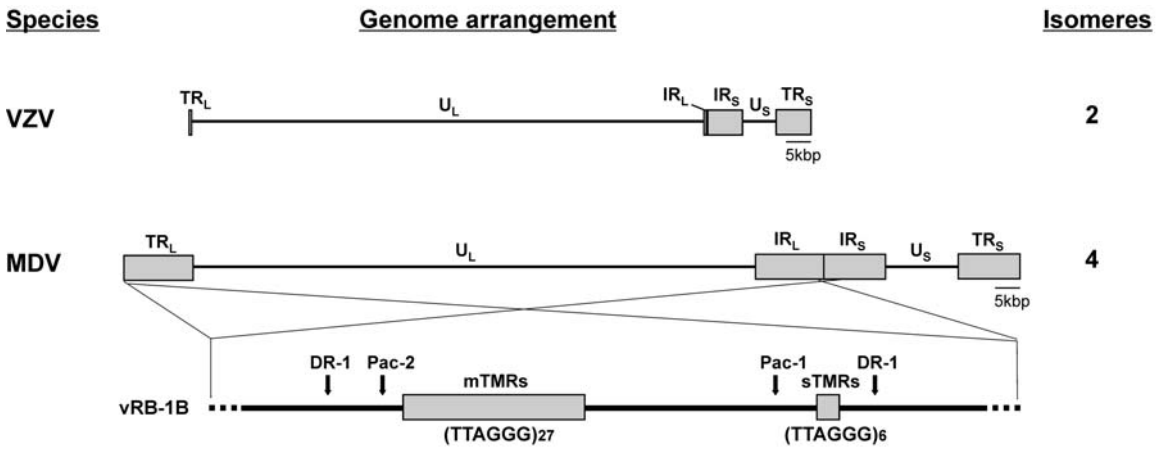


**Figure 1.3.** VZV and MDV genomes. Schematic representation of the VZV (upper panel) and MDV (middle panel) genome. The two unique regions unique long ($U_L$) and short ($U_S$) as well as the terminal ($TR_L$, $TR_S$) and internal ($IR_L$, $IR_S$) inverted repeat regions are shown. A focus on the a-like sequences in MDV is shown including the multiple telomeric repeats (mTMR), short telomeric repeats (sTMR), cleavage and packaging sites pac1 and pac2 as well as DR1 sites (lower panel). The number of isomers in VZV and MDV virions is shown.

### 1.7. Varicella-zoster virus pathogenesis

Primary VZV infection is initiated by the inhalation of aerosolized droplets from, or by direct contact with, individuals with ongoing varicella or reactivated herpes zoster (Fig. 1.4) (35, 86, 87). In the upper respiratory tract, VZV is thought to infect epithelial cells of the oronasal mucosa and is subsequently able to spread to the regional lymphoid tissue (Waldeyer's ring) and lymph nodes where it gains access to highly permissive CD4+ T-cells. The entry of infected T-cells into the bloodstream causes a primary viremia within four to six days of initial infection, which allows the virus to spread to several organs including liver and spleen. VZV then replicates in these organs resulting in a secondary viremia (28). During the incubation period, infected T-cells transport the virus to replication sites in the skin. VZV replication in epidermal cells results in the vesicular rash referred to as chickenpox. Aerosolization of vesicular fluid or direct contact with naïve individual allows the further dissemination of the virus. During primary infection, VZV is able to establish latency in cranial nerves as well as dorsal root and autonomic ganglia, where it remains dormant until a reactivation event occurs (30). In the latent state, the majority of the viral genome is transcriptionally silent and no infectious virus is produced. Reactivation of VZV occurs primarily in the elderly or immunocompromised individuals and results in the development of shingles (herpes zoster), which is often associated with severe pain and postherpetic neuralgia (2).

### 1.8. *Marek's disease virus*

MDV, also known as gallid herpesvirus type 2 (GaHV-2), belongs to the genus *Mardivirus*. Besides MDV, two related but distinct species belong to the same genus, GaHV-3 (previously referred to as MDV-2) and turkey herpes virus 1 (HVT), also known as meleagrid herpesvirus type 1 (MeHV-1) (8).

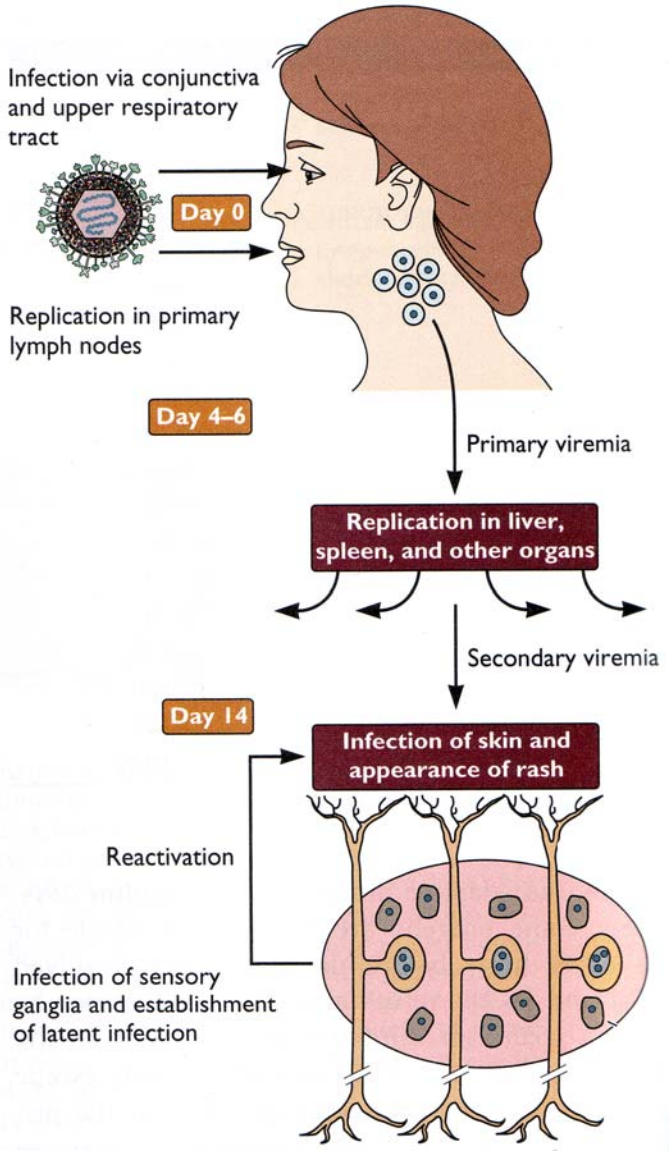


**Figure 1.4.** Model of VZV pathogenesis. VZV infection is initiated by the inhalation of cell free VZV. In the upper respiratory tract, VZV is able to infect epithelia cells and subsequently reaches primary lymph nodes. In a primary viremia, VZV spreads to liver, spleen and other organs where the virus replicates. In a secondary viremia, VZV reaches the skin, which results in the typical rash as well as establishment of latency in neurons of the sensory ganglia. VZV is able to reactivate from the latently infected neurons, which results in a localized vesicular rash. Modified from "Principles of virology"(28).

Marek's disease was named after József Marek who first described the disease as a general polyneuritis in adult animals in 1907 (62). Since then, the clinical picture of the disease has changed dramatically. At first it was described as a sporadic and chronic condition. However over the years the disease developed into an aggressive and acute form, which can cause more than 90% morbidity and mortality in susceptible animal populations (80, 91). The first cases of visceral lymphomas in conjunction with the prevalent neurological symptoms were reported in the mid 1950s. In addition, strains that developed over the past 25 years also cause severe brain edema and acute death even in fully vaccinated animals (80, 101). The virulence of different MDV strains can be classified into mildly virulent (m), virulent (v), very virulent (vv) and very virulent plus (vv+) (102). A number of MDV strains have been cloned as bacterial artificial chromosomes (BAC), which allow manipulation of the viral genome as well as their maintenance in *E. coli* (82, 83, 89).

### 1.9. Marek's disease virus genome structure

The 180-kbp linear, double-stranded DNA genome of MDV consists of two unique sequences ($U_L$ and $U_S$) flanked by terminal ($TR_L$ or $TR_S$) and internal ($IR_L$ or $IR_S$) inverted repeats (Fig. 1.3) (95). MDV also contains a-like sequences, which are present in an identical orientation at both ends of the linear genome as well as in an inverted orientation at the IR L-S junction. Upon circularization, one terminal copy of the a-like sequence is deleted (76). The a-like sequences of MDV have been found to contain a stretch of multiple telomeric repeats (mTMR) of variable lengths flanked by the cleavage and packaging signals *pac1* and *pac2* adjacent to the direct repeat 1 (DR1) (52). In addition, a shorter stretch of telomeric repeats (sTMR) invariably consisting of six TMRs has been identified upstream of the PacI site (Fig. 1.3). Unit length genomes are generated by cleavage of viral concatemeric DNA within DR1,

and are subsequently packaged into preformed capsids within the nucleus (5). Both packaging sites as well as DR1 are required for efficient cleavage and packaging. Whether the TMRs are also required for MDV in these processes has not been shown. However, Dewhurst and colleagues demonstrated that TMRs in HHV-6 are dispensable for virus cleavage and packaging using a plasmid-based approach (23).

### 1.10. Marek's disease virus pathogenesis

The initial infection of the chicken occurs via the respiratory route upon inhalation of infectious, cell-free MDV from a contaminated environment (Fig. 1.5). In the respiratory tract, MDV is able to infect macrophages or dendritic cells (DCs) (9). Infection of these cell types can be facilitated by an initial round of replication in epithelial cells. MDV subsequently uses infected macrophages and DCs as "transport vehicles" to lymphoid organs such as the spleen, thymus and bursa of Fabricius where the virus is detected within 24 hours after initial infection (88). Resident B-cells and later CD4 T-cells in these organs serve as a primary target for the first phase of cytolytic replication. Between days 3 and 6 post infection (dpi), the productive cytolytic replication provokes acute inflammation, which leads to an influx of macrophages, B-cells and T-cells. At 7 to 8 dpi, cytolytic infection in lymphoid organs changes and MDV enters the latent phase (9). Latency largely remains restricted to CD4+ T-cells and rarely occurs in B-cells or CD8+ T-cells (94). Infected CD4+ T-cells not only play an essential role in latency and transformation, but are also crucial for virus spread within the infected animal. Using infected CD4+ T-cells as a "shuttle", MDV is able to enter feather follicle epithelia, where infectious virus is produced and shed into the environment in a cell-free state (47, 80). In addition, MDV also gets transported into several non-lymphoid organs such as liver, lung, kidney, esophagus, proventriculus, intestine and adrenal glands, which serve as sites for the

second phase of cytolytic infection (9). However, MDV is not only able to stay latent in infected lymphocytes and travel throughout an animal, but is also able to transform infected cells, which ultimately leads to cellular immortalization and lymphoma formation in multiple organs.

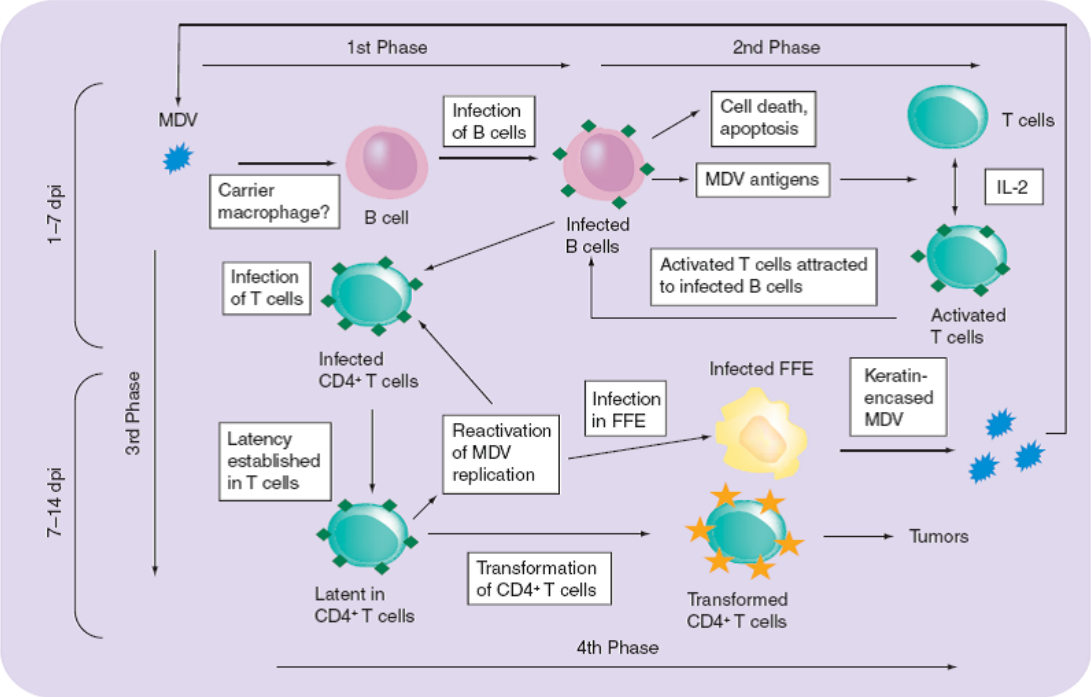


**Figure 1.5.** Model of MDV pathogenesis in chickens. Infection is initiated by the inhalation of cell free MDV. Macrophages are thought to transfer the virus to regional lymph nodes spleen, thymus and bursa, where the virus replicates in B cells and subsequently in T-cells. MDV is able to establish latency in infected T-cells, which transported the virus to the skin and feather follicle epithelia (FFE), where cell free MDV is generated. MDV is also able to transform T-cells, which often results in tumor formation. Obtained from Jarosinski et al. (45).

### 1.11. Herpesvirus genome integration and tumorigenesis

A number of DNA viruses and retroviruses are capable of integrating into the host genome, ensuring viral genome maintenance and replication during cell division.

Several herpesviruses integrate into the host genome, for example EBV, HHV-6, HHV-7 and MDV, whereas others maintain their genome in an episomal state. Delecluse and coworkers demonstrated that MDV integrates predominantly at the distal ends of host chromosomes (22). Strikingly, HHV-6 has also been found to integrate into telomeric regions at the very ends of the chromosomes (61, 72). This indicates that telomeres, which are important for chromosome maintenance via telomerase and an alternative elongation mechanism (ALT) (74), may play a role in the integration and latency of certain herpesviruses. As mentioned above, the MDV genome also contains repeats of telomeric sequences (TTAGGG) at both ends of the genome as well as within the internal repeat region (Fig 1.3). Besides MDV, other herpesviruses from all three classes contain these sequences at the very end of their genome. Among those are viruses closely related to MDV, GaHV-3 and HVT, the β-herpesviruses HHV-6 and HHV-7 as well as the γ-herpesvirus equine herpesvirus type 2 (EHV-2). Intriguingly, viruses that harbor telomeric repeats (TMRs) establish latency in lymphocytes, which requires faithful replication of the viral genome during proliferation of the latently infected host cells (44). The role of the telomeric sequences within the viral genome is not known at present. Several functions are possible, for example i) integration into the host genome via homologuous recombination, ii) recognition of the genome as a mini chromosome by the cell, iii) and/or they play a role in the cleavage and packaging of viral DNA.

### 1.12. Telomere structure and function

Telomeres are specialized structures located at the distal end of eukaryotic chromosomes (Fig. 1.6A). This DNA-protein complex is thought to fulfill at least five vital functions. Firstly, telomeres protect chromosome ends from terminal degradation by exonucleases (98), which would lead to successive loss of genetic information.

Secondly, they prevent illegitimate recombination mediated by the cellular recombination machinery in the presence of free double strand DNA ends (20, 63). Thirdly, telomeres inhibit the activation of DNA damage responses, which recognize genomic double-strand breaks and induce apoptosis in case of severe damage to the genome (98). Fourthly, cytogenetic studies indicate that telomeres are located at the nuclear periphery, suggesting that telomeres might be involved in the chromosomal organization within the nucleus (1). Finally, telomeres including its proteinaceous moieties provide a solution for the end replication problem, which arises from the inability of the replication machinery to amplify the terminal sequences of the lagging strand (100).

In eukaryotes, telomere DNA usually consists of tandem repeats, 5-8 bp in length with a high guanine (G) content (60). In vertebrates, the telomeric repeat sequence is highly conserved and is comprised of the hexanucleotide repeat $(TTAGGG)_n$. Telomeric repeats are protected by a protein complex termed shelterin. Three shelterin proteins, telomere recognition factor 1 and 2 (TRF-1 and TRF-2) and POT1, interact directly with the telomeric repeats (19). Other proteins, such as TIN2, TPP1 and Rap1, interconnect the individual components and facilitate shelterin complex formation (67). At the telomere ends, the G rich strand extends past the complementary strand as a 3′ overhang, which is stabilized by POTI and forms a T loop by invasion into the double-stranded telomeric DNA (42).

Telomere length varies greatly among species and lengths ranging from 20 bp in some ciliated protozoan species such as *Oxytricha* (53), a few hundred bp in *S. cerevisia e*(85), 4-14 kbp in humans (20), 10-150 kbp in mice (51) and 10-2000 kbp in chickens (21).

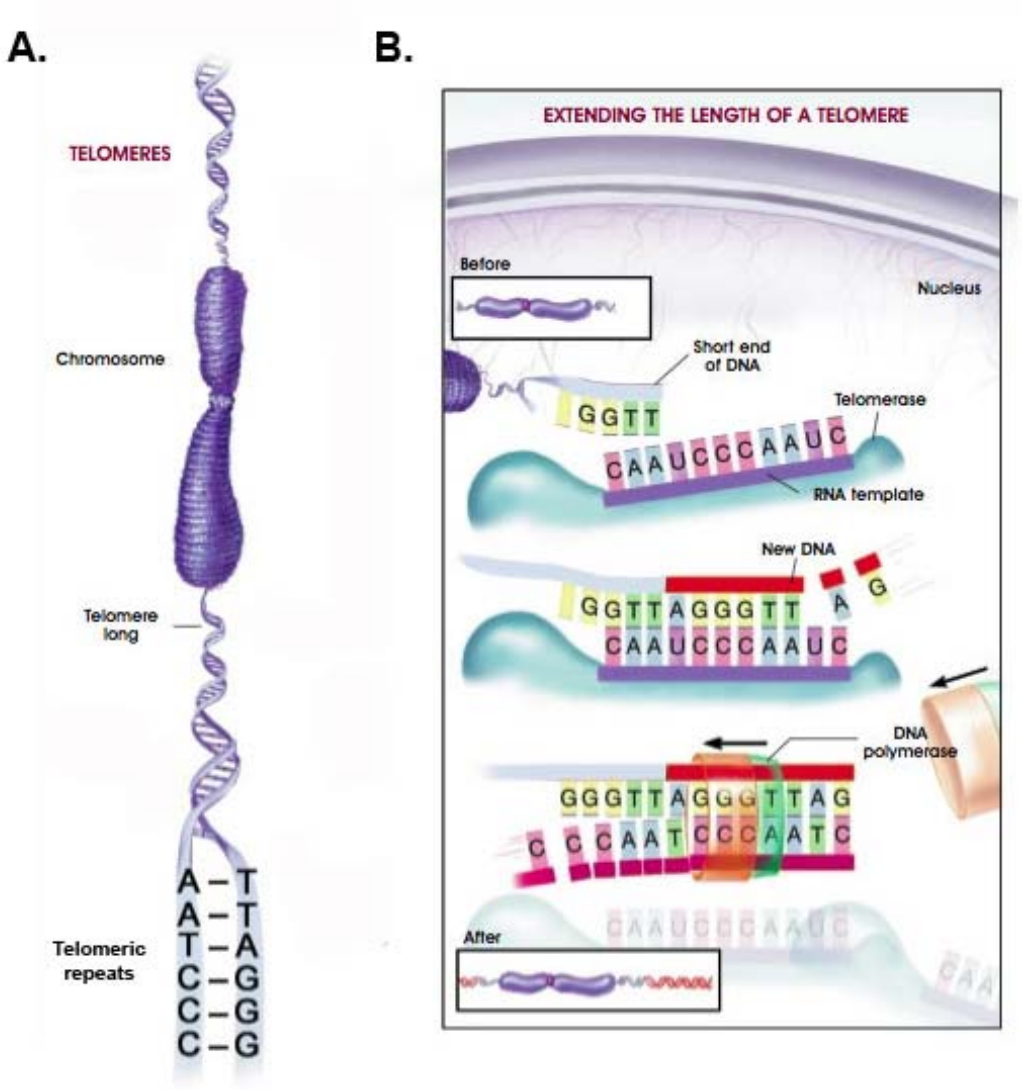


**Figure 1.6.** Telomeres and Telomerase. A) Schematic representation of a eukaryotic chromosome. Telomeres are shown at both ends and telomeric repeat sequences $(TTAGGG)_n$ are indicated. B) Telomerase-mediated telomere extension. The telomerase complex, including telomerase reverse transcriptase (TERT, light blue) and telomerase RNA (TR), bind to the shortened telomere (upper panel) and adds several repeats to the telomere end (middle panel). The complementary strand is subsequently synthesized by the DNA polymerase. Modified from stemcells.nih.gov/info/scireport/appendixC.asp.

### 1.13. Telomere maintenance and telomerase

Replication of chromosome ends poses an intriguing problem, due to the inability of the DNA polymerase to fully replicate the 3′ end of the lagging strand. Watson and Olovnikov independently recognized this phenomenon and hypothesized that the chromosome termini would be progressively shortened with every cell division (78, 79, 100). Indeed, chromosome shortening was observed in proliferating cells *in vitro* corroborating the hypothesis of Watson and Olovnikov (20, 37). In addition, telomere length decreases with age of an individual (38, 59), confirming that telomere shortening also occurs *in vivo*. Furthermore, somatic human cells are limited in the number of cell divisions, suggesting chromosome shortening acts as a molecular clock regulating the replicative potential of cells (39). Continuous cell proliferation occurs until telomeres reach a critical limit which triggers an irreversible growth arrest called cellular senescence (93). Excessive shortening also greatly increases the incidence of end-to-end fusion of chromosomes and the activation of DNA damage responses which can result in the induction of apoptosis (31, 97).

Telomerase, a multi-component ribonucleoprotein complex, counteracts this gradual telomere loss by adding telomeric repeats onto chromosome ends (Fig. 1.6B). The telomerase complex, which was first discovered in the ciliate *Tetrahymena* (33), consists of two main components, telomerase reverse transcriptase (TERT) and telomerase RNA (TR), as well as many associated proteins. As the catalytic subunit of the complex, TERT facilitates the reverse transcriptase reaction, which results in the addition of telomeric repeats to chromosome termini, while TR provides the RNA template for the reaction. Counterparts of TERT have been identified in various organisms including ciliates, yeast, mammalian and avian species. The size of TERT

varies from 103 kDa in *S. cerevisiae*, 127 kDa in humans and mice, 134 kDa in *Tetrahymena* to 155 kDa in chickens (11, 15, 32, 73). All TERT family members contain seven conserved reverse transcriptase (RT) motifs that are located in a central region of the protein (3). TERT harbors two independent RNA binding domains. The first, a high-affinity binding domain is comprised of three conserved telomerase specific motifs that bind a conserved region (CR4-CR5) of human TR (56, 68). A second, low-affinity binding domain is though to interact with human TR within the pseudoknot-template domain (71).

TR contains four structural domains, which are highly conserved regions (CR) in all vertebrates: i) the pseudoknot (core) domain, containing the template sequence (CR1); ii) the H/ACA box and iii) the conserved region (CR) 7 domain, both of which are essential for TR stability and localization; and iv) the CR4-CR5 domain, which is required for efficient TR-TERT complex formation, hence telomerase activity and processivity (12, 29). Besides TERT and TR, several other proteins also directly interact with the telomerase complex in humans, such as the chaperone p23, hStau, ribosomal protein L22 (RPL22) and dyskerin, which are thought to regulate telomerase assembly, modification, localization and enzymatic activity (3, 57, 69, 77). However, TERT and TR alone are sufficient to reconstitute the holoenzyme and to exhibit telomerase activity (34).

While TR is highly expressed in most cell types, TERT expression is limited to only a subset of cell types and is therefore the limiting factor for telomerase activity. Germ-line and stem cells exhibit high telomerase activity that is sufficient to maintain a constant telomere length, allowing the indefinite proliferation of such cells. However, most somatic cells do not exhibit telomerase activity, limiting the number of replication cycles of differentiated cells (92). Expression of telomerase components in somatic cells *in trans* is sufficient to prevent telomere loss and to promote

immortalization and continued proliferation and growth (4). Furthermore, telomerase activity is highly upregulated in more than 90% of human cancers (92), underlining the role of telomere maintenance in tumor development. Inhibition of telomerase activity in immortalized human cells results in telomere shortening and cell death (41), making the system an intriguing target for cancer therapy (24). Some tumors and cells derived thereof, however, are able to maintain their telomeres in the absence of any detectable telomerase activity by an alternative lengthening of telomeres (ALT) pathway (6, 7). The ALT process relies on homologous recombination between telomeres, which will result in the copying of telomere sequences (25). Still, the telomerase complex is the key player in telomere elongation. With its cell type-specific activity, it allows an efficient maintenance of telomeres in germ-line and stem cells, while somatic cells only have a limited proliferative capability, which is thought to keep potential cancer progenitor cells in check.

REFERENCES


1. **Agard, D. A. and J. W. Sedat**. 1983. Three-dimensional architecture of a polytene nucleus. Nature **302**:676-681.

2. **Arvin, A. M.** 1996. Varicella-zoster virus. Clin. Microbiol. Rev. **9**:361-381.

3. **Autexier, C. and N. F. Lue**. 2006. The structure and function of telomerase reverse transcriptase. Annu. Rev. Biochem. **75**:493-517.

4. **Bodnar, A. G., M. Ouellette, M. Frolkis, S. E. Holt, C. P. Chiu, G. B. Morin, C. B. Harley, J. W. Shay, S. Lichtsteiner, and W. E. Wright**. 1998. Extension of life-span by introduction of telomerase into normal human cells. Science **279**:349-352.

5. **Boehmer, P. E. and I. R. Lehman**. 1997. Herpes simplex virus DNA replication. Annu. Rev. Biochem. **66**:347-384.

6. **Bryan, T. M., A. Englezou, L. Dalla-Pozza, M. A. Dunham, and R. R. Reddel**. 1997. Evidence for an alternative mechanism for maintaining telomere length in human tumors and tumor-derived cell lines. Nat. Med. **3**:1271-1274.

7. **Bryan, T. M., A. Englezou, J. Gupta, S. Bacchetti, and R. R. Reddel**. 1995. Telomere elongation in immortal human cells without detectable telomerase activity. EMBO J **14**:4240-4248.

8. **Calnek B.W. and R.L.Witter.** 1991. Marek´s disease, p. 342-385. *In* B.W.Calnek (ed.) (ed.), Diseases of poultry. Iowa State University Press, Ames.

9. **Calnek, B. W.** 2001. Pathogenesis of Marek's disease virus infection. Curr. Top. Microbiol. Immunol. **255**:25-55.

10. **Calnek, B. W., K. A. Schat, L. J. Ross, W. R. Shek, and C. L. Chen**. 1984. Further characterization of Marek's disease virus-infected lymphocytes. I. In vivo infection. Int. J Cancer **33**:389-398.

11. **Chang, H. and M. E. Delany**. 2006. Complicated RNA splicing of chicken telomerase reverse transcriptase revealed by profiling cells both positive and negative for telomerase activity. Gene **379**:33-39.

12. **Chen, J. L., K. K. Opperman, and C. W. Greider**. 2002. A critical stem-loop structure in the CR4-CR5 domain of mammalian telomerase RNA. Nucleic Acids Res. **30**:592-597.

13. **Cohen J.I., Straus S.E, and A. M. Arvin**. 2007. Varicella-Zoster Virus Replication, Pathogenesis and Management, p. 2276-2278. *In* D. M. K. P. M. H. e. al. 5. Ed. B.N.Fields (ed.), Fields Virology. Lippincott-Raven Publishers, Philadelphia.

14. **Cohen, J. I. and K. E. Seidel**. 1993. Generation of varicella-zoster virus (VZV) and viral mutants from cosmid DNAs: VZV thymidylate synthetase is not essential for replication in vitro. Proc. Natl. Acad. Sci. U. S. A **90**:7376-7380.

15. **Collins, K. and L. Gandhi**. 1998. The reverse transcriptase component of the Tetrahymena telomerase ribonucleoprotein complex. Proc. Natl. Acad. Sci. U. S. A **95**:8485-8490.

16. **Davison, A. J.** 1984. Structure of the genome termini of varicella-zoster virus. J Gen Virol **65 ( Pt 11)**:1969-1977.

17. **Davison, A. J., R. Eberle, B. Ehlers, G. S. Hayward, D. J. McGeoch, A. C. Minson, P. E. Pellett, B. Roizman, M. J. Studdert, and E. Thiry**. 2009. The order Herpesvirales. Arch. Virol **154**:171-177.

18. **Davison, A. J. and N. M. Wilkie**. 1983. Location and orientation of homologous sequences in the genomes of five herpesviruses. J Gen Virol **64 (Pt 9)**:1927-1942.

19. **de Lange, T.** 2005. Shelterin: the protein complex that shapes and safeguards human telomeres. Genes Dev. **19**:2100-2110.

20. **de Lange, T., L. Shiue, R. M. Myers, D. R. Cox, S. L. Naylor, A. M. Killery, and H. E. Varmus**. 1990. Structure and variability of human chromosome ends. Mol. Cell Biol. **10**:518-527.

21. **Delany, M. E., L. M. Daniels, S. E. Swanberg, and H. A. Taylor**. 2003. Telomeres in the chicken: genome stability and chromosome ends. Poult. Sci. **82**:917-926.

22. **Delecluse, H. J. and W. Hammerschmidt**. 1993. Status of Marek's disease virus in established lymphoma cell lines: herpesvirus integration is common. J. Virol. **67**:82-92.

23. **Deng, H. and S. Dewhurst**. 1998. Functional identification and analysis of cis-acting sequences which mediate genome cleavage and packaging in human herpesvirus 6. J. Virol. **72**:320-329.

24. **Ducrest, A. L., H. Szutorisz, J. Lingner, and M. Nabholz**. 2002. Regulation of the human telomerase reverse transcriptase gene. Oncogene **21**:541-552.

25. **Dunham, M. A., A. A. Neumann, C. L. Fasching, and R. R. Reddel**. 2000. Telomere maintenance by recombination in human cells. Nat. Genet. **26**:447-450.

26. **Ecker, J. R. and R. W. Hyman**. 1982. Varicella zoster virus DNA exists as two isomers. Proc. Natl. Acad. Sci. U. S. A **79**:156-160.

27. **Fanget, B. and A. Francon**. 1996. A varicella vaccine stable at 5 degrees C. Dev. Biol. Stand. **87**:167-171.

28. **Flint, S. J., L. W. Enquist, V. R. Racaniello, and Skalka A.M.** 2004. Molecular Biology, Pathogenesis, and Control of Animal Viruses. Principles of virology. ASM Press, Washington, D.C.

29. **Fragnet, L., M. A. Blasco, W. Klapper, and D. Rasschaert**. 2003. The RNA subunit of telomerase is encoded by Marek's disease virus. J Virol **77**:5985-5996.

30. **Gilden, D. H., R. Gesser, J. Smith, M. Wellish, J. J. Laguardia, R. J. Cohrs, and R. Mahalingam**. 2001. Presence of VZV and HSV-1 DNA in human nodose and celiac ganglia. Virus Genes **23**:145-147.

31. **Granger, M. P., W. E. Wright, and J. W. Shay**. 2002. Telomerase in cancer and aging. Crit Rev. Oncol. Hematol. **41**:29-40.

32. **Greenberg, R. A., R. C. Allsopp, L. Chin, G. B. Morin, and R. A. DePinho**. 1998. Expression of mouse telomerase reverse transcriptase during development, differentiation and proliferation. Oncogene **16**:1723-1730.

33. **Greider, C. W. and E. H. Blackburn**. 1985. Identification of a specific telomere terminal transferase activity in Tetrahymena extracts. Cell **43**:405-413.

34. **Greider, C. W. and E. H. Blackburn**. 1987. The telomere terminal transferase of Tetrahymena is a ribonucleoprotein enzyme with two kinds of primer specificity. Cell **51**:887-898.

35. **Grose, C.** 1981. Variation on a theme by Fenner: the pathogenesis of chickenpox. Pediatrics **68**:735-737.

36. **Hammerschmidt, W., H. Ludwig, and H. J. Buhk**. 1988. Specificity of cleavage in replicative-form DNA of bovine herpesvirus 1. J Virol **62**:1355-1363.

37. **Harley, C. B., A. B. Futcher, and C. W. Greider**. 1990. Telomeres shorten during ageing of human fibroblasts. Nature **345**:458-460.

38. **Hastie, N. D., M. Dempster, M. G. Dunlop, A. M. Thompson, D. K. Green, and R. C. Allshire**. 1990. Telomere reduction in human colorectal carcinoma and with ageing. Nature **346**:866-868.

39. **Hayflick, L.** 1965. The limited in vitro lifetime of human diploid cell strains. Exp. Cell Res. **37**:614-636.

40. **Heldwein, E. E. and C. Krummenacher**. 2008. Entry of herpesviruses into mammalian cells. Cell Mol. Life Sci. **65**:1653-1668.

41. **Herbert, B., A. E. Pitts, S. I. Baker, S. E. Hamilton, W. E. Wright, J. W. Shay, and D. R. Corey**. 1999. Inhibition of human telomerase in immortal human cells leads to progressive telomere shortening and cell death. Proc. Natl. Acad. Sci. U. S. A **96**:14276-14281.

42. **Hodes, R. J., K. S. Hathcock, and N. P. Weng**. 2002. Telomeres in T and B cells. Nat. Rev. Immunol. **2**:699-706.

43. **Honess, R. W. and B. Roizman**. 1974. Regulation of herpesvirus macromolecular synthesis. I. Cascade regulation of the synthesis of three groups of viral proteins. J. Virol. **14**:8-19.

44. **Izumiya, Y., H. K. Jang, M. Ono, and T. Mikami**. 2001. A complete genomic DNA sequence of Marek's disease virus type 2, strain HPRS24. Curr. Top. Microbiol. Immunol. **255**:191-221.

45. **Jarosinski, K. W., B. K. Tischer, S. Trapp, and N. Osterrieder**. 2006. Marek's disease virus: lytic replication, oncogenesis and control. Expert. Rev. Vaccines. **5**:761-772.

46. **Johnson, D. C. and M. T. Huber**. 2002. Directed egress of animal viruses promotes cell-to-cell spread. J. Virol. **76**:1-8.

47. **Johnson, E. A., C. N. Burke, T. N. Fredrickson, and R. A. DiCapua**. 1975. Morphogenesis of marek's disease virus in feather follicle epithelium. J. Natl. Cancer Inst. **55**:89-99.

48. **Jones, C.** 1998. Alphaherpesvirus latency: its role in disease and survival of the virus in nature. Adv. Virus Res. **51**:81-133.

49. **Kemble, G. W., P. Annunziato, O. Lungu, R. E. Winter, T. A. Cha, S. J. Silverstein, and R. R. Spaete**. 2000. Open reading frame S/L of varicella-zoster virus encodes a cytoplasmic protein expressed in infected cells. J Virol **74**:11311-11321.

50. **Kinchington, P. R., W. C. Reinhold, T. A. Casey, S. E. Straus, J. Hay, and W. T. Ruyechan**. 1985. Inversion and circularization of the varicella-zoster virus genome. J Virol **56**:194-200.

51. **Kipling, D. and H. J. Cooke**. 1990. Hypervariable ultra-long telomeres in mice. Nature **347**:400-402.

52. **Kishi, M., G. Bradley, J. Jessip, A. Tanaka, and M. Nonoyama**. 1991. Inverted repeat regions of Marek's disease virus DNA possess a structure similar to that of the a sequence of herpes simplex virus DNA and contain host cell telomere sequences. J. Virol. **65**:2791-2797.

53. **Klobutcher, L. A., M. T. Swanton, P. Donini, and D. M. Prescott**. 1981. All gene-sized DNA molecules in four species of hypotrichs have the same terminal sequence and an unusual 3' terminus. Proc. Natl. Acad. Sci. U. S. A **78**:3015-3019.

54. **Klupp, B. G., C. J. Hengartner, T. C. Mettenleiter, and L. W. Enquist**. 2004. Complete, annotated sequence of the pseudorabies virus genome. J Virol **78**:424-440.

55. **Ku, C. C., J. Besser, A. Abendroth, C. Grose, and A. M. Arvin**. 2005. Varicella-Zoster virus pathogenesis and immunobiology: new concepts emerging from investigations with the SCIDhu mouse model. J Virol **79**:2651-2658.

56. **Lai, C. K., J. R. Mitchell, and K. Collins**. 2001. RNA binding domain of telomerase reverse transcriptase. Mol. Cell Biol. **21**:990-1000.

57. **Le, S., R. Sternglanz, and C. W. Greider**. 2000. Identification of two RNA-binding proteins associated with human telomerase RNA. Mol. Biol. Cell **11**:999-1010.

58. **Levin, M. J., S. Leventhal, and H. A. Masters**. 1984. Factors influencing quantitative isolation of varicella-zoster virus. J Clin. Microbiol. **19**:880-883.

59. **Lindsey, J., N. I. McGill, L. A. Lindsey, D. K. Green, and H. J. Cooke**. 1991. In vivo loss of telomeric repeats with age in humans. Mutat. Res. **256**:45-48.

60. **Louis, E. J. and A. V. Vershinin**. 2005. Chromosome ends: different sequences may provide conserved functions. Bioessays **27**:685-697.

61. **Luppi, M., P. Barozzi, R. Marasca, and G. Torelli**. 1994. Integration of human herpesvirus-6 (HHV-6) genome in chromosome 17 in two lymphoma patients. Leukemia **8 Suppl 1**:S41-S45.

62. **Marek, J.** 1907. Multiple Nervenentzündung (Polyneuritis) bei Hühnern. Dtsch. Tierärztl. Wochenschr. **15**:417-421.

63. **McClintock, B.** 1941. The Stability of Broken Ends of Chromosomes in Zea Mays. Genetics **26**:234-282.

64. **McGeoch, D. J., S. Cook, A. Dolan, F. E. Jamieson, and E. A. Telford**. 1995. Molecular phylogeny and evolutionary timescale for the family of mammalian herpesviruses. J. Mol. Biol. **247**:443-458.

65. **McVoy, M. A., D. E. Nixon, J. K. Hur, and S. P. Adler**. 2000. The ends on herpesvirus DNA replicative concatemers contain pac2 cis cleavage/packaging elements and their formation is controlled by terminal cis sequences. J. Virol. **74**:1587-1592.

66. **Mettenleiter, T. C.** 2002. Herpesvirus assembly and egress. J. Virol. **76**:1537-1547.

67. **Misri, S., S. Pandita, R. Kumar, and T. K. Pandita**. 2008. Telomeres, histone code, and DNA damage response. Cytogenet. Genome Res. **122**:297-307.

68. **Mitchell, J. R. and K. Collins**. 2000. Human telomerase activation requires two independent interactions between telomerase RNA and telomerase reverse transcriptase. Mol. Cell **6**:361-371.

69. **Mitchell, J. R., E. Wood, and K. Collins**. 1999. A telomerase component is defective in the human disease dyskeratosis congenita. Nature **402**:551-555.

70. **Moffat, J. F., M. D. Stein, H. Kaneshima, and A. M. Arvin**. 1995. Tropism of varicella-zoster virus for human CD4+ and CD8+ T lymphocytes and epidermal cells in SCID-hu mice. J Virol **69**:5236-5242.

71. **Moriarty, T. J., D. T. Marie-Egyptienne, and C. Autexier**. 2004. Functional organization of repeat addition processivity and DNA synthesis determinants in the human telomerase multimer. Mol. Cell Biol. **24**:3720-3733.

72. **Morris, C., M. Luppi, M. McDonald, P. Barozzi, and G. Torelli**. 1999. Fine mapping of an apparently targeted latent human herpesvirus type 6 integration site in chromosome band 17p13.3. J. Med. Virol. **58**:69-75.

73. **Nakamura, T. M., G. B. Morin, K. B. Chapman, S. L. Weinrich, W. H. Andrews, J. Lingner, C. B. Harley, and T. R. Cech**. 1997. Telomerase catalytic subunit homologs from fission yeast and human. Science **277**:955-959.

74. **Nguyen, B., L. W. Elmore, and S. E. Holt**. 2004. Telomere maintenance: at the crossroads of mismatch repair? Cancer Biol. Ther. **3**:293-295.

75. **Niizuma, T., L. Zerboni, M. H. Sommer, H. Ito, S. Hinchliffe, and A. M. Arvin**. 2003. Construction of varicella-zoster virus recombinants from parent Oka cosmids and demonstration that ORF65 protein is dispensable for infection of human skin and T cells in the SCID-hu mouse model. J. Virol. **77**:6062-6065.

76. **Nixon, D. E. and M. A. McVoy**. 2002. Terminally repeated sequences on a herpesvirus genome are deleted following circularization but are reconstituted by duplication during cleavage and packaging of concatemeric DNA. J. Virol. **76**:2009-2013.

77. **Nugent, C. I. and V. Lundblad**. 1998. The telomerase reverse transcriptase: components and regulation. Genes Dev. **12**:1073-1085.

78. **Olovnikov, A. M.** 1971. [Principle of marginotomy in template synthesis of polynucleotides]. Dokl. Akad. Nauk SSSR **201**:1496-1499.

79. **Olovnikov, A. M.** 1973. A theory of marginotomy. The incomplete copying of template margin in enzymic synthesis of polynucleotides and biological significance of the phenomenon. J Theor. Biol. **41**:181-190.

80. **Osterrieder, N., J. P. Kamil, D. Schumacher, B. K. Tischer, and S. Trapp**. 2006. Marek's disease virus: from miasma to model. Nat. Rev. Microbiol. **4**:283-294.

81. **Pellett, P. E. and B. Roizman**. 2007. The Family Herpesviridae: A Brief Introduction, p. 2479-2499. *In* Fields B.N., Howley P.M., and Knipe D.M. (eds.), Fields Virology. Lippincott-Raven Publishers, Philadelphia.

82. **Petherbridge, L., A. C. Brown, S. J. Baigent, K. Howes, M. A. Sacco, N. Osterrieder, and V. K. Nair**. 2004. Oncogenicity of virulent Marek's disease virus cloned as bacterial artificial chromosomes. J. Virol. **78**:13376-13380.

83. **Petherbridge, L., K. Howes, S. J. Baigent, M. A. Sacco, S. Evans, N. Osterrieder, and V. Nair**. 2003. Replication-competent bacterial artificial chromosomes of Marek's disease virus: novel tools for generation of molecularly defined herpesvirus vaccines. J. Virol. **77**:8712-8718.

84. **Roizman, B., L. E. Carmichael, F. Deinhardt, G. de The, A. J. Nahmias, W. Plowright, F. Rapp, P. Sheldrick, M. Takahashi, and K. Wolf**. 1981. Herpesviridae. Definition, provisional nomenclature, and taxonomy. The Herpesvirus Study Group, the International Committee on Taxonomy of Viruses. Intervirology **16**:201-217.

85. **Runge, K. W. and V. A. Zakian**. 1989. Introduction of extra telomeric DNA sequences into Saccharomyces cerevisiae results in telomere elongation. Mol. Cell Biol. **9**:1488-1497.

86. **Sawyer, M. H., C. J. Chamberlin, Y. N. Wu, N. Aintablian, and M. R. Wallace**. 1994. Detection of varicella-zoster virus DNA in air samples from hospital rooms. J Infect. Dis. **169**:91-94.

87. **Sawyer, M. H., Y. N. Wu, C. J. Chamberlin, C. Burgos, S. K. Brodine, W. A. Bowler, A. LaRocco, E. C. Oldfield, III, and M. R. Wallace**. 1992. Detection of varicella-zoster virus DNA in the oropharynx and blood of patients with varicella. J Infect. Dis. **166**:885-888.

88. **Schat, K. A., R. F. Schinazi, and B. W. Calnek**. 1984. Cell-specific antiviral activity of 1-(2-fluoro-2-deoxy-beta-D-arabinofuranosyl)-5-iodocytosine (FIAC) against Marek's disease herpesvirus and turkey herpesvirus. Antiviral Res. **4**:259-270.

89. **Schumacher, D., B. K. Tischer, W. Fuchs, and N. Osterrieder**. 2000. Reconstitution of Marek's disease virus serotype 1 (MDV-1) from DNA cloned as a bacterial artificial chromosome and characterization of a glycoprotein B-negative MDV-1 mutant. J. Virol. **74**:11088-11098.

90. **Sears, J., M. Ujihara, S. Wong, C. Ott, J. Middeldorp, and A. Aiyar**. 2004. The amino terminus of Epstein-Barr Virus (EBV) nuclear antigen 1 contains AT hooks that facilitate the replication and partitioning of latent EBV genomes by tethering them to cellular chromosomes. J Virol **78**:11487-11505.

91. **Shamblin, C. E., N. Greene, V. Arumugaswami, R. L. Dienglewicz, and M. S. Parcells**. 2004. Comparative analysis of Marek's disease virus (MDV) glycoprotein-, lytic antigen pp38- and transformation antigen Meq-encoding genes: association of meq mutations with MDVs of high virulence. Vet. Microbiol. **102**:147-167.

92. **Shay, J. W. and S. Bacchetti**. 1997. A survey of telomerase activity in human cancer. Eur. J Cancer **33**:787-791.

93. **Shay, J. W., O. M. Pereira-Smith, and W. E. Wright**. 1991. A role for both RB and p53 in the regulation of human cellular senescence. Exp. Cell Res. **196**:33-39.

94. **Shek, W. R., B. W. Calnek, K. A. Schat, and C. H. Chen**. 1983. Characterization of Marek's disease virus-infected lymphocytes: discrimination between cytolytically and latently infected cells. J. Natl. Cancer Inst. **70**:485-491.

95. **Silva, R. F., L. F. Lee, and G. F. Kutish**. 2001. The genomic structure of Marek's disease virus. Curr. Top. Microbiol. Immunol. **255**:143-158.

96. **Slobedman, B. and A. Simmons**. 1997. Concatemeric intermediates of equine herpesvirus type 1 DNA replication contain frequent inversions of adjacent long segments of the viral genome. Virology **229**:415-420.

97. **Stewart, S. A. and R. A. Weinberg**. 2002. Senescence: does it all happen at the ends? Oncogene **21**:627-630.

98. **Vaziri, H. and S. Benchimol**. 1996. From telomere loss to p53 induction and activation of a DNA-damage pathway at senescence: the telomere loss/DNA damage model of cell aging. Exp. Gerontol. **31**:295-301.

99. **WALLIS, C., C. S. YANG, and J. L. MELNICK**. 1962. Effect of cations on thermal inactivation of vaccinia, herpes simplex, and adenoviruses. J Immunol. **89**:41-46.

100. **Watson, J. D.** 1972. Origin of concatemeric T7 DNA. Nat. New Biol. **239**:197-201.

101. **Witter, R. L.** 1997. Avian tumor viruses: persistent and evolving pathogens. Acta Vet. Hung. **45**:251-266.

102. **Witter, R. L.** 1997. Increased virulence of Marek's disease virus field isolates. Avian Dis. **41**:149-163.

## CHAPTER TWO

# A Self-Excisable Infectious Bacterial Artificial Chromosome Clone of Varicella-Zoster Virus Allows Analysis of the Essential Tegument Protein Encoded by *ORF9*

***B. Karsten Tischer, *Benedikt B. Kaufer, Marvin Sommer, Felix Wussow, Ann M. Arvin, Nikolaus Osterrieder**. 2007. A self-excisable infectious bacterial artificial chromosome clone of varicella-zoster virus allows analysis of the essential tegument protein encoded by ORF9. J Virol **81**:13200-13208.



***** These authors contributed equally to this work

## 2.1. Abstract

In order to facilitate mutant virus generation in varicella zoster virus (VZV), the agent causing varicella (chickenpox) and herpes zoster (shingles), we generated a full-length infectious bacterial artificial chromosome (BAC) clone of the P-Oka strain. First, mini-F sequences were inserted into a preexisting VZV cosmid, and the SuperCos replicon was removed. Subsequently, mini-F containing recombinant virus was generated from overlapping cosmid clones, and full-length VZV DNA recovered from the recombinant virus was established in *Escherichia coli* as an infectious BAC. An inverted duplication of VZV genomic sequences within the mini-F replicon resulted in markerless excision of vector sequences upon virus reconstitution in eukaryotic cells. Using the novel tool, the role of the major tegument protein encoded by *ORF9* for VZV replication was investigated. A markerless point mutation introduced in the start codon by two-step *en passant* Red mutagenesis abrogated *ORF9* expression and resulted in a dramatic growth defect that was not observed in a revertant virus. The essential nature of *ORF9* for VZV replication was ultimately confirmed by restoration of growth of the *ORF9*-deficient mutant virus using trans-complementation via baculovirus mediated gene transfer.

## 2.2. Introduction

Varicella-zoster virus (VZV), the causative agent of chickenpox (varicella) and shingles (herpes zoster), is a highly cell-associated herpesvirus both *in vitro* and *in vivo* (7, 23). Similar to the situation in a closely related alphaherpesvirus, Marek's disease virus (MDV), VZV spreads directly from cell to cell, presumably utilizing the machinery involved in adherens junction modeling and architecture. Infectious virus is only released into the environment after lytic VZV replication in the skin and respiratory mucous membranes of infected individuals (2, 43). Efficient and timely coordinated interaction between the tegument, a proteinaceous structure surrounding the icosahedral nucleocapsid, and envelope membrane (glyco)proteins plays a crucial role in secondary envelopment and spread of herpesviruses in general and VZV in particular (34). It has been shown for related viruses such as herpes simplex virus (HSV) that the inner layer of tegument is tightly associated with the nucleocapsid, whereas the outer layer of tegument provides the link to envelope proteins (35, 36). The current model of herpesviral tegumentation predicts that the inner layer of tegument is added to the nucleocapsid in the nucleus and de-enveloped particles in the cytoplasm, while proteins representing the outer layer are thought to accumulate at cytoplasmic membranes where they make contact with their respective partners, either other tegument proteins and/or membrane proteins (34-36). Through these intricately regulated interactions, final secondary envelopment of particles is facilitated and, ultimately, infectious virus is produced and released.

Determination of the role of individual tegument or membrane (glyco)proteins in the replication cycle of various herpesviruses is not trivial, because, *in vitro*, many of the functions appear redundant (34, 35). Analyses of viral mutants have shown, however, that similar sets of structural proteins are required for most alphaherpesviruses. VZV and MDV seem to be the exceptions to the rule. Not only

do they share important biological properties with respect to growth *in vitro* and *in vivo*, they also exhibit striking similarities with respect to the membrane (glyco)proteins as well as tegument proteins that they absolutely require for replication. For example, both glycoproteins E and I (gE and gI), which form a noncovalently linked complex in infected cells and virions, are essential for growth of both viruses, at least in certain cell types, while they are dispensable in all other alphaherpesviruses tested (3, 8, 25, 37, 42, 50, 63, 65). In contrast, the major viral transactivator encoded by VZV *ORF10* (MDV *UL48*) is dispensable for growth of either virus, but is essential for most related viruses (17, 19, 20, 58, 61). In this context it must be noted that the MDV *UL49* product, the ORF9 homologue of VZV, was shown to be absolutely required for growth of the chicken virus. The facts that this tegument protein was shown to physically interact with gE in the case of related herpesviruses and that gE is essential for both VZV and MDV (4, 21, 29, 30, 38, 50) prompted us to investigate the role of the *ORF9* product in the VZV life cycle.

Since mutagenesis of herpesviruses using standard techniques that are based on homologous recombination in cultured cells by default results in a steady positive selection for viral replication, manipulation of genes that are crucial for viral replication in non-complementing cells is virtually impossible. In addition, propagation in cultured cells increases the risk of introducing compensatory mutations within the viral genome. Generation of stable trans-complementing cell culture systems for virus mutagenesis is not always possible because herpesviral genes are expressed at a defined stage of viral replication, at a certain level, and can even be toxic if expressed in the absence of other viral proteins. These drawbacks of conventional mutagenesis are even more dominant in the case of slowly replicating, highly cell-associated viruses, making it virtually impossible to transfer virus from trans-complementing to non-complementing cells. As the first step out of this

predicament, herpesviral genomes were cloned as overlapping cosmid clones in *E. coli*, which makes all the bacterial methods for sequence modification available, but is also prone to selective pressure, at least at the sites of recombination of the individual cosmids during virus reconstitution (15, 48, 57, 59). In the case of a replication-deficient virus reconstituted from cosmid clone, it is virtually impossible to discriminate between failure of cosmid recombination, a lack of trans-complementation, the essential nature of the manipulated sequence or any unwanted fatal second site mutations within viral sequences. As an improvement over cosmid cloning and a logical next step, a number of herpesviral genomes, including the VZV genome, were previously cloned as bacterial artificial chromosomes (BAC). Full-length viral DNA sequences can be maintained in *E. coli*, manipulated with targeted or random techniques, and finally mutant viruses are derived right after transfection of permissive cells (1, 5, 14, 32, 33, 40, 47, 49, 52, 53).

Herpesviral genomes range from approximately 100 to 300 kb in size and are densely packed with open reading frames totaling ~70 to ~220 genes. They also contain direct and indirect repeat sequences and sequence duplications (10, 31, 60). Having such optimized genomes also means that overlapping regulatory sequences are found within open reading frames, along with polycistronic transcription units, expression of multiple splice variants, anti-sense RNAs, and miRNA's (11, 12, 22, 26, 45, 46). To avoid collateral and spurious effects of herpesvirus mutagenesis, the need for minimal sequence modifications emerges. Such techniques, in addition to the desirable removal of previously introduced mini-F sequences that are necessary for maintenance in bacteria, should result in markerless modification or at least in modifications that will only result in the introduction of very small sequences, such as *frt* or *loxP* sites (59).

We here report on the generation of an infectious clone of the intensively characterized and fully sequenced VZV strain P-Oka, which served as the starting point for the generation of the widely used V-Oka vaccine strain (54). The infectious BAC was generated utilizing previously generated cosmid clones that were modified using Red recombination technique (39, 41, 64). A recently developed method that allows markerless modification of cloned DNA in *E. coli* was used to introduce a sequence duplication into the mini-F vector, which results in removal of all vector sequences upon virus reconstitution in eukaryotic cells (55). Finally mutants were generated that were unable to express the major tegument protein encoded by *ORF9*, which were unable to replicate unless the protein was provided *in trans*, indicating that this major regulatory and structural tegument protein is essential for VZV replication.

## 2.3. Material and Methods

**Viruses and Cells.** Wild-type P-Oka and mutant viruses were propagated and passaged in human melanoma cells (MeWo) grown Dulbecco's minimal essential medium (DMEM) or in minimal essential medium (MEM) containing, 10% fetal bovine serum (FCS) and a mixture of penicillin and streptomycin (Invitrogen). Virus was passaged and amplified by cocultivation of infected with uninfected cell at a ratio of 1/2 to 1/5. Virus stocks were frozen down in growth media supplemented with 8% DMSO and stored in liquid nitrogen.

**Construction of transfer vectors.** For construction of the mini-F transfer vector, plasmid pUC18 was PCR amplified with primers (5'-CTT CTA GAC ACG TGT TCG CTA CCT TAG GAC CGT TAT AGT TAC GAG TAA TCA TGG TCA TAG CTG TTT C-3' and 5'-TGT CTA GAA GCC GGC ACT CGA GCA CGT GTT CGC TAC CTT AGG ACC GTT ATA GTT ACG TCA CTG GCC GTC GTT TTA C-3'), cleaved with XbaI and re-ligated to derive p*Ceu*2. The 2.6 kb *Sal*I fragment of the

rightmost cosmid, pSpe23 (41), was ligated into the *Xba*I site of p*Ceu*2. The entire construct was amplified via inverse PCR using primers (5'-AGA GCT AGC GGA TAA AAG CGT ACT GTT TTT TAT T-3' and 5'-AGA GCT AGC CGG TGT ATG TTT TAA ATT TAT T-3') inserting an *Nhe*I restriction site between the polyA sites of *ORF64* and *ORF65*. The resulting plasmid was termed p*Ceu*2.6*Nhe* (Fig. 2.1A).

To introduce a *Nhe*I site into the mini-F vector pBeloBAC11 (New England Biolabs) and to remove its *cos* and *loxP* sequences, the mini-F plasmid was cleaved with SalI and the 6.4 kb fragment was ligated with the XhoI-treated oligo-homodimer of primer 5'-AGC CTC GAG CTA GCT CGA GGC TA-3'. The derived plasmid, pBelo*Nhe*, was cleaved with NheI and cloned into the *Nhe*I site of p*Ceu*2.6*Nh*e, resulting in recombinant plasmid pBelo-P-Oka-in (Fig. 2.1A).

**T**he pEP-P-Oka-DX-in transfer vector for insertion of duplicated sequences into the mini-F plasmid was generated as follows. First, a 1.7 kb *Bgl*II-*Sca*I-fragment was cloned via *Bam*HI/*Sma*I into pCU*Ceu* (56). The segment flanked by *Nru*I and *Eco*RI was replaced by a PCR product (5'-TAC GGA ATT CCG GAT GAG CAT TC-3' and 5'-CCC GGG ATC CTG CAG TCG ACA CGT GGC GCG CCT AGG TAT AAA TAC CTG TGA CGG AAG ATC AC-3') of the equivalent sequence extended with a multiple cloning site (*MCS*). Then, an *aphAI*-I-*Sce*I PCR product derived from pEPkan-S using primers (5'-GGC GCG CCG GCC AGT GTT ACA ACC AAT TAA CC-3'; 5'-TCG CGA TAA GCT CAT GGA GCG GCG TAA CCG TCG CAC AGG AAG GAC AGA GAT AGG GAT AAC AGG GTA ATC GAT TT-3'), which included a short duplication of pBeloBAC11 sequences, was inserted into a singular *Nru*I site (55), ultimately resulting in the universal transfer vector pEP*MCS*-in-Belo (Fig. 2.1C). A 1.6 kb PCR fragment of P-Oka (Primer: 5'-ACT AGT GCT TCT GCG CAC AAT GCC ACA G-3' and 5'-ACT AGT GAA CGG TAC TTC GCC GCC GCG C-3') was cloned into *Bln*I of the MCS to derive pEP-P-Oka-DX-in (Fig. 2.2).

**Figure 2.1.** Schematic of vector construction. A) pBelo-P-Oka-in. In a first step, recombinant plasmid pCeu2 was constructed by inverse PCR and self-ligation of pUC18 modifying the multiple cloning site (MCS). The 2.6 kb *Sal*I fragment of P-Oka was cloned into the engineered *Xba*I site. Another inverse PCR/ligation step was used to insert an *Nhe*I site close to the border of $IR_S$ and $U_S$ sequences. The mini-F replicon, pBelo*Nhe*, was linearized and cloned into the newly inserted *Nhe*I site. B) pSpe23-Belo. The mini-F replicon with adjoining flanks A and B was released from plasmid pBelo-P-Oka-in by cleavage with I-CeuI and inserted into pSpe23 via Red recombination (55). Subsequently, SuperCos sequences were removed by AscI digest and self-ligation. C) pEP*MCS*-in-Belo. The 1.7 kb *Bgl*II/*Sca*I fragment of pBeloBAC11 was cloned into pCU*Ceu* (56). A small portion of the pBelo sequence was replaced by a PCR product to introduce a multiple cloning site (*MCS*). A PCR was performed to add *Nae*I and *Nru*I sites and a small sequence duplication (arrowheads) to the *aphAI*-I-*Sce*I cassette. Cloning of that fragment into the *Nru*I site of the *MCS* resulted in the *en passant*-ready transfer vector pEP*MCS*-in-Belo. The pBelo flanks used for Red recombination with pBelo-derived BACs are indicated with striped bars.

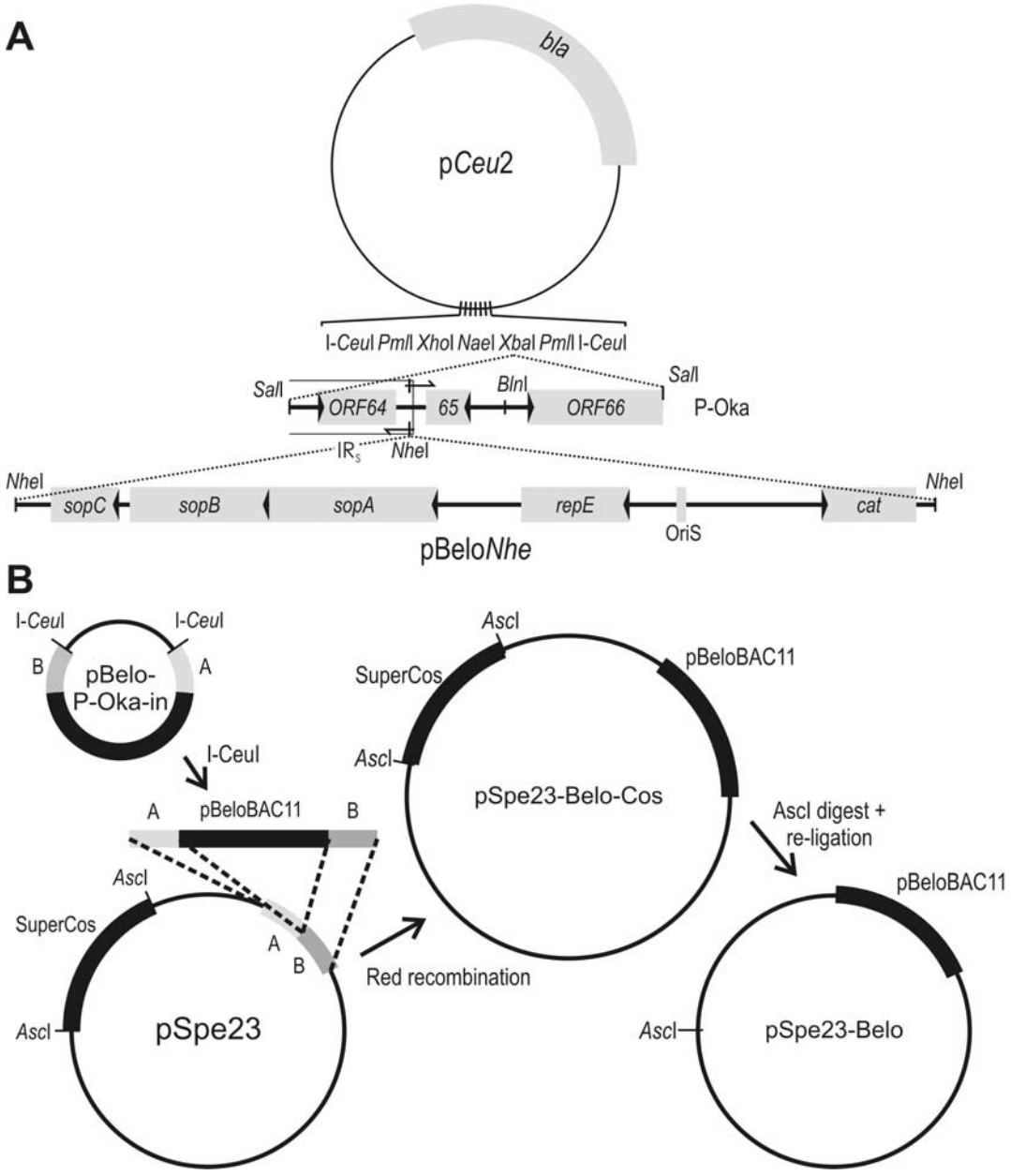
A
bla
pCeu2
I-CeuI PmlI XhoI NaeI XbaI PmlI I-CeuI
SalI
ORF64
65
BlnI
ORF66
SalI
P-Oka
IR5
NheI
NheI
sopC
sopB
sopA
repE
cat
NheI
OriS
pBeloNhe
B
I-CeuI
I-CeuI
B
pBelo-
P-Oka-in
A
I-CeuI
A
pBeloBAC11
B
AscI
SuperCos
A
B
AscI
pSpe23
Red recombination
AscI
SuperCos
pBeloBAC11
AscI
pSpe23-Belo-Cos
AscI digest +
re-ligation
pBeloBAC11
AscI
pSpe23-Belo

**Figure 2.1** (continued)

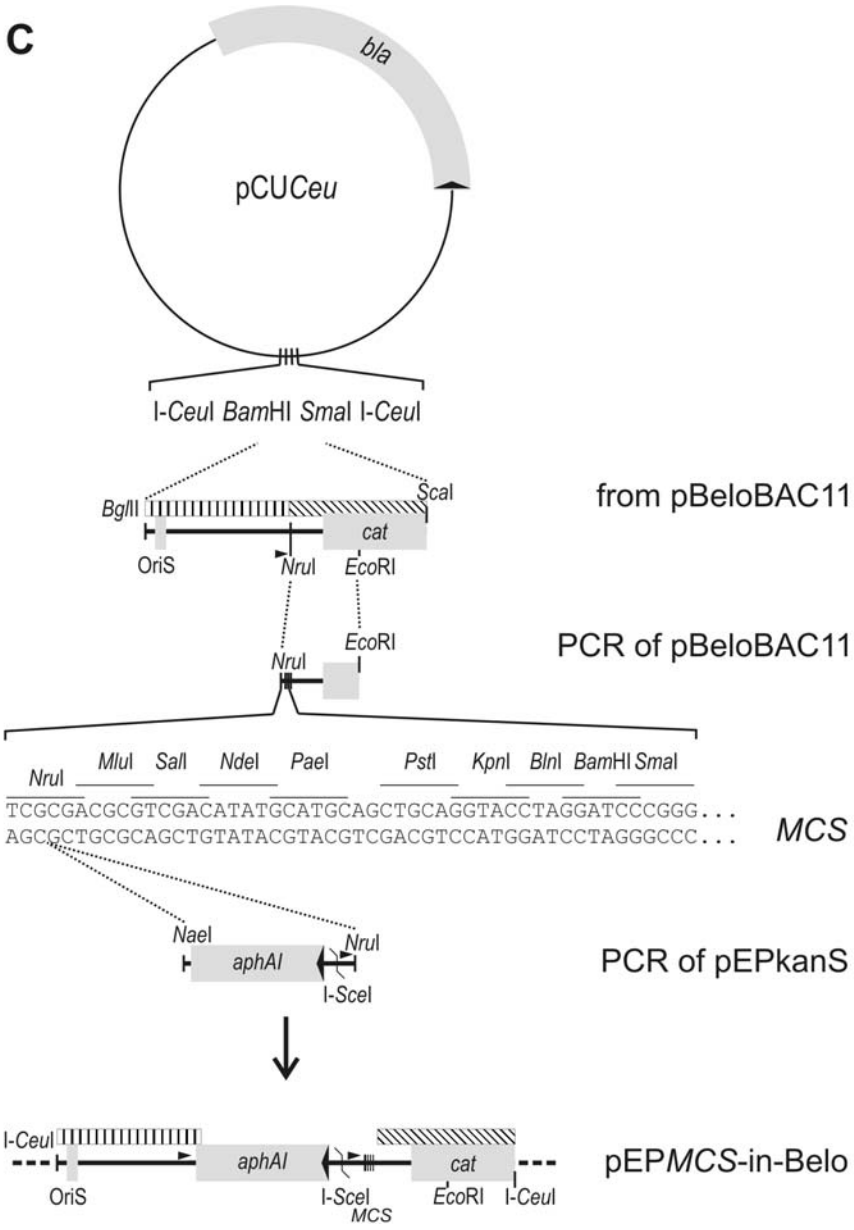

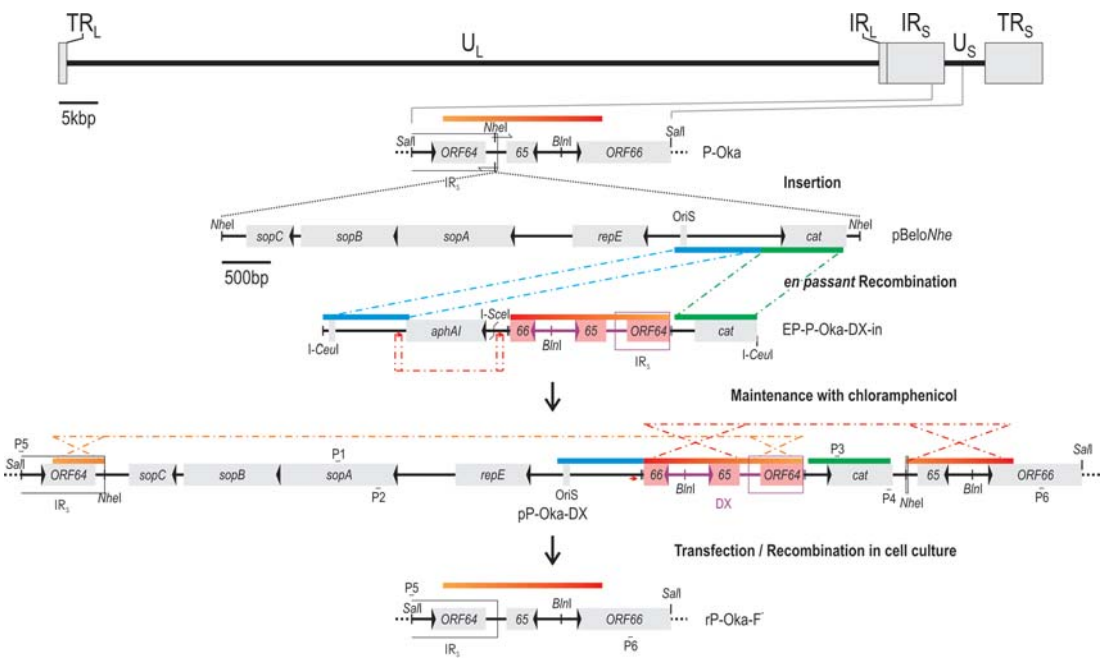


**Figure 2.2.** Insertion and self-excision of mini-F replicon. Schematic of the insertion of pBelo sequences between *ORF64* and *ORF65* (lines 1 to 3). A 1.6 kb sequence of P-Oka was inserted between the bacterial origin of replication ($Ori_S$) and *cat* to create an inverse duplication of VZV sequences adjoining the mini-F replicon. The orange-red gradient bar indicates such duplicate sequences and their orientation. Dotted lines indicate recombination events of identical sequences (same colored bars) for a first Red recombination and of short duplications (red arrow) for the removal of the kanamycin resistance gene *aphAI*. The BAC with duplicated sequences was termed pP-Oka-DX and maintained in *E. coli* under steady chloramphenicol selection. Upon transfection of MeWo cells, two anti-parallel recombination events (orange and red dotted lines) released mini-F sequences and resulted in rP-Oka-F¯. Primers P1 (5'-TTA ACT CAG TTT CAA TAC GGT GCA G-3') and P2 (5'-TGG GGT TTC TTC TCA GGC TAT C-3') were used to screen for presence of mini-F sequences, as well as P3 (5'-AGG CAT TTC AGT CAG TTG CTC-3') and P4 (5'-TGC CAC TCA TCG CAG TAC TG-3') for the presence of *cat*. The loss of the pBelo insert was detected utilizing primers P5 (5'-ATT GGA AGC GAC GTC GAC AC-3') and P6 (5'-TGT AAC GCG CGT AAT ACA GAT CG-3').

**Red recombination.** Red recombination was performed exactly as described earlier using *E. coli* strain EL250 harboring the respective cosmid or BAC DNA (27, 55). All primers used for mutagenesis were PAGE purified (Integrated DNA Technologies, IDT). To perform *en passant* mutagenesis, a linear DNA fragment (PCR products using pEPkan-S as a template or a linearized plasmids) was used to introduce a cassette of *aphAI*, an I-*Sce*I site and a short sequence duplication into the target sequence in a first step. The resulting intermediates were selected with 30 µg/ml kanamycin and 30 µg/ml chloramphenicol on agar plates. An I-SceI expressing plasmid (pBAD-*I-sceI*) was then introduced into EL250 harboring desired co-integrates, the expression of the homing endonuclease was induced with 0.5% arabinose, and a second Red recombination was performed. The loss of the *aphAI*-I-*Sce*I cassette was detected via replica plating, RFLP analysis and the identity of the introduced mutations was confirmed by nucleotide sequencing (55).

**Reconstitution of recombinant VZV from cosmid DNA.** Recombinant pP-Oka-derived VZV was reconstituted by transfecting human melonama (MeWo) cells with pSpe23-Belo and the three other cosmid clones pFsp73, pSpe14 and pPme2 using the CalPhos Mammalian Transfection Kit (Clontech) exactly as previously described (14, 41).

**Generation of *ORF9* mutants by *en passant* mutagenesis.** Primers 5'-TTT GGA TAT TTC ACG ACC CTA TCG TTT ATT TAC GTG CCG GCA TCT TCC GAC GGT GAT AGG GAT AAC AGG GTA ATC GAT TT-3' and 5'-TTA GAG CGA CAA AGT CTG TCA CCG TCG GAA GAT GCC GGC ACG TAA ATA AAC GAT AGG CCA GTG TTA CAA CCA ATT AAC C-3' were used to amplify the *aphAI*-I-*Sce*I cassette present in pEPkan-S. The pP-Oka9ΔM mutants resulting from the *en passant* procedure were analyzed by RFLP and sequencing (data not shown). Using primers 5'-TGG ATA TTT CAC GAC CCT ATC GTT TAT TTA CGT AAT

GGC TAG CTC CGA CGG TGA CAT AGG GAT AAC AGG GTA ATC GAT TT-3' and 5'-TGC ATT AGA GCG ACA AAG TCT GTC ACC GTC GGA GCT AGC CAT TAC GTA AAT AAA CGG CCA GTG TTA CAC CAA TTA ACC-3', a revertant clone from pP-OkaΔ*9*M termed pP-Oka9Mr was generated by *en passant* mutagenesis as well. The repaired *ORF9* encoded for the wild-type amino acid sequence, but harbored a *Nhe*I site close to its start codon, which allowed unequivocal identification via RFLP (Fig. 2.5A).

**Reconstitution of VZV from BAC DNA.** BAC DNA for transfections was prepared using affinity chromatography following the manufacturer's instructions (DNA Maxiprep system, Qiagen). Subsequently, MeWo cells were transfected with Lipofectamin 2000 (Invitrogen). Briefly, 1 to 4 μg BAC DNA were cotransfected with 200 ng pCMV62, a plasmid which contains the VZV IE gene ORF62 under the control of a CMV promoter (44). The DNA lipofectamin solution was added onto the cells in 1 ml of MEM and incubated for 4 h. Transfection medium was then replaced with MEM-10% FBS.

**Immunofluoescence.** Cells were fixed with 2% paraformaldehyde in PBS, permeabilized with 0.1% saponin, and blocked with 10% neonatal calf serum (NCS) in PBS. Primary antibodies, monoclonal anti-ORF62 antibody (Chemicon), monoclonal anti-gB antibody (US Biological), and ORF-9 polyclonal antibody (6) (a kind gift of Dr. William Ruyechan, SUNY Buffalo, NY), were each diluted 1:500 in PBS containing 10% NCS and 0.02% sodium azide. Secondary antibodies, including Alexa 568-conjugated goat anti-rabbit and Alexa 488-conjugated goat anti-mouse antibodies, were diluted 1:1,000 in PBS. Samples were examined under a fluorescence microscope and photographed with a digital camera (Zeiss Axiovert 25 and Axiocam).

**Multi-step growth kinetics.** Multi-step growth kinetics of P-Oka, rP-Oka, rP-Oka*9*ΔM and rP-Oka*9*Mr derived viruses were determined by inoculating $1x10^6$ MeWo cells with 100 plaque-forming units (pfu) of cell-associated virus. Infected cells were trypsinized on days 1, 2, 3, 4 and 5 and titrated by co-cultivation of 10-fold dilutions of trypsinized cells with fresh MeWo cells. Five days after co-seeding, viral plaques were stained by indirect immunofluorescence using anti-gB antibodies (US Biological) and counted, exactly as described elsewhere (56). All titer determinations were done in triplicate.

**Generation of recombinant baculoviruses expressing ORF9.** A shuttle plasmid for the generation of recombinant baculoviruses by Tn7 transposition was generated as described earlier (9). Briefly, the polyhedron promotor of the shuttle plasmid pFastBac1 (Invitrogen) was removed by digestion with SnaBI and HpaI and replaced with a 3.1 kb *Nru*I-*Bst*1107I fragment from pcDNA3, which contains the HCMV-IE promoter/enhancer, the multiple cloning site and polyadenylation signal followed by the simian virus 40 (SV40) promoter-neomycin phosphotransferase II expression cassette. The resulting plasmid was named pFastM. *ORF9* was inserted into the multiple cloning site of pFastM using *Bam*HI and *Xho*I restriction sites resulting in recombinant plasmid pFastM*ORF9*.

The expression cassette of pFastM*ORF9* was incorporated into the baculovirus genome by using Tn7 site-specific transposition according to the manufacturer's instructions for the Bac-to-Bac™ expression system (Invitrogen). Resulting bacmid DNA was purified and transfected into Sf9 cells using Cellfectin (Invitrogen). After incubation at 27°C for 4 days, the resulting recombinant baculovirus, bM*ORF9*, was propagated in Sf9 cells and viral titers were determined in a conventional plaque assay using neutral red agarose overlays (9). One milliliter of bM*ORF9*–containing supernatant was used for infection of MeWo cells seeded in 6-well-plates (25

pfu/cell). Incubation was allowed for 30 min at RT, centrifuged for 5 min at 200 x g, and finally 10 mM butyrate was added to the cells to facilitate transgene expression (9). After 4 h of incubation, cells were washed and 2 ml of DMEM-10% FBS was applied.

## 2.4. Results

**Generation of an infectious P-Oka BAC clone.** The generation of the P-Oka BAC was based on overlapping cosmid clones that had been established earlier (41). Mini-F vector sequences were inserted into one of the P-Oka cosmids via Red recombination. Briefly, the pSpe23 cosmid was electroporated into *E. coli* strain EL250 (27) and recombinant plasmid pBelo-P-Oka-in (Fig. 2.1B) was linearized with I-CeuI. The 9.4 kbp fragment containing linear mini-F sequence and sequences flanking the junction between the VZV internal repeat short ($IR_S$) and unique short ($U_S$) was electroporated into recombination-competent EL250 harboring pSpe23 (27, 55). Chloramphenicol resistant bacteria were selected and screened by restriction fragment length polymporphism (RFLP) analyses for correct insertion of the pBeloBac sequences into the rightmost P-Oka cosmid (data not shown). The derived construct, pSpe23-Belo-Cos, was cleaved with AscI to remove the SuperCos sequences and re-ligated resulting in pSpe23-Belo (Fig. 2.1B). The generated mini-F clone, which now was located within the rightmost P-Oka sequences, was transfected with the other overlapping cosmid clones to reconstitute a P-Oka virus mutant with the mini-F insertion. Total cellular and viral DNA isolated from MeWo cells infected with the P-Oka-BAC virus was cleaved with the enzymes AscI, which is unable to cleave P-Oka-BAC sequences, and λ exonuclease to digest cellular DNA. Remaining P-Oka-BAC DNA (pP-Oka) was precipitated and electroporated into EL250 cells. Bacteria

containing the full-length VZV genome were selected with chloramphenicol and screened by RFLP analysis (Fig. 2.3A).

**Reconstitution and characterization of recombinant pP-Oka-derived VZV.** In order to demonstrate that the insertion the mini-F sequence in the VZV genome did not have a detrimental effect on viral replication *in vitro*, recombinant rP-Oka was reconstituted from the full-length infectious clone (pP-Oka) and growth kinetics were determined. Human melanoma cells (MeWo) were transfected with pP-Oka clones by lipofection. Efficiency was increased by cotransfection with the pCMV62 plasmid (44). Transfected cells were analyzed by immunofluorescence microscopy to detect plaque formation as early as 4 days post transfection. Multi-step growth kinetics revealed that BAC derived rP-Oka exhibited growth properties that were virtually identical to those of parental, wild-type P-Oka virus (Fig. 2.3B). Therefore, neither the increased size of the viral genome nor the insertion of the mini-F sequences into the chosen genomic locus had measurable effects on viral replication.

**Self-excision of mini-F sequences upon rP-Oka reconstitution.** Mini-F sequences of pP-Oka were removed employing a stabilized inverse sequence duplication. The self-excision is based on the duplication within the mini-F of a VZV sequence that is present adjacent to the mini-F insertion site. The duplication was introduced between the origin of replication and the antibiotic resistance gene (Fig. 2.2) by first constructing an *en passant*-ready transfer construct, pEP-P-Oka-DX-in (43, 55) (Fig. 2.1C). A 4.5 kb I-*Ceu*I fragment was used to insert the 1.6 kb sequence duplication into mini-F sequences of pP-Oka via *en passant* mutagenesis in inverse orientation. The resulting BAC, pP-Oka-DX, was maintained in *E. coli* by standard chloramphenicol selection. The loss of vector sequences in *E. coli* through intramolecular recombination is prevented by the inverse orientation of the internal sequence duplication and its placement between the chloramphenicol resistance gene

**Figure 2.3.** Confirmation of P-Oka BAC. A) Southern Blot of P-Oka, pP-Oka, pP-Oka-DX, and rP-Oka-F$^-$. BAC DNA was prepared from *E. coli* harboring pP-Oka or pP-Oka-DX. MeWo cells were infected with the parental virus P-Oka or with the recombinant rP-Oka-F$^-$, harvested at >80% of infection, and total DNA was prepared. BAC DNA (10 μg) or viral DNA (20 μg) was digested with *Bam*HI or *Nco*I, separated on a 1% agarose gel, and transferred to a nylon membrane. VZV BAC specific bands were detected using random DIG-labeled (DIG DNA labeling kit, Roche) sonicated pP-Oka DNA. B) rP-Oka has growth kinetics that are very similar to those of wild-type P-Oka. Multi-step growth kinetics of P-Oka and rP-Oka were performed using MeWo cells. Means and standard deviations of three independent experiments are given.

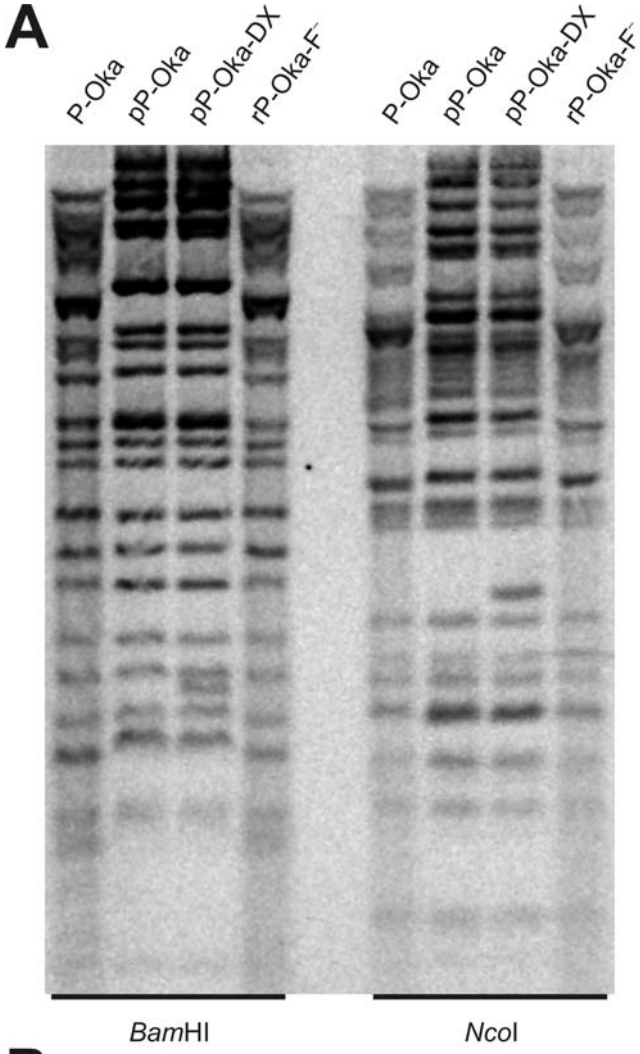
A
P-Oka
pP-Oka
pP-Oka-DX
rP-Oka-F
P-Oka
pP-Oka
pP-Oka-DX
rP-Oka-F
BamHI
NcoI
B
P-Oka
rP-Oka
pfu
10^6
10^5
10^4
10^3
10^2
0
40
t [h]
80
120

*cat* and the mini-F origin $Ori_S$ (data not shown). Also, recombination of the duplication and identical sequences present in the terminal repeat short ($TR_S$) would separate the resistance gene and the mini-F replicon, which would be lethal to the bacteria. Consequently, pP-Oka-DX was stable in *E. coli* due to the constant selective pressure for plasmid replication and chloramphenicol resistance.

After establishing stable maintenance of pP-Oka-DX in *E. coli*, MeWo cells were transfected with pP-Oka-DX. Since there is no positive selection for maintenance of the mini-F replicon or chloramphenicol resistance in eukaryotic cells, intra- and intermolecular recombination leading to removal of the chlorampenicol resistance gene, the mini-F replicon, and the duplicated sequences can take place. Reconstituted rP-Oka-$F^-$ virus reconstituted from the pP-Oka-DX BAC was passaged, harvested for DNA preparation, and the loss of the mini-F sequences was confirmed via PCR and sequencing (Fig. 2.2 and 2.4). After the first passage of rP-Oka-$F^-$ the absence of the pBeloBAC cassette was observed in the majority of genomes, but a small fraction of viral genomes still harbored *cat* or the mini-F replicon until passage 4. The rP-Oka-$F^-$ genome was also analyzed via Southern Blot analysis and its restriction enzyme pattern was indistinguishable from that of P-Oka DNA (Fig. 2.3A).

**Characterization of an *ORF9* deficient VZV mutant.** To create a P-Oka mutant unable to express ORF9 protein, the start codon of the corresponding open reading frame (*ORF9*) was inactivated by markerless *en passant* mutagenesis (55). A revertant was also generated in which the start codon was repaired and a *Nhe*I site was introduced to allow unequivocal identification of the revertant (Fig. 2.5A). MeWo cells were transfected with pP-Oka DNA, DNA of the start codon mutant pP-Oka9ΔM or the revertant pP-Oka9Mr to reconstitute the respective recombinant viruses (rP-Oka, rP-Oka9ΔM and rP-Oka9Mr). Upon reconstitution, rP-Oka9ΔM exhibited drastically decreased plaque sizes when compared to parental rP-Oka and the revertant

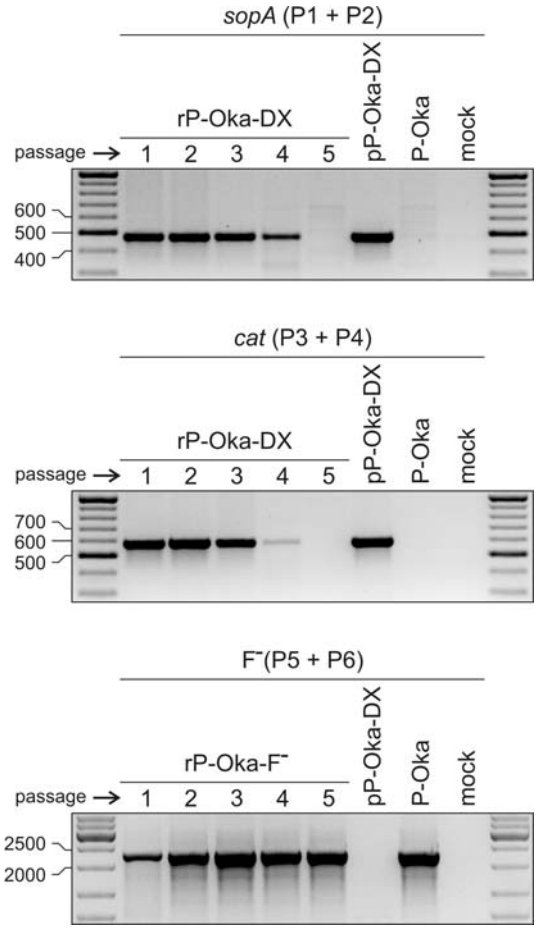


**Figure 2.4.** PCR analysis of mini-F self excision upon transfection. MeWo cells were transfected with pP-Oka-DX. Reconstituted virus was passaged by mixing infected and uninfected cells at a ratio of 1 to 5. DNA from virus passages was used to perform a PCR reaction with primers P1 and P2 (top panel) or P3 and P4 (middle panel) to detect remaining pBelo sequences in viruses reconstituted from pP-Oka-DX. Primers P5 and P6 were used to show the restoration of the P-Oka wild-type genomic organization in rP-Oka-F⁻ (see also Fig. 2.2). pP-Oka-DX DNA isolated from *E. coli* as well as total DNA of MeWo infected with P-Oka or uninfected MeWo cells were used as controls. Mini-F sequences are not detectable after 5 passages and in a significant portion of reconstituted virus the pBelo insert is lost right upon transfection.

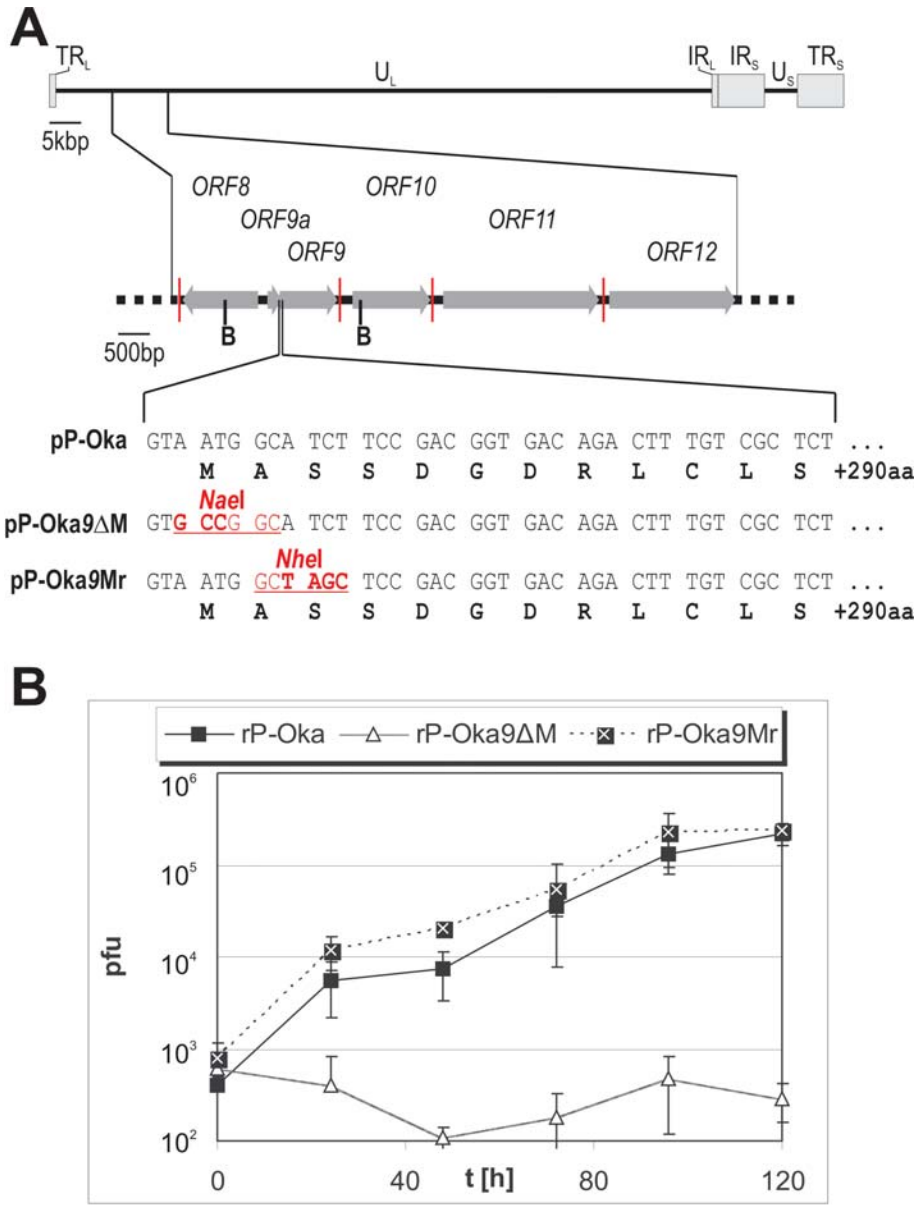


**Figure 2.5.** Growth properties of an ORF9-negative VZV. A) Genomic region of VZV *ORF9* with a focus on the aminoterminal sequence of *ORF9* is shown. The original nucleotide and amino acid sequences (black) are given, as are the mutations introduced in pP-Oka9ΔM and its revertant (lines 2 and 3). B) Multi-step growth kinetics of rP-Oka, rP-Oka9ΔM and rP-Oka9ΔMr. Kinetics were performed in triplicate and means and standard deviations are given.

virus pP-Oka*9*Mr (Fig. 2.6A). IF analysis using ORF9-specific polyclonal antibodies revealed that, as expected, rP-Oka*9*ΔM does not express ORF9 (Fig. 2.6A upper panel) (6). On the other hand, ORF62 could readily be detected in the parental, the *ORF9* deletion, and the revertant virus (Fig. 2.6A lower panel). In order to confirm the dramatic growth defect of rP-Oka*9*ΔM, multi-step growth kinetics were performed. In contrast to rP-Oka*9*ΔM whose growth curve stayed flat, the rP-Oka*9*Mr revertant virus, in which the start codon of *ORF9* had been repaired, grew with kinetics that were virtually indistinguishable from those of wild-type P-Oka and parental rP-Oka virus (Fig. 2.5B). Since rP-Oka*9*ΔM showed no replication that would be sufficient for virus propagation leading to self excision of mini-F sequences, characterization of ORF9 was performed using recombinant viruses still harboring pBeloBAC sequences.

To confirm that the impaired growth was only due to the lack of *ORF9* expression, we used baculovirus mediated gene delivery to complement growth of rP-OkaΔ*9*M. Baculoviruses have been shown to be an effective vehicle for introduction of DNA sequences into mammalian cells since they neither replicate nor cause cytopathic effects (24). MeWo cells were transfected with pP-OkaΔ*9*M DNA and infected at 1, 2, 3, 4 or 5 days post-transfection with a recombinant baculovirus expressing *ORF9* under the control of the HCMV-IE promoter. After BAC transfection and baculovirus infection, cells were analyzed via immunofluorescence using anti-gB and anti-ORF9 antibodies at day 7 post transfection (6). The *trans*-complementation via baculoviruses at days 1, 2 and 3 post transfection resulted in replication, and, consequently, significantly increased plaque sizes of rP-OkaΔ*9*M (Fig. 2.6B).

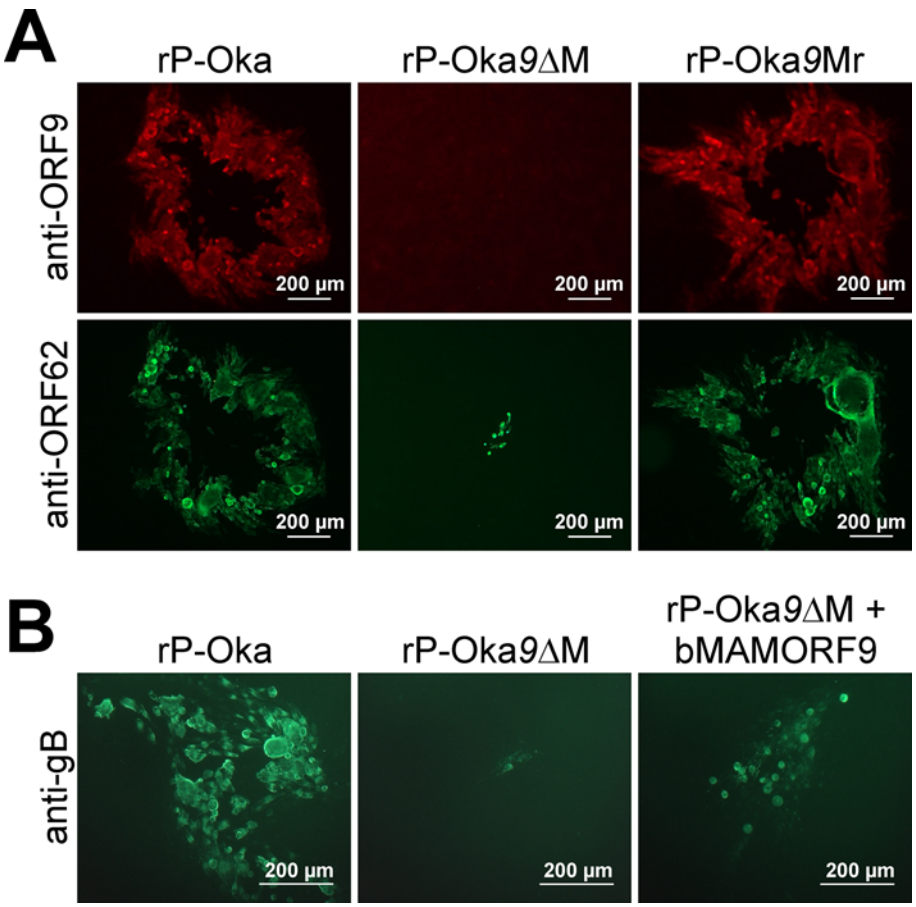


**Figure 2.6.** Immunofluorescence analysis and trans-complementation via baculovirus mediated gene transfer. A) Plaque analysis of rP-Oka (left panels), rP-Oka*9*ΔM (middle panels) and rP-Oka*9*Mr (right panels). Plaques were analyzed by indirect immunofluorescence using anti-ORF9 polyclonal (6) and anti-ORF62 monoclonal antibodies (Chemicon, USA) at day 7 post transfection. B) Plaque analysis of rP-Oka (left panel), rP-Oka*9*ΔM (middle panel) and rP-Oka*9*ΔM rescued with baculovirus gene delivery at day 2 post transfection (right panel). Plaques were analyzed via indirect immunofluorescence using anti-gB monoclonal antibody (US Scientific, USA) at day 7 post transfection.

## 2.5. Discussion

In this study we demonstrated that the generation of a full-length bacterial artificial chromosome (BAC) directly from overlapping cosmid clones is possible. We could show that Red mutagenesis proved an efficient means to transfer a second bacterial origin of replication, here the mini-F replicon, into a pre-existing cosmid clone. Having the BAC cassette within viral sequences ahead of virus reconstitution from the cosmids produces VZV BAC genomes without the need of (mostly inefficient) selection in cell culture. Furthermore, removal of contaminating cellular chromosomal DNA from BAC DNA using restriction enzyme cleavage and λ exonuclease digestion before electroporation of the infectious VZV genome into *E. coli* was found to be more efficient than standard methods of DNA preparation (33, 49). The strategy as described here, therefore, has the potential to be widely applicable for the cloning of herpesvirus genomes from already established cosmid clone systems, particularly with regard to highly cell-associated viruses.

Whenever bacterial sequences are used to manipulate viral genomes, the overall effect of introduced, foreign sequence scars, like the mini-F cassette itself, for viral replication is not predictable. The newly developed system applying an inversely oriented sequence duplication between the selection marker (antibiotic resistance gene) and the bacterial replicon allows stable maintainenance of the herpesviral genome in *E. coli*. It also presents an *in cis* tool to remove the mini-F cassette upon transfection. In the particular case described here, four passages in cultured cells were required to completely remove mini-F sequences from recombinant genomes as assayed by PCR. The highly cell-associated nature and slow replication kinetics of VZV, which could account for polyclonal growth of VZV within the same infected cell, could be one possible explanation for the maintenance of a few mini-F containing

genomes in the first few cell culture passages. In addition, the lack of a growth advantage of recombinant virus devoid of mini-F sequences (rP-Oka-F$^-$) over viruses still carrying vector (rP-Oka-DX) could also contribute to the detection of mini-F sequences until passage 4. Placing mini-F sequences within a gene that is essential for virus replication or using the developed methodology in faster replicating viruses producing cell-free infectivity would increase the efficiency of self excision of vector sequences (Wussow and Tischer, unpublished data). The combination of the VZV-BAC clone at hand, the established techniques to perform markerless mutagenesis in *E. coli*, and the construction of a self-excisable BAC allows the creation of clonal virus progeny with minimal sequence modification.

Similar to the situation in MDV, the generation of the full length P-Oka BAC clone, from the already established system of overlapping cosmid clones, allowed us to address genes that likely were crucial for VZV growth in cell culture. We were able to characterize the role of *ORF9* in VZV replication. Immunofluorescence analyses of rP-OkaΔ9M with an ORF9 specific moloclonal antibody showed the lack of ORF9 production in infected cells, which were, however, reactive with an anti-ORF62 antibody. The repair of the ORF9 start codon restored ORF9 expression as well as virus growth in cell culture to levels observed with parental virus (Fig. 2.6A). Complementation via baculovirus-mediated gene delivery was also able to rescue productive viral replication. These results clearly demonstrated that *ORF9* is essential for productive replication of VZV in cell culture, as is the case for MDV but unlike the situation in related human or animal alphaherpesviruses (13, 17, 18, 28). That supports the theory that highly cell-associated alphaherpesviruses mainly utilize the UL49-gE/gI pathway to spread from cell to cell, whereas the loss of the UL49 homologue in herpesviruses that produce cell-free virions is less crucial for virus propagation. The characterization of UL49 negative mutants with less cell associated viruses allows the

analysis of other, nonstructural functions of that tegument protein as well (51, 62), while with VZV and MDV such a detailed characterization would required a very detailed dissection of respective functional domains. In addition, the highly cell-associated nature of VZV makes it virtually impossible to work with phenotypically rescued mutant viruses because such viruses cannot be purified from trans-complementing cells.

Complementation of rP-OkaΔ9M with the baculovirus expression system, however, was able to restore virus growth and significantly increase plaque sizes, albeit not to the level of wild-type or revertant viruses. One explanation for the failure to completely restore VZV growth is that baculovirus mediated gene expression decreases with time; therefore, the amounts of ORF9 produced may not be sufficient at the end of the experiment. Another reason might be that relatively low doses of recombinant baculovirus (MOI=25) were used, which resulted in the absence of *ORF9* expression in a subset of cells limiting the availability of ORF9 for replication of rP-OkaΔ9M. Low MOI infection was chosen to prevent overexpression of *ORF9*, which had been shown to lead to cytotoxic effects and likely is one of the reasons for the failure to generate permanent cell lines (Kaufer, Tischer and Osterrieder, unpublished observations). Another explanation might be that *ORF9* expression is controlled by the strong HCMV-IE promoter. This promoter is constitutively active and transgene expression, therefore, cannot be modulated during the course of infection by virus-encoded transcription factors as is the case during regular VZV infection. Constant, not synchronized, high-level expression of *ORF9* may be detrimental to virus replication as has been suggested in the MDV system (16, 17).

In summary, we have generated an infectious herpesvirus (VZV) BAC clone from overlapping pieces of cloned viral DNA. Advances of focused and minimal sequence modification in bacteria allowed characterization of the essential nature of ORF9 of

the highly cell associated herpesvirus VZV for *in vitro* replication. The established methodology is likely applicable to many other (herpes)viruses and has the advantage that the initial cloning step is independent of virus replication and that no selective pressure is applied because cosmid clones are usually derived from viral DNA packaged in nucleocapsids. Employing an inverse sequence duplication in the infectious BAC for *cis*-recombination allowed scarless self-excision of the mini-F replicon, which is not only important for the generation of viruses and mutants free of foreign sequences, but also represents an important step forward with respect to recombineering of viral sequences in eukaryotic cells. In addition, since cosmid and mini-F plasmid origins of replication can be maintained in the same bacterial cell as demonstrated here, successive assembly of a full-length viral mini-F clone from overlapping cosmid clones in bacteria applying Red recombination seems feasible and is currently being attempted. Viral genome assembly would avoid a eukaryotic stage in the generation of an infectious clone and be obtained without applying any positive or negative selection on the viral genomes.

### 2.6. Acknowledgments

The expert technical assistance of Neil G. Margulis is greatly appreciated. We thank Paul Kinchington, University of Pittsburgh, for providing the pCMV62 plasmid and William Ruyechan, SUNY Buffalo, for the anti-ORF9 antibodies. The study was supported by PHS grant 1R21AI061412 to NO. FW was funded by a grant from the Medical Faculty of Christian-Albrecht University of Kiel (Research Center Integrative Neurobiology). We thank Helmut Fickenscher for inspiring discussions and careful perusal of the manuscript.

REFERENCES


1. **Adler, H., M. Messerle, M. Wagner, and U. H. Koszinowski**. 2000. Cloning and mutagenesis of the murine gammaherpesvirus 68 genome as an infectious bacterial artificial chromosome. J. Virol. **74**:6964-6974.

2. **Arvin, A. M.** 2006. Investigations of the pathogenesis of Varicella zoster virus infection in the SCIDhu mouse model. Herpes. **13**:75-80.

3. **Balan, P., N. Davis-Poynter, S. Bell, H. Atkinson, H. Browne, and T. Minson**. 1994. An analysis of the in vitro and in vivo phenotypes of mutants of herpes simplex virus type 1 lacking glycoproteins gG, gE, gI or the putative gJ. J. Gen. Virol. **75 ( Pt 6)**:1245-1258.

4. **Berarducci, B., M. Ikoma, S. Stamatis, M. Sommer, C. Grose, and A. M. Arvin**. 2006. Essential functions of the unique N-terminal region of the varicella-zoster virus glycoprotein E ectodomain in viral replication and in the pathogenesis of skin infection. J. Virol. **80**:9481-9496.

5. **Borst, E. M., G. Hahn, U. H. Koszinowski, and M. Messerle**. 1999. Cloning of the human cytomegalovirus (HCMV) genome as an infectious bacterial artificial chromosome in Escherichia coli: a new approach for construction of HCMV mutants. J. Virol. **73**:8320-8329.

6. **Cilloniz, C., W. Jackson, C. Grose, D. Czechowski, J. Hay, and W. T. Ruyechan**. 2007. The varicella-zoster virus (VZV) ORF9 protein interacts with the IE62 major VZV transactivator. J. Virol. **81**:761-774.

7. **Cohen, J. I.** 1996. Varicella-zoster virus. The virus. Infect. Dis. Clin. North Am. **10**:457-468.

8. **Cohen, J. I. and H. Nguyen**. 1997. Varicella-zoster virus glycoprotein I is essential for growth of virus in Vero cells. J. Virol. **71**:6913-6920.

9. **Condreay, J. P., S. M. Witherspoon, W. C. Clay, and T. A. Kost**. 1999. Transient and stable gene expression in mammalian cells transduced with a recombinant baculovirus vector. Proc. Natl. Acad. Sci. USA **96**:127-132.

10. **Davison, A. J.** 2002. Evolution of the herpesviruses. Vet. Microbiol. **86**:69-88.

11. **Davison, A. J., D. J. Dargan, and N. D. Stow**. 2002. Fundamental and accessory systems in herpesviruses. Antiviral Res. **56**:1-11.

12. **Davison, A. J. and J. E. Scott**. 1986. The complete DNA sequence of varicella-zoster virus. J. Gen. Virol. **67 ( Pt 9)**:1759-1816.

13. **del Rio, T., H. C. Werner, and L. W. Enquist**. 2002. The pseudorabies virus VP22 homologue (UL49) is dispensable for virus growth in vitro and has no effect on virulence and neuronal spread in rodents. J. Virol. **76**:774-782.

14. **Delecluse, H. J., T. Hilsendegen, D. Pich, R. Zeidler, and W. Hammerschmidt**. 1998. Propagation and recovery of intact, infectious Epstein-Barr virus from prokaryotic to human cells. Proc. Natl. Acad. Sci. USA **95**:8245-8250.

15. **DeLuca, N. A. and P. A. Schaffer**. 1985. Activation of immediate-early, early, and late promoters by temperature-sensitive and wild-type forms of herpes simplex virus type 1 protein ICP4. Mol. Cell Biol. **5**:1997-2008.

16. **Dorange, F., S. El Mehdaoui, C. Pichon, P. Coursaget, and J. F. Vautherot**. 2000. Marek's disease virus (MDV) homologues of herpes simplex virus type 1 UL49 (VP22) and UL48 (VP16) genes: high-level expression and characterization of MDV-1 VP22 and VP16. J. Gen. Virol. **81**:2219-2230.

17. **Dorange, F., B. K. Tischer, J. F. Vautherot, and N. Osterrieder**. 2002. Characterization of Marek's disease virus serotype 1 (MDV-1) deletion mutants that lack UL46 to UL49 genes: MDV-1 UL49, encoding VP22, is indispensable for virus growth. J. Virol. **76**:1959-1970.

18. **Elliott, G., W. Hafezi, A. Whiteley, and E. Bernard**. 2005. Deletion of the herpes simplex virus VP22-encoding gene (UL49) alters the expression, localization, and virion incorporation of ICP0. J. Virol. **79**:9735-9745.

19. **Fuchs, W., H. Granzow, B. G. Klupp, M. Kopp, and T. C. Mettenleiter**. 2002. The UL48 tegument protein of pseudorabies virus is critical for intracytoplasmic assembly of infectious virions. J. Virol. **76**:6729-6742.

20. **Fuchs, W., H. Granzow, and T. C. Mettenleiter**. 2003. A pseudorabies virus recombinant simultaneously lacking the major tegument proteins encoded by the UL46, UL47, UL48, and UL49 genes is viable in cultured cells. J. Virol. **77**:12891-12900.

21. **Fuchs, W., B. G. Klupp, H. Granzow, C. Hengartner, A. Brack, A. Mundt, L. W. Enquist, and T. C. Mettenleiter**. 2002. Physical interaction between envelope glycoproteins E and M of pseudorabies virus and the major tegument protein UL49. J. Virol. **76**:8208-8217.

22. **Gomi, Y., H. Sunamachi, Y. Mori, K. Nagaike, M. Takahashi, and K. Yamanishi**. 2002. Comparison of the complete DNA sequences of the Oka varicella vaccine and its parental virus. J. Virol. **76**:11447-11459.

23. **Grose, C. and T. I. Ng**. 1992. Intracellular synthesis of varicella-zoster virus. J. Infect. Dis. **166 Suppl 1**:S7-12.

24. **Hu, Y. C., C. T. Tsai, Y. J. Chang, and J. H. Huang**. 2003. Enhancement and prolongation of baculovirus-mediated expression in mammalian cells: focuses on strategic infection and feeding. Biotechnol. Prog. **19**:373-379.

25. **Kimura, H., S. E. Straus, and R. K. Williams**. 1997. Varicella-zoster virus glycoproteins E and I expressed in insect cells form a heterodimer that requires the N-terminal domain of glycoprotein I. Virology **233**:382-391.

26. **Krause, P. R., K. D. Croen, S. E. Straus, and J. M. Ostrove**. 1988. Detection and preliminary characterization of herpes simplex virus type 1 transcripts in latently infected human trigeminal ganglia. J. Virol. **62**:4819-4823.

27. **Lee, E. C., D. Yu, J. Martinez de Velasco, L. Tessarollo, D. A. Swing, Court DL, N. A. Jenkins, and N. G. Copeland**. 2001. A highly efficient Escherichia coli-based chromosome engineering system adapted for recombinogenic targeting and subcloning of BAC DNA. Genomics **73**:56-65.

28. **Liang, X., B. Chow, Y. Li, C. Raggo, D. Yoo, S. ttah-Poku, and L. A. Babiuk**. 1995. Characterization of bovine herpesvirus 1 UL49 homolog gene and product: bovine herpesvirus 1 UL49 homolog is dispensable for virus growth. J. Virol. **69**:3863-3867.

29. **Mallory, S., M. Sommer, and A. M. Arvin**. 1997. Mutational analysis of the role of glycoprotein I in varicella-zoster virus replication and its effects on glycoprotein E conformation and trafficking. J. Virol. **71**:8279-8288.

30. **Mallory, S., M. Sommer, and A. M. Arvin**. 1998. Analysis of the glycoproteins I and E of varicella-zoster virus (VZV) using deletional mutations of VZV cosmids. J. Infect. Dis. **178 Suppl 1**:S22-S26.

31. **McGeoch, D. J., F. J. Rixon, and A. J. Davison**. 2006. Topics in herpesvirus genomics and evolution. Virus Res. **117**:90-104.

32. **McGregor, A. and M. R. Schleiss**. 2001. Molecular cloning of the guinea pig cytomegalovirus (GPCMV) genome as an infectious bacterial artificial chromosome (BAC) in Escherichia coli. Mol. Genet. Metab **72**:15-26.

33. **Messerle, M., I. Crnkovic, W. Hammerschmidt, H. Ziegler, and U. H. Koszinowski**. 1997. Cloning and mutagenesis of a herpesvirus genome as an infectious bacterial artificial chromosome. Proc. Natl. Acad. Sci. USA **94**:14759-14763.

34. **Mettenleiter, T. C.** 2002. Herpesvirus assembly and egress. J. Virol. **76**:1537-1547.

35. **Mettenleiter, T. C.** 2006. Intriguing interplay between viral proteins during herpesvirus assembly or: the herpesvirus assembly puzzle. Vet. Microbiol. **113**:163-169.

36. **Mettenleiter, T. C., B. G. Klupp, and H. Granzow**. 2006. Herpesvirus assembly: a tale of two membranes. Curr. Opin. Microbiol. **9**:423-429.

37. **Mijnes, J. D., L. M. van der Horst, A. E. van, M. C. Horzinek, P. J. Rottier, and R. J. de Groot**. 1996. Biosynthesis of glycoproteins E and I of feline herpesvirus: gE-gI interaction is required for intracellular transport. J. Virol. **70**:5466-5475.

38. **Moffat, J., C. Mo, J. J. Cheng, M. Sommer, L. Zerboni, S. Stamatis, and A. M. Arvin**. 2004. Functions of the C-terminal domain of varicella-zoster virus glycoprotein E in viral replication in vitro and skin and T-cell tropism in vivo. J. Virol. **78**:12406-12415.

39. **Murphy, K. C.** 1998. Use of bacteriophage lambda recombination functions to promote gene replacement in Escherichia coli. J. Bacteriol. **180**:2063-2071.

40. **Nagaike, K., Y. Mori, Y. Gomi, H. Yoshii, M. Takahashi, M. Wagner, U. Koszinowski, and K. Yamanishi**. 2004. Cloning of the varicella-zoster virus genome as an infectious bacterial artificial chromosome in Escherichia coli. Vaccine **22**:4069-4074.

41. **Niizuma, T., L. Zerboni, M. H. Sommer, H. Ito, S. Hinchliffe, and A. M. Arvin**. 2003. Construction of varicella-zoster virus recombinants from parent Oka cosmids and demonstration that ORF65 protein is dispensable for infection of human skin and T cells in the SCID-hu mouse model. J. Virol. **77**:6062-6065.

42. **Olson, J. K. and C. Grose**. 1998. Complex formation facilitates endocytosis of the varicella-zoster virus gE:gI Fc receptor. J. Virol. **72**:1542-1551.

43. **Osterrieder, N., J. P. Kamil, D. Schumacher, B. K. Tischer, and S. Trapp**. 2006. Marek's disease virus: from miasma to model. Nat. Rev. Microbiol. **4**:283-294.

44. **Perera, L. P., J. D. Mosca, W. T. Ruyechan, and J. Hay**. 1992. Regulation of varicella-zoster virus gene expression in human T lymphocytes. J. Virol. **66**:5298-5304.

45. **Pfeffer, S., M. Zavolan, F. A. Grasser, M. Chien, J. J. Russo, J. Ju, B. John, A. J. Enright, D. Marks, C. Sander, and T. Tuschl**. 2004. Identification of virus-encoded microRNAs. Science **304**:734-736.

46. **Roizman, B., T. Kristie, J. L. McKnight, N. Michael, P. Mavromara-Nazos, and D. Spector**. 1988. The trans-activation of herpes simplex virus gene

expression: comparison of two factors and their cis sites. Biochimie **70**:1031-1043.

47. **Rudolph, J. and N. Osterrieder**. 2002. Equine herpesvirus type 1 devoid of gM and gp2 is severely impaired in virus egress but not direct cell-to-cell spread. Virology **293**:356-367.

48. **Schaffer, P. A., S. K. Weller, B. A. Pancake, and D. M. Coen**. 1984. Genetics of herpes simplex virus. J. Invest Dermatol. **83**:42s-47s.

49. **Schumacher, D., B. K. Tischer, W. Fuchs, and N. Osterrieder**. 2000. Reconstitution of Marek's disease virus serotype 1 (MDV-1) from DNA cloned as a bacterial artificial chromosome and characterization of a glycoprotein B-negative MDV-1 mutant. J. Virol. **74**:11088-11098.

50. **Schumacher, D., B. K. Tischer, S. M. Reddy, and N. Osterrieder**. 2001. Glycoproteins E and I of Marek's disease virus serotype 1 are essential for virus growth in cultured cells. J. Virol. **75**:11307-11318.

51. **Sciortino, M. T., B. Taddeo, M. Giuffre-Cuculletto, M. A. Medici, A. Mastino, and B. Roizman**. 2007. Replication competent herpes simplex virus 1 isolates selected from cells transfected with a BAC-DNA lacking solely the UL49 gene vary with respect to the defect in the UL41 gene encoding the host shutoff RNase. J. Virol.

52. **Smith, G. A. and L. W. Enquist**. 1999. Construction and transposon mutagenesis in Escherichia coli of a full-length infectious clone of pseudorabies virus, an alphaherpesvirus. J. Virol. **73**:6405-6414.

53. **Suter, M., A. M. Lew, P. Grob, G. J. Adema, M. Ackermann, K. Shortman, and C. Fraefel**. 1999. BAC-VAC, a novel generation of (DNA) vaccines: A bacterial artificial chromosome (BAC) containing a replication-competent, packaging-defective virus genome induces protective immunity against herpes simplex virus 1. Proc. Natl. Acad. Sci. USA **96**:12697-12702.

54. **Takahashi, M., T. Otsuka, Y. Okuno, Y. Asano, and T. Yazaki**. 1974. Live vaccine used to prevent the spread of varicella in children in hospital. Lancet **2**:1288-1290.

55. **Tischer, B. K., J. von Einem, B. Kaufer, and N. Osterrieder**. 2006. Two-step red-mediated recombination for versatile high-efficiency markerless DNA manipulation in Escherichia coli. Biotechniques **40**:191-197.

56. **Trapp, S., M. S. Parcells, J. P. Kamil, D. Schumacher, B. K. Tischer, P. M. Kumar, V. K. Nair, and N. Osterrieder**. 2006. A virus-encoded telomerase RNA promotes malignant T cell lymphomagenesis. J. Exp. Med. **203**:1307-1317.

57. **van, Z. M., W. Quint, J. Briaire, R. T. de, A. Gielkens, and A. Berns**. 1988. Regeneration of herpesviruses from molecularly cloned subgenomic fragments. J. Virol. **62**:2191-2195.

58. **von Einem, J., D. Schumacher, D. J. O'Callaghan, and N. Osterrieder**. 2006. The alpha-TIF (VP16) homologue (ETIF) of equine herpesvirus 1 is essential for secondary envelopment and virus egress. J Virol **80**:2609-2620.

59. **Wagner, M., Z. Ruzsics, and U. H. Koszinowski**. 2002. Herpesvirus genetics has come of age. Trends Microbiol. **10**:318-324.

60. **Wang, N., P. F. Baldi, and B. S. Gaut**. 2006. Phylogenetic analysis, genome evolution and the rate of gene gain in the Herpesviridae. Mol. Phylogenet. Evol.

61. **Weinheimer, S. P., B. A. Boyd, S. K. Durham, J. L. Resnick, and D. R. O'Boyle**. 1992. Deletion of the VP16 open reading frame of herpes simplex virus type 1. J. Virol. **66**:258-269.

62. **Yedowitz, J. C., A. Kotsakis, E. F. Schlegel, and J. A. Blaho**. 2005. Nuclear localizations of the herpes simplex virus type 1 tegument proteins VP13/14, vhs, and VP16 precede VP22-dependent microtubule reorganization and VP22 nuclear import. J. Virol. **79**:4730-4743.

63. **Yoshitake, N., X. Xuan, and H. Otsuka**. 1997. Identification and characterization of bovine herpesvirus-1 glycoproteins E and I. J. Gen. Virol. **78 ( Pt 6)**:1399-1403.

64. **Zhang, Y., F. Buchholz, J. P. Muyrers, and A. F. Stewart**. 1998. A new logic for DNA engineering using recombination in Escherichia coli. Nat. Genet. **20**:123-128.

65. **Zuckermann, F. A., T. C. Mettenleiter, C. Schreurs, N. Sugg, and T. Ben Porat**. 1988. Complex between glycoproteins gI and gp63 of pseudorabies virus: its effect on virus replication. J. Virol. **62**:4622-4626.

# CHAPTER THREE

## Varicella-Zoster Virus (VZV) ORFS/L is Required for Efficient Viral Replication and Contains an Element Critical For DNA Cleavage and Packaging

**Benedikt B. Kaufer, Benjamin Smejkal, Nikolaus Osterrieder**. Varicella-Zoster Virus (VZV) ORFS/L is Required for Efficient Viral Replication and Contains an Element Critical For DNA Cleavage and Packaging.
Submitted to Journal of Virology 2010

## 3.1. Abstract

The genome of varicella-zoster virus (VZV), a human alphaherpesvirus, consists of two unique regions, unique long ($U_L$) and unique short ($U_S$), each of which is flanked by inverted repeats. During replication, four isomers of the viral DNA are generated, which are distinguished by the relative orientations of $U_L$ and $U_S$. VZV virions predominantly package two isomeric forms of the genome that have a fixed orientation of the $U_L$. ORFS/L, an open reading frame (ORF) with unknown function is located at the extreme terminus of $U_L$, directly adjacent to the a-like sequences, which are known to be involved in cleavage and packaging of viral DNA. We demonstrate here that ORFS/L localizes to the Golgi network in infected and transfected cells. Furthermore, we were able to demonstrate that deletion of the complete ORFS/L gene is lethal, while retention of the N-terminal 28 amino acids resulted in viable virus. The growth defect was only partially attributable to the expression of the ORFS/L product, suggesting that the 5′ region of ORFS/L contains a sequence element crucial for cleavage/packaging of viral DNA. Consequently, mutations introduced into the 5′ region of ORFS/L resulted in a defect in DNA cleavage, indicating that the region is indeed involved in processing of viral DNA. Since the sequence element has no counterpart on the opposite end of $U_L$, our results provide an explanation for the almost exclusive orientation of the $U_L$ seen in packaged VZV DNA.

## 3.2. Introduction

Varicella-zoster virus (VZV), also known as *Human herpesvirus 3* is a highly cell-associated human alphaherpesvirus that causes chicken pox (varicella) upon infection of naïve individuals (2). During primary infection, VZV is able to establish latency in cranial nerves as well as dorsal root and autonomic ganglia, where it remains dormant until a reactivation event occurs (8). Reactivation of VZV occurs primarily in the elderly or immunocompromised individuals and results in the development of shingles (herpes zoster), which is often associated with severe pain and postherpetic neuralgia (1).

The VZV genome, the smallest among the human herpesviruses, is approximately 125 kbp in size and encodes at least 70 unique open reading frames (ORFs) (1). As has been reported for all alphaherpesviruses, the VZV genome consists of two unique regions, the unique long ($U_L$) and unique short ($U_S$) segment, each flanked by inverted repeat regions ($TR_L$, $IR_L$, $TR_S$, $IR_S$) (6). In contrast to herpes simplex virus type 1 (HSV-1), the prototype alphaherpesvirus, VZV contains only very short repeats (88 bp) on either end of the $U_L$ (5). During alphaherpesvirus replication, four isomers of viral DNA are generated, which can be distinguished by the orientation of $U_L$ and $U_S$ relative to each other. While all four possible isomers of HSV-1 DNA are represented in the virion as equimolar populations, virions produced by VZV and other members of the genus *Varicellovirus*, such as equine herpesvirus type 1 (EHV-1), predominantly contain only two isomeric forms of the genome (5, 7, 9, 13, 21). Southern blot analysis of VZV virion DNA demonstrated that inversion of the $U_L$ region is rare (about 5%) (5) and could also be attributed to a rare circular configuration of the genome within the virion (12). A previous report on EHV-1 suggested that inversion of the $U_L$ region in infected cells is common, but that

packaging occurs in a directional manner (21). For both VZV and EHV-1, the reason for the more or less exclusive orientation of the $U_L$ is unknown.

The organization of the VZV genome is similar to that of HSV-1 and over 90% of the VZV ORFs have a counterpart in the HSV-1 genome (1, 11). One of the genes without a direct counterpart in HSV-1 is VZV ORFS/L, also known as ORF0, that was discovered by Kemble and coworkers (10). No known function is attributed to the gene or its product, which is predicted as a 157 amino acid (aa) type 2 transmembrane protein with a C-terminal transmembrane domain (11). The gene is located at the very beginning of $U_L$, directly adjacent to the a-like sequences that also includes PacI and PacII sites crucial for cleavage and packaging of concatameric VZV DNA (Fig 3.1) (11, 17). One potential homologue of ORFS/L is HSV-1 UL56, also a type 2 transmembrane protein. While UL56 is dispensable for HSV-1 replication *in vitro*, it plays an important role in pathogenicity *in vivo* (3, 19) although little is known about the molecular mechanism of its function. UL56 orthologues are expressed by most members of the *Alphaherpesvirinae* subfamily (24). For example, HSV-2 UL56 localizes to the Golgi network and interacts with KIF1A, a kinesin motor protein suggesting a role in vesicular trafficking (14, 15).

A previous study of Kemble and coworkers addressed the localization of ORFS/L using a rabbit polyclonal antibody and reported that ORFS/L is localized to the cytoplasm (11) Furthermore, ORFS/L was found to be expressed in skin lesions of individuals as well as neurons of a dorsal root ganglion during virus reactivation. Recently, deletion of aa29 to aa157 of ORFS/L was shown to have an effect on viral replication *in vitro* and *in vivo* in the SCID-hu mouse model (26). However, it still remains unknown whether the growth defect is dependent on ORFS/L gene function or is due to the deletion of another critical sequence element.

In this study, we demonstrate that ORFS/L localizes to the Golgi network in infected

and transfected cells, suggesting that it is a true functional orthologue of HSV-2 UL56. In addition, we could prove that the ORFS/L gene product is important for efficient VZV replication. We also identified a 5′ region of ORFS/L that is essential for replication and plays a role in cleavage and packaging of viral DNA, previously suggested by Davison and colleagues (5). Since this essential region has no homology to the opposite end of $U_L$, it could provide an explanation for the almost exclusive packaging in VZV virions of two viral DNA isomers with an invariable $U_L$ orientation.

### 3.3. Material and Methods

**Cells and Viruses.** Human melanoma cells (MeWo) were grown and maintained in growth medium (minimal essential medium (MEM) supplemented with 10% fetal bovine serum (FBS), 100 U/ml penicillin and 0.1mg/ml streptomycin) at 37°C under a 5% $CO_2$ atmosphere. Wild-type and mutant viruses were reconstituted, grown and amplified on MeWo cells by co-cultivation of infected with uninfected cells at a ratio of 1:2 to 1:5. Virus stocks were frozen in growth media supplemented with 8% dimethyl sulfoxide (DMSO) and stored in liquid nitrogen.

**Generation of *ORFS/L* mutants and revertants via *en passant* mutagenesis.** Mutants with a deletion of ORFS/L (Δaa1-157), a start codon knockout (aa1stop) in which the ATG was replaced by a stop codon (TAG), a C-terminal deletion (Δaa34-157), a stop codon insertion at amino acid position 34 (aa34stop) or with an HA-tagged ORFS/L (S/L_cHA) were generated based on pP-Oka, an infectious bacterial artificial chromosome (BAC) clone of the P-Oka strain (22), via two-step red-mediated *en passant* mutagenesis as described previously (23). In order to generate revertants of the respective ORFS/L mutants, a transfer vector was generated. Briefly, a region containing ORFS/L and flanking sequences was amplified from pP-Oka by

polymerase chain reaction, cloned into the pcDNA3.1 TOPO vector (Invitrogen) and termed prORFS/L. The *aphAI*-I-*Sce*I cassette was amplified from pEPkan-SII (23) and inserted into prORFS/L using a unique EcoRI restriction site within ORFS/L resulting in plasmid prORFS/L-*aphAI*-I-*Sce*I. The entire rORFS/L-*aphAI*-I-*Sce*I cassette was amplified and used for two-step Red-mediated mutagenesis. Revertant viruses of Δaa1-157, Δaa1stop, Δaa34-157 and Δaa34stop were termed Δaa1-157-rev, Δaa1stop-rev, Δaa34-157-rev and Δaa34stop-rev, respectively. All clones were confirmed by PCR and DNA sequencing of the ORFS/L region (Fig. 3.1A) as well as multiple restriction fragment length polymorphism analyses (RFLP) to ensure the integrity of the genome (data not shown). All oligonucleotides used are given in Table 3.1.

**Reconstitution of VZV from BAC DNA.** BAC DNA used for transfection was isolated with the Qiagen Midiprep system according to the manufacturer's (Qiagen) instruction. Subsequently, MeWo cells were transfected with Lipofectamin 2000 (Invitrogen) as described previously (22). Briefly, 1 µg BAC DNA was co-transfected with 200 ng pCMV62, a plasmid, which contains the VZV IE gene ORF62 under the control of a CMV promoter (kindly provided by Dr. Kip Kinchington, University of Pittsburgh Medical School). The DNA-lipofectamin solution was added onto the cells and incubated for 4 h. Transfection medium was then replaced with growth medium. Resulting viruses were termed vΔaa1-157, vΔaa1-157-rev, vΔaa1stop, vΔaa1stop-rev, vΔaa34-157, vΔaa34-157-rev, vΔaa34stop and vS/L_cHA.

**Multi-step growth kinetics and plaque size assay. 1x10$^6$** MeWo cells were inoculated with 100 plaque-forming units (pfu) of cell-associated viruses. For multi-step growth kinetics, infected cells were trypsinized on days 1, 2, 3, 4 and 5 post infection (p.i.) and titrated in 10-fold dilutions with fresh MeWo cells and the number of plaques determined by indirect immunofluorescence using an anti-gB antibody (US Biological). Three independent experiments were performed in triplicates. For plaque

**Table 3.1.** Primers used for cloning and mutagenesis. Underlined sequences indicate restriction enzyme sites. Bold indicates mutated sequences.

| Construct name | | sequence (5' → 3') |
|---|---|---|
| **Δaa1-157** | for | CCCACCTCCCCGCGCGTTTGCGGGGCGACCATCGGGGGGGTGAAACTACTGTCCGG AAGGGTAGGGATAACAGGGTAATCGATTTATTC |
| | rev | GCAAGCGAGAATAAATACCTTCCCCTTCCGGACAGTAGTTTCACCCCCCCGATGGTCG CCCCGCGCCAGTGTTACAACCAATTAACC |
| **Δaa1 stop** | for | CCCCACCTCCCCGCGCGTTTGCGGGGCGACCATCGGGGGGG**TAG**GGGATTTTTTGC CGGGAAACCTAGGGATAACAGGGTAATCGATTTA |
| | rev | GTTAAAGGCTGGCGGGGGGGGTTTCCCGGCAAAAAATCCC**CTA**CCCCCCCGATGGTC GCCCCGCGCCAGTGTTACAACCAATTAACCAA |
| **Δaa34-157** | for | GCGTCCACCCCTCGTTTACTGCTCGGATGGCGACCGTGCACTGAAACTACTGTCCGG AAGGGGTAGGGATAACAGGGTAATCGATTT |
| | rev | GCAAGCGAGAATAAATACCTTCCCCTTCCGGACAGTAGTTTCAGTGCACGGTCGCCAT CCGAGCGCCAGTGTTACAACCAATTAACC |
| **Δaa34 stop** | for | GTCCACCCCTCGTTTACTGCTCGGATGGCGACCGTGCAC**TAG**TCCCGCCGACCTGGG ACCCTAGGGATAACAGGGTAATCGATTT |
| | rev | GACGACGTGAGGGTGACCGGCGGGGTCCCAGGTCGGCGGGA**CTA**GTGCACGGTCG CCATCCGGCCAGTGTTACAACCAATTAACC |
| **S/L_cHA** | for | CCGTTTTTCCCGAGGAACCTCCCAACTCAACTACA**TATCCGTATGATGTGCCGGATTA TGCG**TGAAACTAGGGATAACAGGGTAATCGAT |
| | rev | GAATAAATACCTTCCCCTTCCGGACAGTAGTTTCA**CGCATAATCCGGCACATCATACG GATA**TGTAGGCCAGTGTTACAACCAATTAACC |
| **prORFS/L** | for | AGCGACCCCACCTCCCC |
| | rev | CGACAAGCTGCAAGCGAGAA |
| **prORFS/L-*aphAI*-I-*Sce*I** | for | CTAA*GAATTC*GCAAATGCTGTGTACCGGCTAGGGATAACAGGGTAATCGATTT |
| | rev | TTGC*GAATTC*TTAGAAAAGCCAGCTGAAGTCTGGCCAGTGTTACAACCAATTAACC |
| **pCDNA-ORFS/L** | for | ATGGGATTTTTTGCCGGG |
| | rev | TGTAGTTGAGTTGGGAGGTTCCTC |
| **Southern probe VZV terminus** | for | GACGCACCGGGGTCATC |
| | rev | TGTAGTTGAGTTGGGAGGTTCCTC |

size assays, cells were fixed 6 days p.i., stained, and plaques imaged with a digital camera (Zeiss Axiovert 25 and Axiocam). Areas of 60 individual plaques were evaluated with the Axiovision software (Zeiss).

**Generation of ORFS/L expression plasmids.** ORFS/L was amplified from pP-Oka and inserted into pcDNA*3.1/V5*-His TOPO vector (Invitrogen). The resulting plasmid was sequenced and termed pORFS/L-His. It was then transfected with Lipofectamin 2000 according to the manufacturer's recommendation (Invitrogen).

**Indirect immunofluorescence labeling and confocal microscopy.** MeWo cells were fixed with 3% paraformaldehyde (PFA) and permeabilized with 0.1% saponin 48 h after infection or transfection. Cells were stained with mouse monoclonal anti-GM130 antibody (BD Transduction Laboratories), rabbit polyclonal anti-HIS antibodies (Genscript Cooperation) or rabbit polyclonal anti-HA antibodies (Zymed Laboratory) at 1:200 dilutions. Secondary antibodies, including AlexaFluor568-conjugated goat anti-mouse and AlexaFluor488-conjugated goat anti-rabbit (Molecular probes) were diluted 1:1,000. Cells were washed with PBS and mounted with DAPI Vectashield (Vector Laboratories). Cells were examined using a SP5 confocal microscope system (Leica). Collected images were arranged using Photoshop 7.0 (Adobe).

**Prediction software.** NetStart 1 for vertebrates was used to predict translation initiation sites of ORFS/L (http://www.cbs.dtu.dk/services/NetStart/) (18). N- and O-glycosylation (http://www.cbs.dtu.dk/services/NetNGlyc/ and http://www.cbs.dtu.dk/services/NetOGlyc/) sites were predicted using NetNGlyc 1.0 and NetOGlyc 3.1. The presence of signal peptides for ER translocation was analyzed with SignalP 3.0 (http://www.cbs.dtu.dk/services/SignalP/). Myristoylation were predicted with Myristoylator program (http://ca.expasy.org/tools/myristoylator/).

**Cleavage assay**. $1x10^7$ MeWo cells were infected with $1x10^4$ pfu of vP-Oka,

vΔaa1stop or vΔaa1stop-rev and harvested at the time of complete cytopathic effect as observed after about 48 h, 72 h or 48 h respectively and documented via bright field microscopy. Cells were washed with ice-cold PBS and lysed in buffer A (10mM Tris pH7.4, 10mM NaCl, 3mM $MgCl_2$, 0.5% NP40). Either purified nuclei or whole cell lysates were digested with proteinase K (Qiagen) in the presence of 1% SDS and 5 mM EDTA, and DNA was purified by phenol/chloroform extraction (20). Equivalent amounts of purified nuclear or whole cell DNA were digested with *BamHI* overnight and separated by agarose gel electrophoresis. Southern blot analysis allowed the detection of VZV terminal fragments using a digoxigenin-labeled probe, generated with the PCR Dig Synthesis kit (Roche) according to manufacturer's instruction. Oligonucleotides used for amplification are given in Table 3.1. Southern blot signals were detected by chemiluminescence as recorded with a Chemi-Genius Bio Imaging System and quantified with the GeneTool software (Syngene, Cambridge, UK).

### 3.4. Results

**Analysis of ORFS/L in infected cells.** ORFS/L, predicted as a 157 aa protein, harbors two alternative start codons (29 aa and 51 aa). In order to identify protein species generated by this open reading frame, we inserted a HA-tag at the C-terminus (pS/L_cHA) in pP-Oka, an infectious BAC clone of the P-Oka strain (Fig 3.1A and B) (22). Multi-step growth kinetics and plaque size assays demonstrated that S/L_cHA virus (vS/L_cHA) is capable of replicating with kinetics comparable to those of parental BAC-derived vP-Oka, indicating that HA-tag insertion had no effect on viral replication *in vitro* (Fig. 3.2A and B). Western blot analysis of vS/L_cHA infected MeWo cells revealed that ORFS/L is expressed as a single species of about 18 kDa, corresponding well to the predicted molecular mass of the full-length, 157 amino acid (aa) protein (Fig. 3.1C). Protein predictions programs (Myristoylator, SignalP 3.0,

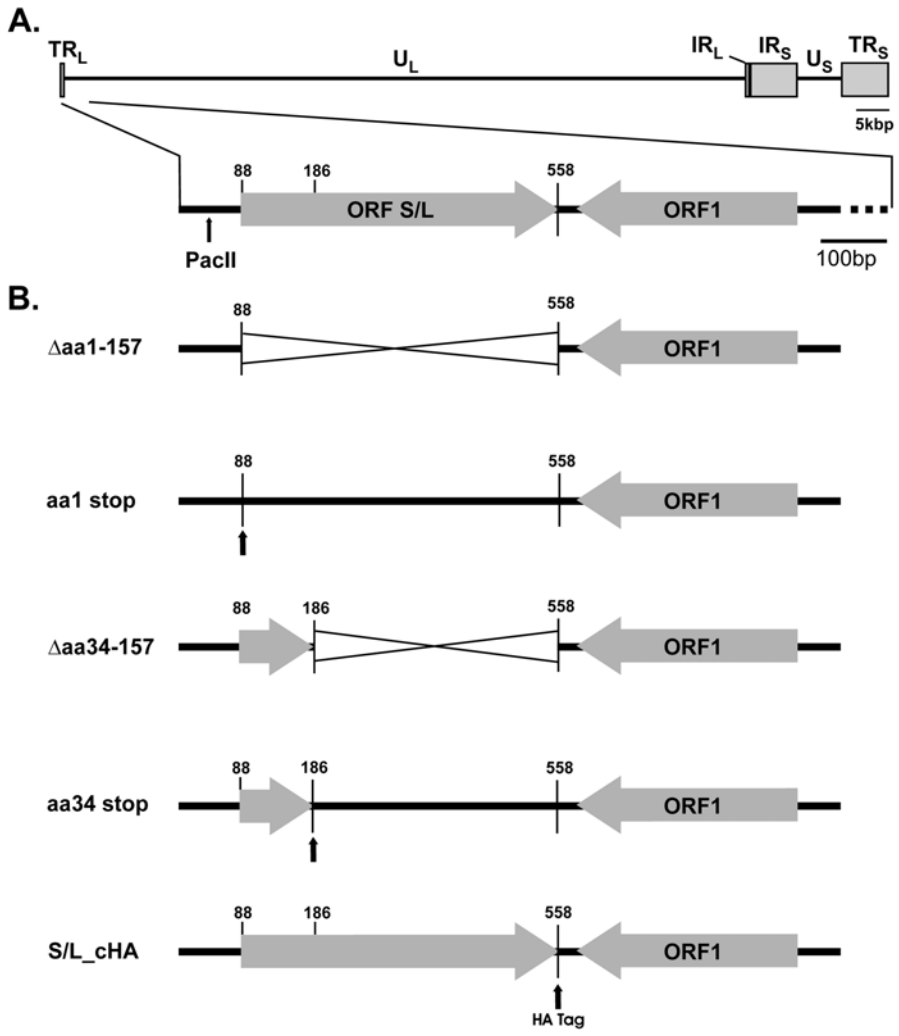


**Figure 3.1.** Overview of the VZV ORFS/L genomic region and the generated mutants. A) Schematic representation of the VZV genome with a focus on the terminal region containing ORFS/L. Scale bars provide an accurate measure of the genome and the expanded region. B) Overview of the mutants generated in the ORFS/L region. The X indicates the deletion of the corresponding region. Arrows indicate the loci of stop codon or HA-tag insertion.

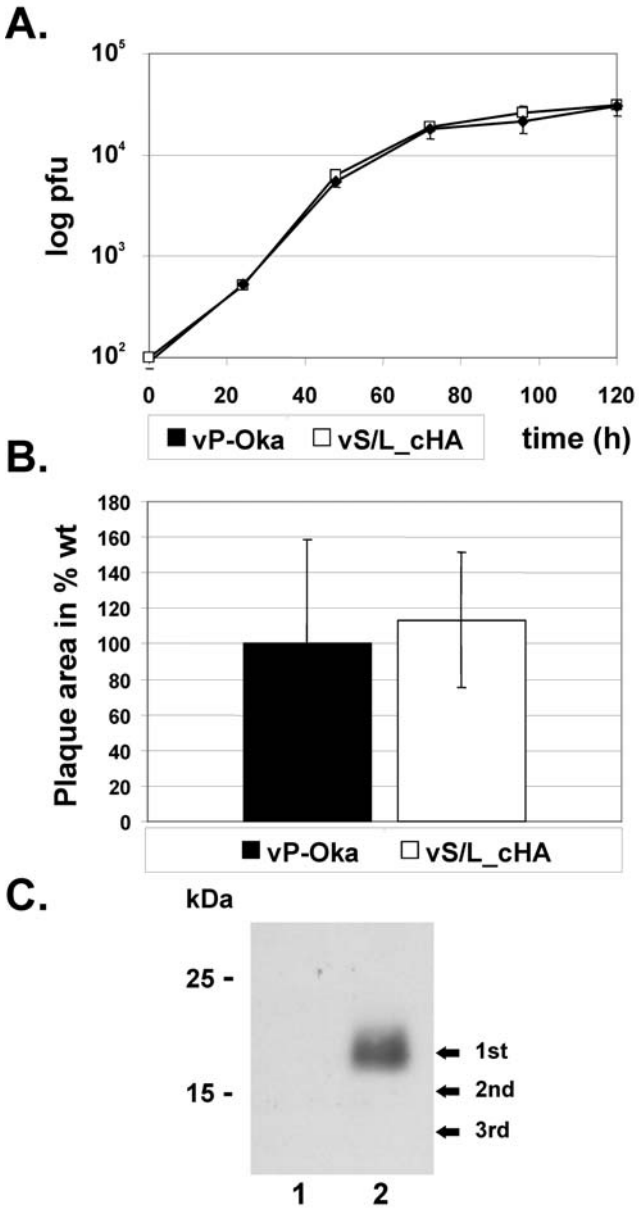


**Figure 3.2.** Growth properties of vS/L_cHA and size determination of ORFS/L. A) Multi-step growth kinetics of vS/L_cHA and vP-Oka. Shown are the means of three independent experiments including the standard error (error bars). B) Plaque size measurements of vS/L_cHA and vP-Oka. Shown are relative average plaque areas of 60 individual plaques with standard deviations (error bars), with the sizes of vP-Oka plaques set at 100%. C) Western blot analysis of cells infected with vP-Oka (lane 1) or vS/L_cHA (lane 2). Arrows indicate the predicted molecular mass of the unmodified ORFS/L protein when initiated from the first (aa1), second (aa29) or third methionine codon (aa51).

NetNGlyc 1.0 and NetOGlyc 3.1) indicated that ORFS/L is not myristoylated and posseses an ER-localization signal, which is a prerequisite for modification in the ER or Golgi. Our data, therefore, suggest that ORFS/L is exclusively expressed as the full-length protein and that that the two alternative start codons (aa 29 and aa 51) are not used for translation initiation.

**ORFS/L localizes to the trans-Golgi network (TGN) in infected and transfected cells.** To determine the subcellular localization of ORFS/L in VZV infected cells, we infected MeWo cells with vS/L_cHA. Confocal microscopy revealed that ORFS/L colocalizes with GM130, a marker for the Golgi apparatus, in infected MeWo cells (Fig. 3.3A, upper panel). Besides the Golgi network, ORFS/L was found to localize to the nuclear envelope upon syncytia formation (Fig. 3.3A, middle and lower panels). To address the question whether localization of ORFS/L to the Golgi network is dependent on other viral proteins, we determined the localization of ORFS/L in transfected cells. MeWo cells were transfected with pcDNA-ORFS/L-His. Similar to the situation in infected cells, ORFS/L was localized to the Golgi network after expression of the His-tagged protein under a strong herpesvirus (CMV-IE) promoter. We concluded, therefore, that localization of the ORFS/L protein to the Golgi apparatus is independent of the presence of other viral proteins (Fig. 3.3B) and that ORFS/L likely represents an orthologue of HSV-1 UL56.

**Deletion of the entire ORFS/L is lethal for VZV replication *in vitro*.** Previously, a recombinant virus containing a deletion of the C-terminal 129 aa, downstream of the second start codon of ORFS/L was reported to have an effect on viral replication *in vitro* and *in vivo* (26). To confirm the role of ORFS/L in VZV replication, we deleted the entire ORF (aa 1 to aa 157) corresponding to base pair (bp) 88 to 558 of pP-Oka

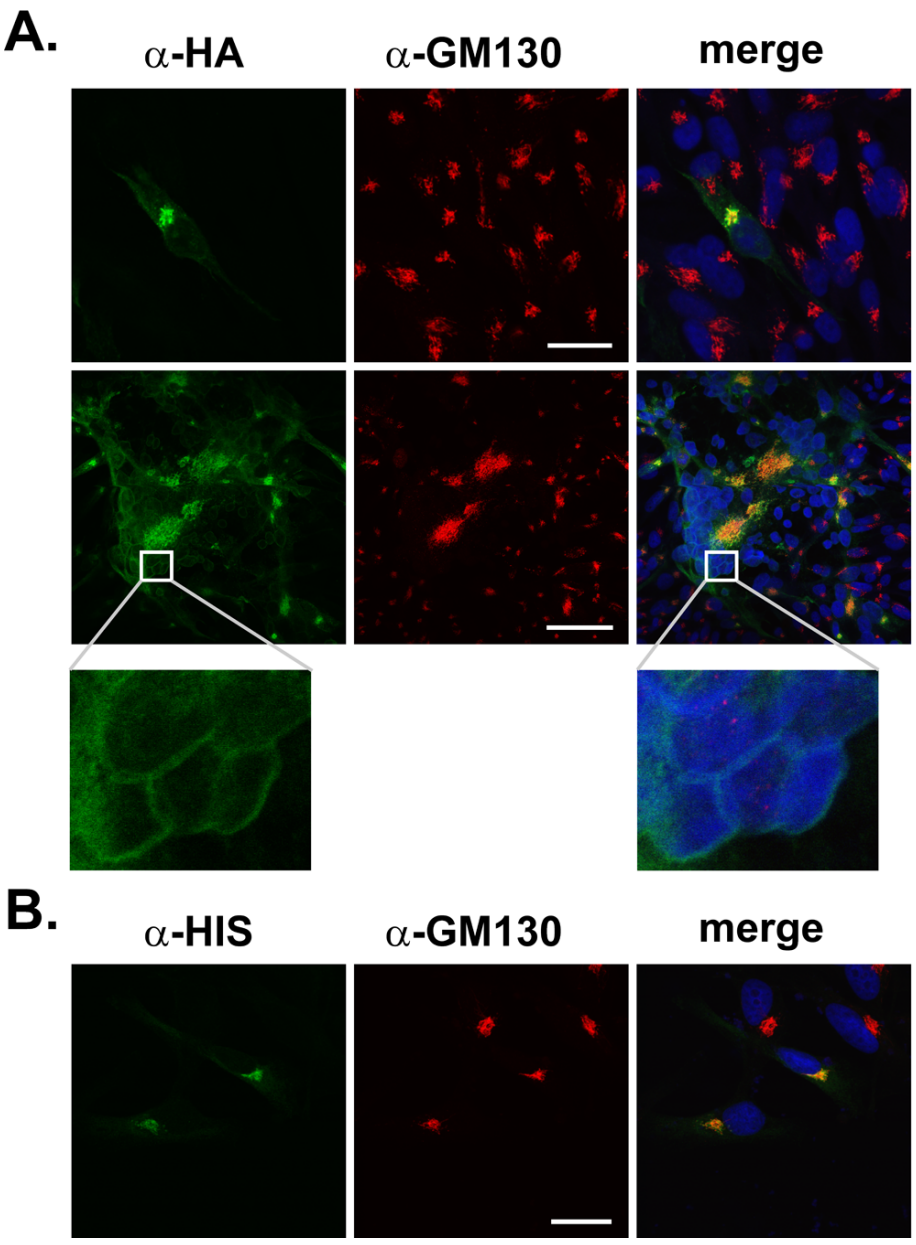


**Figure 3.3**. Localization of ORFS/L in infected and transfected cells. A) Localization of ORFS/L (green) with GM130 (red), a marker for the Golgi apparatus, and DAPI (blue) is shown for single infected MeWo cells (upper panel) or in syncytia (middle panel). The lower panel shows a focus on the nuclei within a syncytium that confirms a colocalization of ORFS/L and the nuclear envelope. Scale bars correspond to 30 µm (upper panel) and 100 µm (middle panel). B) MeWo cells were transfected with expression plasmid pORFS/L-His and analyzed 48 h after transfection. ORFS/L (green) and GM130 (red) were detected with indicated antibodies. The infected and transfected cells are representative for the cell population. Scale bars correspond to 20 µm.

(Fig. 3.1) (22). In addition, a revertant BAC clone (pΔaa1-157rev) was generated in which the original ORFS/L sequence was restored. Subsequently, the constructs were transfected into MeWo cells resulting in the reconstitution of recombinant viruses vΔaa1-157 and vΔaa1-157rev. Upon virus reconstitution, wt independent vΔaa1-157 clones exhibited a severe replication defect while the revertant virus grew with kinetics that were virtually indistinguishable from those of parental vP-Oka. Plaque size measurements confirmed this significant growth defect (Fig. 3.4A and B). The replication defect of both vΔaa1-157 clones was so severe that the viruses could not be amplified by passaging.

**ORFS/L gene product plays a role in replication in vitro.** To determine whether the observed growth effect was due to the lack of the ORFS/L gene product or an essential DNA element within ORFS/L, we generated a series of additional mutant viruses. In order to abrogate ORFS/L gene expression, we either replaced the first start codon (vaa1stop) or the codon for amino acid 34 (vaa34stop), just downstream of the second start codon, with a stop codon (Fig 3.1). We also generated a C-terminal deletion of aa34 to 157 (vΔaa34-157) similar to previous reports (11, 26). In addition, revertant viruses of vaa1stop (vaa1stop-rev) and vΔaa34-157 (vΔaa34-157-rev) were generated. Multi-step growth kinetics revealed that vaa1stop, vaa34stop and vΔaa34-157 were significantly impaired in viral replication when compared to vP-Oka or revertant viruses (Fig 3.5A). While vaa34stop and vΔaa34-157 replication was reduced by about 5-fold, vaa1stop was reduced by about 10-fold. In order to confirm the growth defect, we performed plaque size assays. In agreement with the multi-step growth kinetics, vaa1stop, vaa34stop and vΔaa34-157 showed a significant defect in plaque formation when compared to vP-Oka or revertant viruses (Fig. 3.5B). Plaque areas of vaa1stop, vaa34stop and vΔaa34-157 were reduced by 69%, 45% and 38%, respectively, when

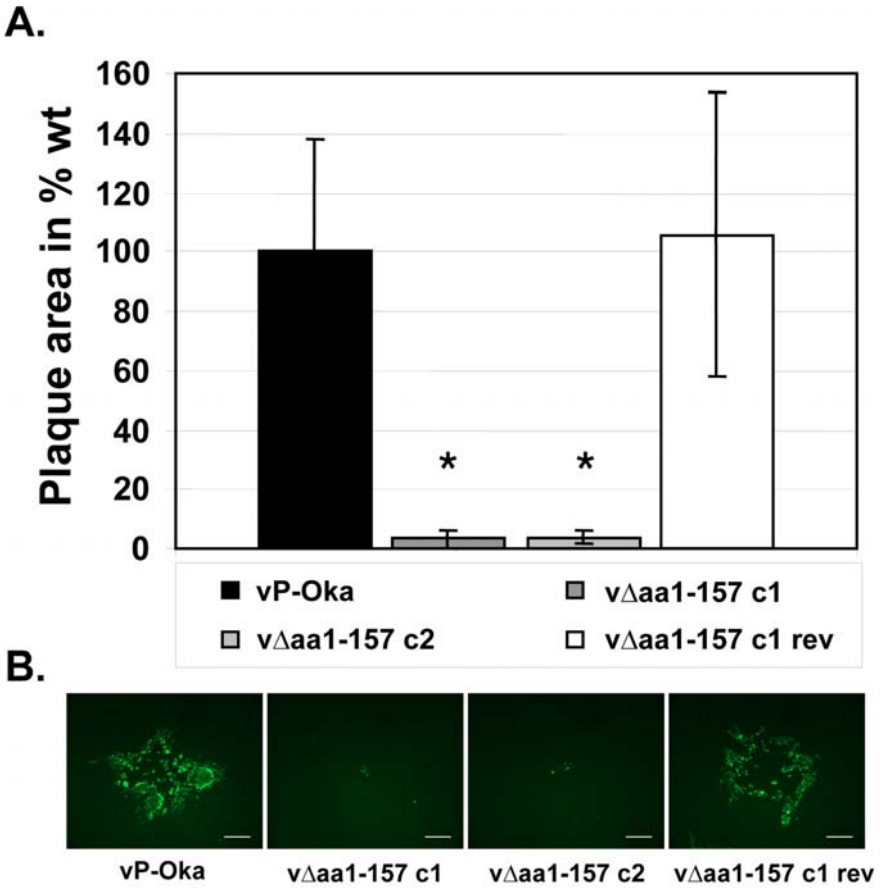


**Figure 3.4.** Growth properties of viruses lacking the entire ORFS/L. A) Plaque size measurements of vΔaa1-157 (clones 1 and 2), vP-Oka and revertant vΔaa1-157 generated from clone 1. Twenty individual plaque areas were measured and are shown as means (vP-Oka plaques were set at 100%) with standard deviations (error bars). Plaque areas induced by Δaa1-157 mutants were significantly reduced ($p<0.0001$) when compared to those of parental vP-Oka or or the revertant virus using Student's t-test. B) Representative plaque images for vΔaa1-157 (clones 1 and 2), vP-Oka and vΔaa1-157-rev. Scale bars correspond to 200 μm.

compared with parental vP-Oka or the revertant virues. Replication defects seen with both stop codon mutants confirmed that the ORFS/L gene product is crucial for efficient VZV replication. The results of the experiments also led us to conclude that the sequence encoding the amino-terminal 33 aa of ORFS/L contain an essential sequence element that does not directly relate to the function of the ORFS/L protein.

**Cleavage defect of vaa1 stop contributes to its growth defect.** To elucidate whether the observed differences in viral replication of vaa1stop and vaa34stop (Fig. 3.5A and B) was due to a structural function of the extreme 5′-end of ORFS/L, we examined the cleavage and packaging of VZV genomes from concatemeric replication intermediates in cells infected with mutant or parental viruses. We infected MeWo cells with vaa1stop, vaa1stop-rev or vP-Oka, harvested the cells at 90-100% cytopathic effect, prepared nuclear or whole cell DNA, digested it with *BamHI* and probed for the genomic termini (Fig 3.6A). While vaa1stop-rev viruses showed a cleavage pattern comparable to parental vP-Oka, viral DNA in cells infected with the vaa1stop showed a significant increase in uncleaved VZV termini in whole cell DNA (Fig. 3.6B). Since the quantity of cytosolic virions has an effect on the amount of cleaved termini, we also analyzed nuclear DNA. A comparable increase in uncleaved VZV termini was observed in nuclear preparations (data not shown). The relative quantity of uncleaved genomes was increased by more than 3.6-fold, indicating that the 5′-region of ORFS/L is involved in cleavage of unit-length genomes from concatameric replicative form DNA, before packaging into newly formed nucleocapsids. This reduction in DNA cleavage could subsequently result in impaired packaging of VZV genomes, which would account for the more severe growth defect of vaa1stop when compared to vaa34stop or vΔaa34-157. From the results we, therefore, concluded that the ORFS/L 5′ region contains an essential sequence element and that this element is likely involved in cleavage and packaging of viral DNA.

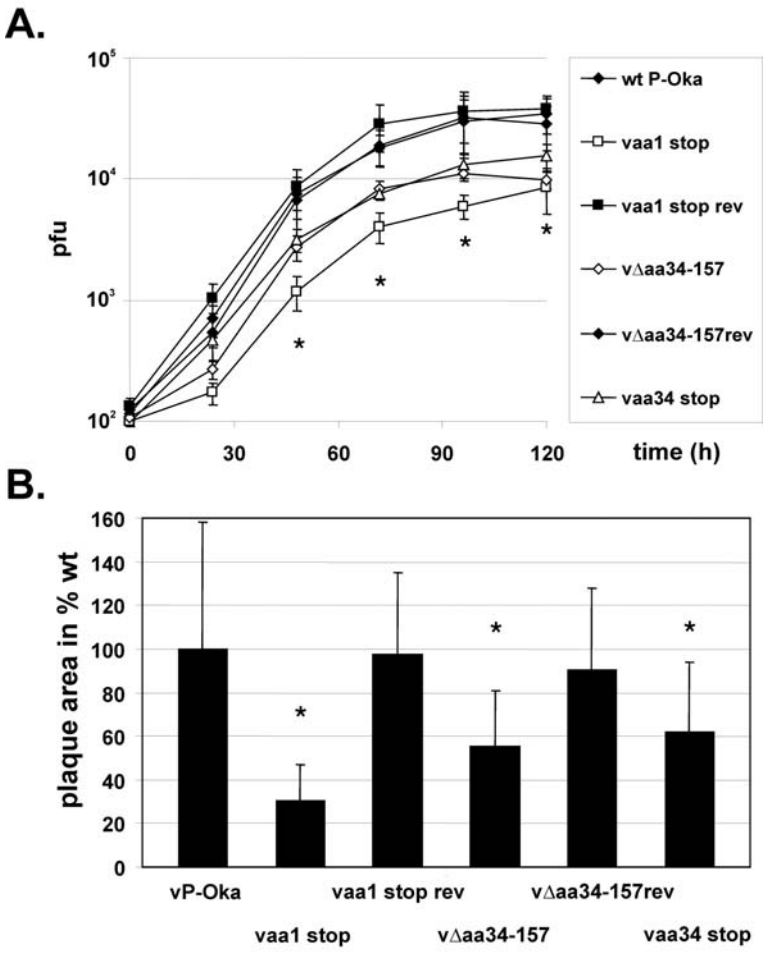


**Figure 3.5.** Growth properties of a panel of ORFS/L mutants. A) Multi-step growth kinetics of indicated viruses. Virus replication of vaa1stop, vaa34stop and vΔaa34-157 was significantly reduced ($p<0.05$) at indicated time points (asterisk) when compared to vP-Oka or corresponding revertant virus as determined using the Student's t-test. B) Plaque size measurements of indicated viruses. Plaque areas of vaa1stop, vaa34stop and vΔaa34-157 were significantly reduced ($p<0.001$) when compared to those of vP-Oka (set to 100%) or the corresponding revertant virus as determined by Student's t-test. Shown are means of 60 individual plaques per virus and standard deviations (error bars).

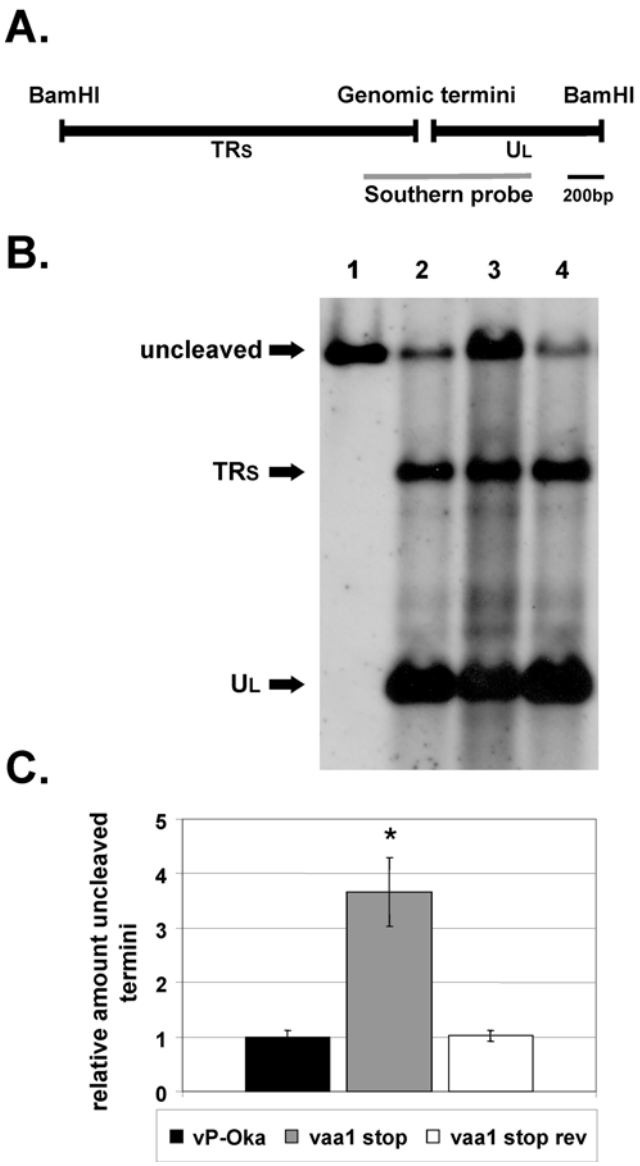


**Figure 3.6.** Cleavage of the viral genome in cells infected with mutant virus. A) Schematic representation of the terminal fragments, $TR_S$ and $U_L$, generated after restriction enzyme digestion with BamHI. The probe used to detect the genomic termini by Southern blotting is indicated. The scale bar provides an accurate measure of the sizes of the fragments expected after cleavage and of the probe. B) Cleavage analysis of vP-Oka (lane 2), vaa1stop (lane 3) and vaa1stop-rev (lane 4). The P-Oka BAC (lane 1) served as a standard for uncleaved termini. The Southern blot shown is representative of three independent experiments. C) Quantification of band intensities of three independent cleavage assays. The ratio of uncleaved and cleaved DNA is shown relative to vP-Oka. The relative amount of uncleaved termini of vaa1stop was significantly increased ($p<0.05$) when compared to vP-Oka and vaa1stop-rev as determined by Student's t-test.

### 3.5. Discussion

Although the molecular tools available to study VZV replication in vitro and in vivo have considerably improved over the past decade, the functions of several of the 70 unique VZV ORFs still remain unknown. While sequence similarities between herpesviruses ORFs can often provide valuable information on protein localization and function, such predictions only provide testable hypotheses but no formal proof of the role these proteins or genetic elements play in related viruses. Furthermore, some of the VZV ORFs, such as ORFS/L, ORF1, ORF2, ORF13, ORF32 and ORF57, do not have known orthologues in the prototype alphaherpesvirus, HSV-1 (10).

For example, the function of ORFS/L, an ORF located at the very end of the $U_L$, remains enigmatic. Previously, a report demonstrated that a deletion of the C-terminal portion of ORFS/L resulted in a viral growth defect in vitro and in vivo (26). It has remained unclear, however, whether this defect is due to ORFS/L gene function or a critical sequence element that is independent of protein function. A second study also suggested that the ORFS/L protein localizes to the cytoplasm. Here, we chose to revisit both ORFS/L function and the localization of the encoded protein and also sought to dissect putatively overlapping functions of this genomic region. We surmised that important functions are attributable to nucleotide sequences specified in this region, which has close proximity to the DNA processing elements involved in cleavage and packaging of the viral DNA in newly formed nucleocapsids.

We first addressed the subcellular distribution of the ORFS/L protein and were able to demonstrate that it localizes to the Golgi apparatus in infected and transfected cells, which supports previous bioinformatic predictions that suggested it is homologue of the HSV-1 and HSV-2 UL56 gene product. Besides its subcellular localization, the position of ORFS/L within the VZV genome, in close proximity to ORF3 representing the VZV homologue of UL55, also supports this assumption. In

addition, the ORFS/L protein shares 20% sequence identity with the UL56 gene of HSV-1 and -2 and contains two of the three conserved PY motifs (L/PPXY). The PY motifs of HSV-2 UL56 were shown to facilitate binding to Nedd4, an E3 ubiquitin ligase involved in protein sorting and trafficking (4, 24, 25). Although we show here that subcellular localization of the ORFS/L protein is consistent with an involvement of Nedd4-dependent sorting, further studies will be necessary to analyze the exact molecular functions of the ORFS/L product and its interaction with cellular proteins. The putative interaction partners include KIF1A, a member of the kinesin family that is involved in vesicular trafficking along microtubules and for which an interaction with the HSV-2 UL56 product was identified (15).

Western blot analysis suggested that the P-Oka ORFS/L is solely expressed as a protein of 18 kDa in size, and that the alternative start codons present in the ORF are not used during infection. In addition, post-translational modifications that could account for size differences, such as myristoylation, N- and O-glycolylations seem unlikely based on in silico predictions. The lack of an ER signal peptide indicates that ORFS/L is likely not translated at the rough ER or translated or modified in the ER or Golgi network. Similar to the HSV-1 and HSV-2 UL56 proteins, the VZV ORFS/L product is predicted to encode a C-terminal-anchored, type II transmembrane protein. This protein class does not possess an N-terminal signal sequence that would provide a signal for membrane insertion. Instead, type II transmembrane proteins contain a C-terminal hydrophobic region facilitating insertion and orienting the N-terminus of the protein towards the cytoplasm (16). In the case of the HSV-2 UL56 protein, the C-terminal hydrophobic region was indeed shown to be responsible for membrane insertion and its localization to the Golgi apparatus (14, 15).

It is notable that analysis of genome sequences of several other VZV strains suggested that ORFS/L translation might not be initiated from the first start codon,

because a frame shift mutation reported to occur immediately downstream of the first AUG would terminate translation prematurely. However, this frame shift was identified to be caused by an additional cytosine within a stretch of eight consecutive cytosines, which could be a sequencing error caused by polymerase slippage. In contrast to the 17 wild type VZV strain sequences available in GenBank (http://www.ncbi.nlm.nih.gov/), the vaccine strains vOka, VariVax and VarilRix, have a mutation in the stop codon that extends the open reading frame by 276 bp (92 aa). This extension could affect the insertion of ORFS/L into membranes and as such contribute to the attenuated phenotype of the vaccine viruses. More detailed sequence analyses and identification of whether or not ORFS/L is expressed in the strains in question will be necessary to confirm or refute the potential variation with respect to ORFS/L expression discussed for VZV strains other than P-Oka.

Mutations of the first codon and immediately downstream of the second start codon confirmed that the ORFS/L gene product plays an important, albeit not essential, role in VZV replication. The involvement in vesicular trafficking, as shown for HSV-2 UL56, could account for the growth defect observed in cultured MeWo and HFF cells. In contrast, partial and complete deletions of ORFS/L sequences revealed that the 5′ region of ORFS/L is essential for replication. Analysis of the status of viral DNA in cells infected with the mutant viruses showed that a sequence element contained in ORFS/L is involved in cleavage and packaging of single unit genomes from concatemeric replication intermediates. Intriguingly, this sequence that we showed is essential for efficient cleavage and packaging of viral DNA is not present at the opposite end of the $U_L$. Consequently, inversion of the $U_L$ would theoretically lead to a potentially lethal cleavage and packaging defect, which may explain why there is preferential packaging of viral DNA with only one orientation of the $U_L$. The asymmetry of the ends of the VZV $U_L$ region was first detected and discussed by

Davison and coworkers, who predicted a cleavage element within the $U_L$ region that resides at least 90 bp from the genomic terminus, which exactly corresponds to the 5' region of ORFS/L. This hypothesis is also in agreement with data suggesting directional packaging of EHV-1 into virions, with the EHV-1 genomic organization being very similar to that of VZV (21).

In conclusion, our study provides the first evidence that the ORFS/L gene product plays a role in VZV replication and that the 5′ region is involved in cleavage and packaging. Further studies of ORFS/L function and its potential interaction partners will shed light on its detailed role in VZV replication. In addition, defining the essential sequence elements within the 5′ region of ORFS/L may increase the understanding of its role in cleavage and packaging as well as the almost exclusive orientation of the $U_L$ in VZV virions.

### 3.6. Acknowledgments

This study was supported by PHS grant 1R21AI061412 and an unrestricted grant from the Freie Universität Berlin to N.O.

REFERENCES


1. **Arvin, A. M.** 1996. Varicella-zoster virus. Clin. Microbiol. Rev. **9**:361-381.

2. **Arvin, A. M.** 2001. Varicella-zoster virus, p. 2731-2767. *In* B. N. Fields, D. M. Knipe, and P. M. Howley (eds.), Virology. Lippincott-Raven Publishers, Philadelphia.

3. **Berkowitz, C., M. Moyal, A. Rosen-Wolff, G. Darai, and Y. Becker**. 1994. Herpes simplex virus type 1 (HSV-1) UL56 gene is involved in viral intraperitoneal pathogenicity to immunocompetent mice. Arch. Virol **134**:73-83.

4. **Bruce, M. C., V. Kanelis, F. Fouladkou, A. Debonneville, O. Staub, and D. Rotin**. 2008. Regulation of Nedd4-2 self-ubiquitination and stability by a PY motif located within its HECT-domain. Biochem. J **415**:155-163.

5. **Davison, A. J.** 1984. Structure of the genome termini of varicella-zoster virus. J Gen Virol **65 ( Pt 11)**:1969-1977.

6. **Davison, A. J. and N. M. Wilkie**. 1983. Location and orientation of homologous sequences in the genomes of five herpesviruses. J Gen Virol **64 (Pt 9)**:1927-1942.

7. **Ecker, J. R. and R. W. Hyman**. 1982. Varicella zoster virus DNA exists as two isomers. Proc. Natl. Acad. Sci. U. S. A **79**:156-160.

8. **Gilden, D. H., R. Gesser, J. Smith, M. Wellish, J. J. Laguardia, R. J. Cohrs, and R. Mahalingam**. 2001. Presence of VZV and HSV-1 DNA in human nodose and celiac ganglia. Virus Genes **23**:145-147.

9. **Hammerschmidt, W., H. Ludwig, and H. J. Buhk**. 1988. Specificity of cleavage in replicative-form DNA of bovine herpesvirus 1. J Virol **62**:1355-1363.

10. **Jeffrey I.Cohen, Stephen E.Straus, and Ann M.Arvin**. 2007. Fields Virology, p. 2276-2278. *In* D. M. K. P. M. H. e. al. 5. Ed. B.N.Fields (ed.). Lippincott-Raven Publishers, Philadelphia.

11. **Kemble, G. W., P. Annunziato, O. Lungu, R. E. Winter, T. A. Cha, S. J. Silverstein, and R. R. Spaete**. 2000. Open reading frame S/L of varicella-zoster virus encodes a cytoplasmic protein expressed in infected cells. J Virol **74**:11311-11321.

12. **Kinchington, P. R., W. C. Reinhold, T. A. Casey, S. E. Straus, J. Hay, and W. T. Ruyechan**. 1985. Inversion and circularization of the varicella-zoster virus genome. J Virol **56**:194-200.

13. **Klupp, B. G., C. J. Hengartner, T. C. Mettenleiter, and L. W. Enquist**. 2004. Complete, annotated sequence of the pseudorabies virus genome. J Virol **78**:424-440.

14. **Koshizuka, T., F. Goshima, H. Takakuwa, N. Nozawa, T. Daikoku, O. Koiwai, and Y. Nishiyama**. 2002. Identification and characterization of the UL56 gene product of herpes simplex virus type 2. J Virol **76**:6718-6728.

15. **Koshizuka, T., Y. Kawaguchi, and Y. Nishiyama**. 2005. Herpes simplex virus type 2 membrane protein UL56 associates with the kinesin motor protein KIF1A. J Gen Virol **86**:527-533.

16. **Kutay, U., E. Hartmann, and T. A. Rapoport**. 1993. A class of membrane proteins with a C-terminal anchor. Trends Cell Biol. **3**:72-75.

17. **McVoy, M. A., D. E. Nixon, J. K. Hur, and S. P. Adler**. 2000. The ends on herpesvirus DNA replicative concatemers contain pac2 cis cleavage/packaging elements and their formation is controlled by terminal cis sequences. J. Virol. **74**:1587-1592.

18. **Pedersen, A. G. and H. Nielsen**. 1997. Neural network prediction of translation initiation sites in eukaryotes: perspectives for EST and genome analysis. Proc. Int. Conf. Intell. Syst. Mol. Biol. **5**:226-233.

19. **Rosen-Wolff, A. and G. Darai**. 1991. Identification and mapping of the UL56 gene transcript of herpes simplex virus type 1. Virus Res. **19**:115-126.

20. **Sambrook, J. and D.F.Fritsch and T.Maniatis**. 1989. Molecular cloning: a laboratory manual. Cold Spring Harbor, N.Y..

21. **Slobedman, B. and A. Simmons**. 1997. Concatemeric intermediates of equine herpesvirus type 1 DNA replication contain frequent inversions of adjacent long segments of the viral genome. Virology **229**:415-420.

22. **Tischer, B. K., B. B. Kaufer, M. Sommer, F. Wussow, A. M. Arvin, and N. Osterrieder**. 2007. A self-excisable infectious bacterial artificial chromosome clone of varicella-zoster virus allows analysis of the essential tegument protein encoded by ORF9. J Virol **81**:13200-13208.

23. **Tischer, B. K., J. von Einem, B. Kaufer, and N. Osterrieder**. 2006. Two-step red-mediated recombination for versatile high-efficiency markerless DNA manipulation in Escherichia coli. Biotechniques **40**:191-197.

24. **Ushijima, Y., F. Goshima, H. Kimura, and Y. Nishiyama**. 2009. Herpes simplex virus type 2 tegument protein UL56 relocalizes ubiquitin ligase Nedd4 and has a role in transport and/or release of virions. Virol J **6**:168.

25. **Ushijima, Y., T. Koshizuka, F. Goshima, H. Kimura, and Y. Nishiyama**. 2008. Herpes simplex virus type 2 UL56 interacts with the ubiquitin ligase Nedd4 and increases its ubiquitination. J Virol **82**:5220-5233.

26. **Zhang, Z., J. Rowe, W. Wang, M. Sommer, A. Arvin, J. Moffat, and H. Zhu**. 2007. Genetic analysis of varicella-zoster virus ORF0 to ORF4 by use of a novel luciferase bacterial artificial chromosome system. J Virol **81**:9024-9033.

# CHAPTER FOUR

## Herpesvirus-induced lymphoma formation is independent of the interaction between viral telomerase RNA and telomerase reverse transcriptase

**Benedikt B. Kaufer, Sascha Trapp, Keith Jarosinski, Nikolaus Osterrieder**.
Herpesvirus-induced lymphoma formation is independent of the interaction between viral telomerase RNA and telomerase reverse transcriptase
Submitted to PLoS Pathogens 2010

## 4.1. Abstract

Telomerase is a ribonucleoprotein complex involved in the maintenance of telomeres, a protective structure at the chromosome termini. The enzyme complex contains two main components, telomerase reverse transcriptase (TERT), the catalytic subunit, and the telomerase RNA (TR), which serves as a template for the addition of telomeric repeats $(TTAGGG)_n$. Marek's disease virus (MDV), an oncogenic herpesvirus, encodes a TR homologue, viral TR (vTR), which significantly contributes to MDV-induced lymphomagenesis. As recent studies suggest that TRs possess telomerase-independent functions, we investigated if the tumor-promoting capacity of vTR is dependent on formation of a functional telomerase complex. We show that vTR-TERT interaction and telomerase activity was efficiently abrogated by the disruption of the vTR P6.1 stem-loop (P6.1mut). Recombinant MDV carrying the P6.1 stem-loop mutation were generated and tested in the natural host, the chicken, in which MDV readily induces fatal lymphomas. In contrast to viruses lacking vTR, all animals infected with P6.1mut viruses developed MDV-induced lymphomas, but onset of tumor formation was significantly delayed. P6.1mut viruses induced enhanced metastasis, indicating functionality of non-complexed vTR in tumor dissemination. We discovered that vTR interacts with RPL22, a cellular factor involved in T-cell development and virus-induced transformation. The interaction is enhanced in the presence of vTR harboring the P6.1 stem-loop mutation when compared to wild-type vTR. Our study provides the first evidence that expression of TR, in this case encoded by a herpesvirus, is pro-oncogenic in the absence of telomerase activity.

## 4.2. Author Summary

The telomerase complex with its two main components, telomerase reverse transcriptase and telomerase RNA, plays an important role in telomere maintenance and is involved in tumor development. Recent studies suggest telomerase RNAs can function independently of the telomerase complex, and possibly promote tumor development. Here we demonstrate that vTR, a herpesvirus encoded telomerase RNA, serves two distinct functions in MDV-induced tumor formation. The first is dependent on increased telomerase activity, which is crucial for rapid onset of lymphomas in infected animals. vTR becomes part of the telomerase complex and contributes to the survival of rapidly dividing transformed cells. The second function of vTR is entirely independent of telomerase action and is crucial for tumor formation and metastasis. This latter function is likely a consequence of vTR-mediated gene regulation that is at least in part controlled by interaction of vTR with RPL22, a cellular factor involved in T-cell development and virus-induced transformation. Taken together, our study demonstrates that telomerase RNA encoded by a herpesvirus is directly involved in tumor formation *in vivo*, in a fashion that is largely independent of its function within an active telomerase complex.

## 4.3. Introduction

Telomerase is a multi-component ribonucleoprotein complex. One of its main functions is the maintenance of telomeres, a protective structure at the termini of linear chromosomes. The telomerase complex consists of two essential core components, telomerase reverse transcriptase (TERT) and telomerase RNA (TR), which serves as a template for the catalytically active subunit in the elongation of telomeric repeats $(TTAGGG)_n$ at the end of chromosomes (11). TR contains four structural domains, which are highly conserved regions (CR) in all vertebrates: i) the pseudoknot (core)

domain, containing the template sequence (CR1); ii) the H/ACA box and iii) the conserved region (CR) 7 domain. Both the H/ACA box and CR7 are essential for TR stability and localization; and iv) the CR4-CR5 domain, which is required for efficient TR-TERT complex formation, and subsequent telomerase activity and processivity (7, 9). An essential structure within the CR4-CR5 domain is the P6.1 stem-loop. Base pairing of the P6.1 stem is completely conserved in all vertebrates. Disruption of the base pairing of the P6.1 stem was shown to interfere with proper TR-TERT interaction and resulted in absent telomerase activity *in vitro* and *in vivo* (4, 7, 33). In addition, the P6.1 stem-loop was shown to interact with conserved sequences of the template region CR1, which also plays a critical role in the catalytic activity of the telomerase complex (33).

Telomerase activity is tightly regulated and varies amongst cell types. While it is commonly up-regulated in germ-line, stem and cancer cells, it is absent in most somatic cells (28). The absence of telomerase activity often leads to progressive telomere shortening, known to initiate cellular senescence and irreversible cell cycle arrest (2). Several tumor-inducing viruses have evolved strategies to evade and subvert this mechanism of cellular senescence, mainly via the up-regulation of TERT, which was shown to be the limiting factor of telomerase activity in some organisms, such as the human and the chicken (2). It has been suggested that up-regulation of TERT expression and provision of more active telomerase increases the proliferative potential of cells persistently infected with virus, which in turn might be beneficial to accumulating genetic alterations and transformation after infection (2).

One of the most remarkable viruses with respect to the efficiency of the induction of fatal tumors is Marek's disease virus (MDV), a lymphotropic alphaherpesvirus, that causes Marek's disease (MD) in chickens, characterized by neurological disorders, immune suppression and, primarily, malignant T cell lymphomas (32). The rapid onset

of MD-induced lymphomas, as early as 2 weeks post-infection, and high tumor-induced mortality (90-100% in susceptible animals), suggests a direct involvement of virus-encoded oncogenes in the process. The major MDV oncogene, *meq*, encodes a basic leucine zipper (bZIP) transcription factor (TF) that was shown to interact with Rb, cdk2 and p53, proteins involved in cell-cycle control, and several cellular TFs including c-Jun, c-Fos and c-Myc, an oncogene known to regulate TERT expression (6, 24). In addition, and as a unique feature, the MDV genome harbors two copies of its own TR subunit, termed viral TR (vTR), that shares 88% sequence identity with chicken TR (chTR), contains all four conserved structural TR domains, and was likely acquired from the chicken genome (9). The 180-kbp linear, double-stranded DNA genome of MDV consists of a long (L) and short (S) unique region ($U_L$ and $U_S$) flanked by terminal ($TR_L$ or $TR_S$) and internal ($IR_L$ or $IR_S$) inverted repeats. Both vTR copies are located in the repeats flanking the $U_L$, $TR_L$ and $IR_L$. Besides the presence of vTR in the $TR_L$ and $IR_L$, MDV also contains two sets of tandem repeats in very close proximity to the genomic termini that represent perfect telomeres (18).

vTR is expressed during both lytic and latent MDV infection. It is functionally active and was shown to efficiently induce higher telomerase activity and processivity with respect to telomere elongation *in vitro* than its cellular homologue, chTR (10, 32). Although dispensable for lytic replication *in vitro* and *in vivo*, vTR is required for efficient MDV-induced tumorigenesis, as MDV mutants lacking both copies of vTR were severely impaired in lymphoma formation and dissemination (32).

Recent reports suggest that both TERT and TR may also have roles in tumorigenesis aside from their role the maintenance of telomere length in rapidly dividing cells (3, 5, 20). For example, human TR has been shown to restrain ATR activity, a factor in the DNA damage response pathway, in a telomerase-independent fashion allowing the survival of cells after cellular stress such as UV radiation (16).

Furthermore, knockdown of TR in human cancer cells induced rapid changes in the global gene expression profiles that were independent of telomere maintenance and DNA damage responses. Induced changes in expression levels included genes involved in cell cycle progression (Cyclin G2 and Cdc27) and adhesion (integrin αV), that may have an effect on MDV pathogenesis and tumorigenesis as well (20). Similarly, expression of vTR in the chicken fibroblast DF-1 cell line that does not exhibit telomerase activity induced a 2-fold increase of integrin αV expression, suggesting a telomerase-independent function for vTR (17, 20, 32).

A potential interaction partner of vTR is ribosomal protein L22 (RPL22), previously shown to interact with human TR (19). Besides associating with ribosomes, RPL22 is also involved in T-cell development (1, 22). T-cells are the target of MDV transformation. Epstein-Barr virus (EBV), a herpesvirus that shares many pathobiological similarities with MDV, encodes two RNAs termed EBER 1 and 2. EBER-1 is highly abundant in latently infected cells (12, 32) and was shown to mediate transformation through an RPL22-binding RNA, which was termed EBV encoded RNA 1 (EBER-1) (31).

In order to elucidate whether MDV vTR has functions that are independent of telomere maintenance and the formation of a functional telomerase complex, we mutated the P6.1 stem-loop present in CR4-CR5 of MDV-encoded vTR. The mutation was shown to efficiently abrogate vTR-mediated telomerase activity *in vitro*. *In vivo* studies analyzing MD incidence, tumor development and dissemination confirmed that vTR contains functions dependent and independent of the formation of an active telomerase complex. In addition, we identified RPL22 as a novel interaction partner of vTR. To our knowledge, the data presented here provide the first *in vivo* evidence that a TR executes functions important for tumor formation that are independent of

telomerase activity and likely depend on the alternate usage of RPL22 in the transformation process.

### 4.4. Results and Discussion

**vTR P6.1 stem-loop mutation efficiently disrupts telomerase activity.** To ensure that the disruption of the vTR P6.1 stem-loop, as previously shown for cellular TRs, efficiently abrogates vTR-TERT interaction and consequently telomerase activity, we performed gel-based telomere repeat amplification protocol (TRAP) assays. Base pairing of the P6.1 stem-loop was disrupted by mutating base pairs (bp) 295-298 of vTR from 5′-AGAG-3′ to 5′-UCUC-3′ as shown in figure 4.1A. In order to confirm the absence of telomerase activity via TRAP assay, *in vitro* transcription was used to generate various vTR's that were used in the TRAP assays (Fig. 4.1B): wild-type (wt) vTR, vTR containing the P6.1 mutation (Fig 4.1A), or, as a negative control, vTR containing a mutation in the template sequence (AU5) resulting in the addition of $(TATATA)_n$ repeats that are not amplified in the TRAP assay. Functional chTERT protein was obtained by *in vitro* transcription of a synthetic cDNA followed by translation using a rabbit reticulocyte lysate system (Fig. 4.1C). In order to reconstitute the telomerase complex, chTERT was incubated with vTR variants or actin control RNA and telomerase activity analyzed by TRAP assay. While telomerase activity was readily detected with wt vTR confirming earlier results (10), no TRAP products could be detected when vTR was used harboring the P6.1 mutation, the AU5 mutation or when negative control RNA was added to the reaction (Fig. 4.1D). Although clearly detectable, few TRAP products were obtained with the vTR-TERT combination. The relatively low activity of reconstituted vTR-TERT compared with the positive control TR could be due to the low TERT levels generated by *in vitro* transcription/translation, the lack of accessory telomerase factors, or a high protein

**Figure 4.1.** Effect of the P6.1 mutation on telomerase activity. A) Schematic of the CR4-CR5 domain including a detailed representation of the P6.1 stem-loop. Structure of wild-type P6.1 (left) and mutant P6.1 stem-loop (P6.1 mut) (right) is shown. Nucleotide changes of the wt P6.1 stem-loop (blue) are shown in red. B) *In vitro* transcribed β-actin control RNA, wt vTR RNA, vTR containing the P6.1 mutation (P6.1) or a mutation in the template sequence (AU5) was analyzed on a 2% denaturing agarose-formaldehyde gel. Expected vTR size is indicated by the black arrow. C) Chicken TERT-His was translated *in vitro* using rabbit reticulocyte lysates and subsequently analyzed via Western blotting using an anti-5x-His antibody. The expected size of TERT-His is indicated with the black arrow. D) Telomerase activity of the *in vitro* transcribed vTR variants was analyzed using gel based TRAP-assays. TRAP products and the internal control (IC) are indicated. The results shown are representative for three independent experiments showing similar results.

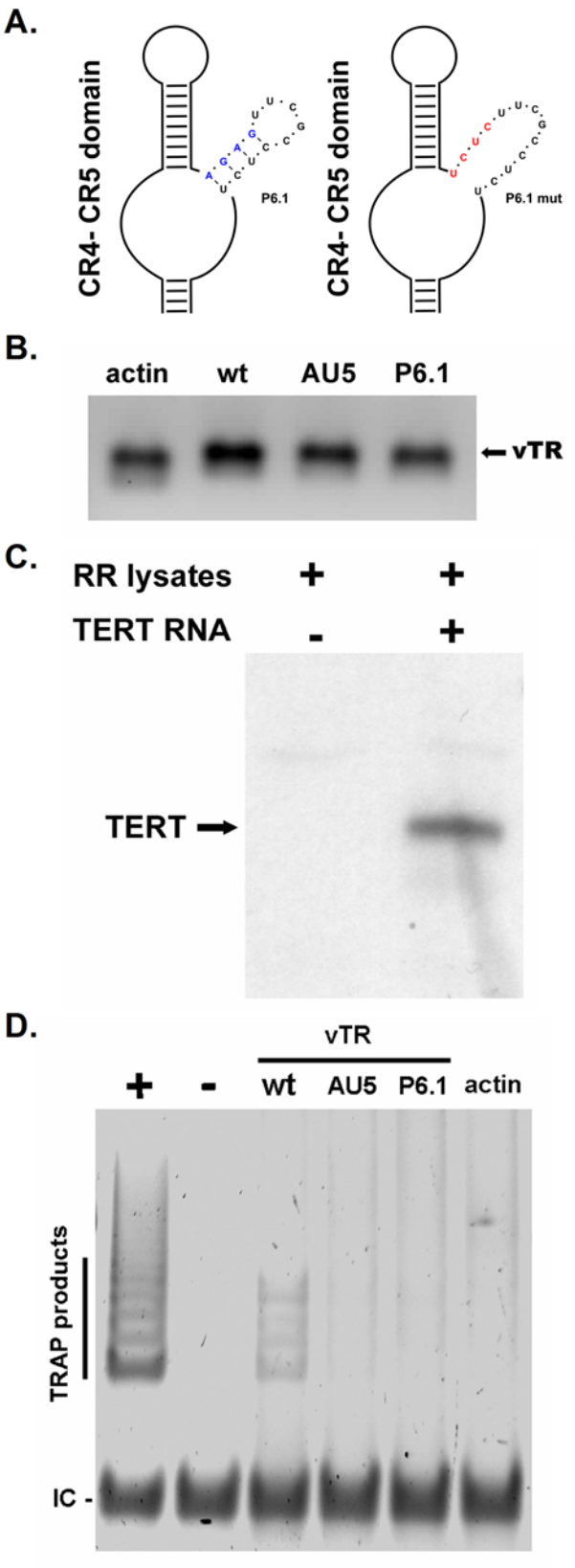
A.
CR4- CR5 domain
P6.1
CR4- CR5 domain
P6.1 mut
B.
actin
wt
AU5
P6.1
vTR
C.
RR lysates + +
TERT RNA - +
TERT
D.
vTR
+ -
wt
AU5
P6.1
actin
TRAP products
IC -

content of the reticulocyte lysates known to reduce TRAP product generation (21). Our results clearly demonstrated that the introduced mutation within the vTR P6.1 stem-loop completely abrogates the formation of an active telomerase complex.

**Construction of MDV bacterial artificial chromosome (BAC) mutants.** To determine whether the established tumor-promoting function of vTR is dependent on the formation of an enzymatically active telomerase complex, we manipulated the P6.1 stem-loop in pRB-1B, an infectious BAC clone of the highly oncogenic RB-1B MDV strain (Fig. 4.2A) (25). Base pairing of the P6.1 stem-loop was disrupted by mutating base pairs (bp) 295-298 of vTR, as described above, by two-step Red-mediated mutagenesis (30) (Fig. 4.1A). The mutation was introduced into both copies of the diploid vTR gene within the MDV genome, and the resulting mutant infectious clone was termed pP6.1mut. In addition, a revertant BAC clone (pP6.1rev) was generated in which the original sequence was restored in both alleles. All clones were confirmed by PCR, DNA sequencing and multiple restriction fragment length polymorphism analyses (RFLP) to ensure the integrity of the genome (Fig. 4.2B)

**vTR-TERT interaction and telomerase activity are dispensable for efficient lytic viral replication *in vitro* and *in vivo*.** In order to investigate the effect of the P6.1 stem-loop mutation on virus replication *in vitro*, wt pRB-1B, pP6.1mut and pP6.1rev BACs were transfected into chicken embryo cells (CEC) resulting in the reconstitution of recombinant viruses termed vRB-1B, vP6.1mut and vP6.1rev. Multi-step growth kinetics revealed that replication of vP6.1mut was unaffected *in vitro* when compared to that of wt vRB-1B or vP6.1rev (Fig 4.3A). In addition, mutation of the P6.1 stem-loop had no effect on plaque sizes induced by the P6.1 virus mutant (Fig 4.3B). These findings were consistent with previous data on vTR deficient viruses, which had shown that vTR is dispensable for lytic virus growth *in vitro* (32).

**Figure 4.2.** MDV genome organization and P6.1 stem-loop mutation. A) Schematic representation of the MDV genome including the unique-short and -long regions ($U_S$, $U_L$) flanked by terminal and internal repeat regions ($TR_S$, $TR_L$, $IR_S$, $IR_L$). The focus on the vTR-containing regions shows the telomeric repeat region present in the MDV genome (left), vTR including its conserved regions (CR) 1-8, and the three exons of the neighboring vIL-8 gene (right). B) Restriction fragment length polymorphism analyses of pRB-1B (lane 2, 6, 10), vP6.1mut (lane 3, 7, 11) and vP6.1rev (lane 4, 8, 12) using the indicated restriction enzymes. Lane 1, 5, and 9 show the 1 kb plus ladder (Invitrogen) ranging from 2 kbp (lowest band) to 12 kbp (highest band) in 1 kbp increments.

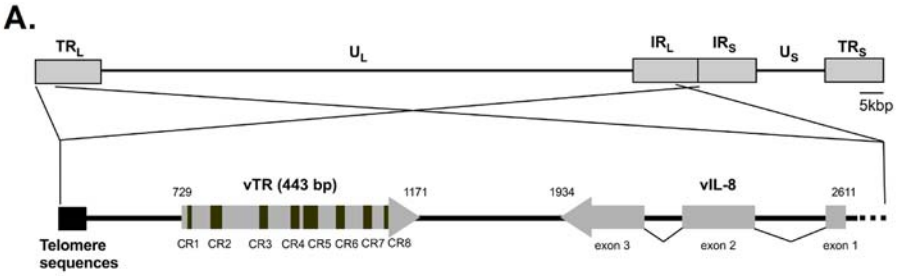
A.
TRL
UL
IRL
IRS
US
TRS
5kbp
729
vTR (443 bp)
1171
1934
vIL-8
2611
Telomere sequences
CR1 CR2 CR3 CR4 CR5 CR6 CR7 CR8
exon 3
exon 2
exon 1

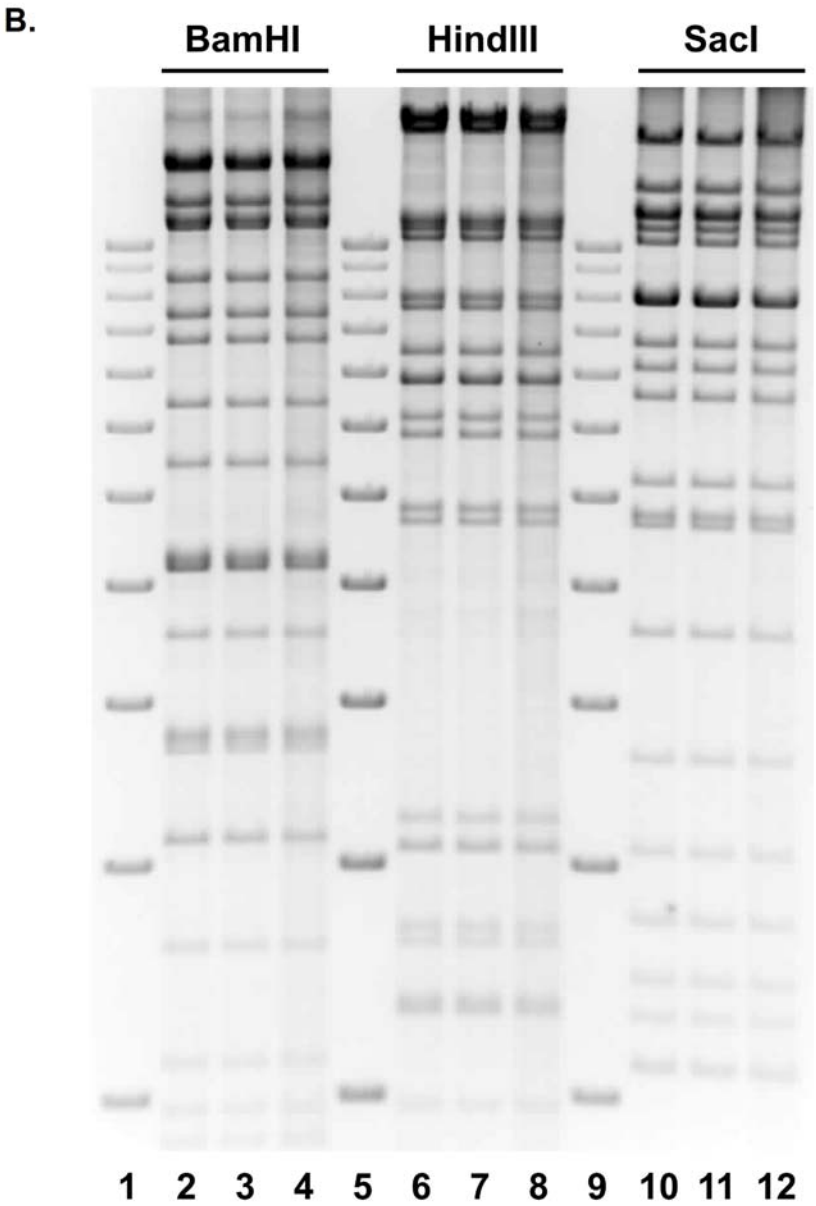
B.
BamHI
HindIII
SacI
1 2 3 4 5 6 7 8 9 10 11 12

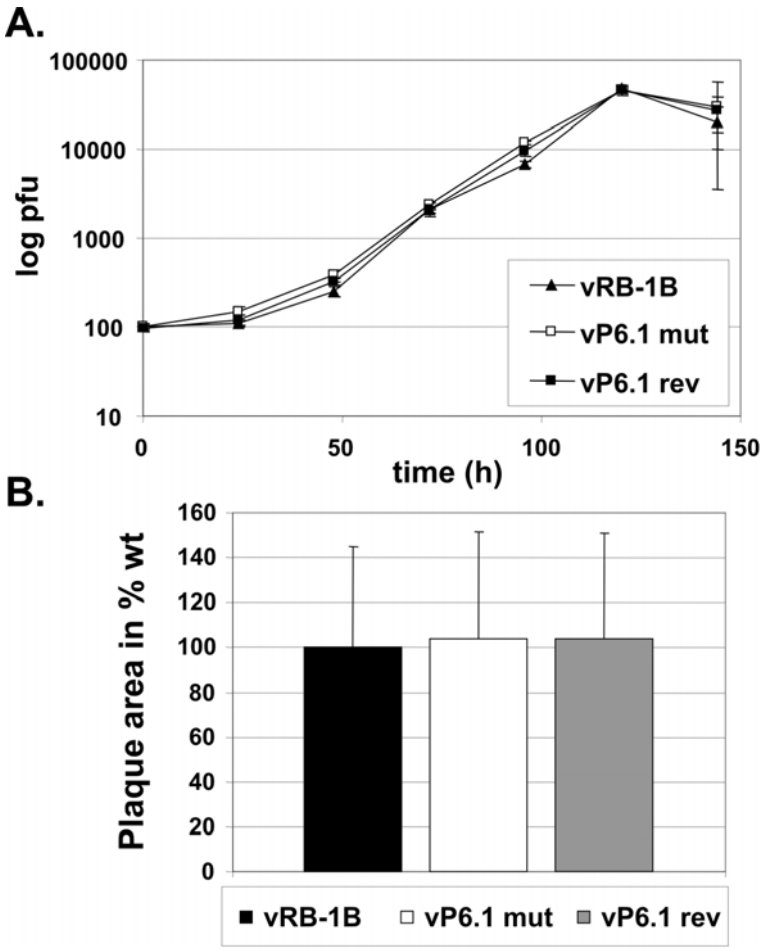


**Figure 4.3.** Growth properties of viruses containing the P6.1 stem-loop mutation. A) Multi-step growth kinetics of wt vRB-1B, vP6.1mut and vP6.1rev were performed in triplicates and are shown as means with standard deviations (error bars). B) Plaque size assay. Results are shown for the three recombinant viruses as the relative mean plaque area in percent of 100 randomly selected plaques induced by each of the viruses with the corresponding standard deviations (error bars).

Since efficient lytic replication *in vivo* is considered a prerequisite for efficient lymphomagenesis, we analyzed the replicative potential of the various mutant viruses in the natural host. We infected 1-day-old chickens and monitored virus levels by qPCR using DNA isolated from whole blood obtained by wing vein puncture until 28 days post infection (dpi). MDV is present in peripheral blood mononuclear cells (PBMC) and qPCR analyses showed that vP6.1mut replicated in those cells to levels that were comparable to those of wt vRB-1B or vP6.1rev (Fig. 4.4A). The results were again consistent with published data on the lytic replication of vTR deficient viruses, which were shown to be fully capable of robust lytic replication (32). The observed dispensability for lytic replication of vTR-TERT interaction and vTR-mediated telomerase activity in general can be explained by the fact that the initial virus production in chicken B and T cells does not require long-term survival of the host cell or host cell proliferation. Survival of the latently infected host cell is, however, a prerequisite for, or consequence of transformation and tumor formation. From the results of the experiments on lytic replication of the P6.1mut viruses we concluded that viruses containing the P6.1 stem-loop mutation are capable of efficient replication in cultured cells *in vitro* as well as in the target cells *in vivo*. Therefore, a functional vTR-TERT interaction is not needed for replication *in vivo*, a prerequisite for MDV-induced disease.

**Onset of MDV-induced lymphoma is delayed in the absence of vTR-TERT interaction and vTR-mediated telomerase activity.** We have previously shown that MD lymphoma formation was significantly reduced in the absence of vTR (32). To address whether the observed reduction is dependent on the interaction of vTR with TERT, we performed two independent animal experiments in which we monitored the temporal occurrence of virus-induced lymphoma in chickens infected with vRB-1B, vP6.1mut or P6.1rev. In a trial experiment, we established that abrogation of vTR-

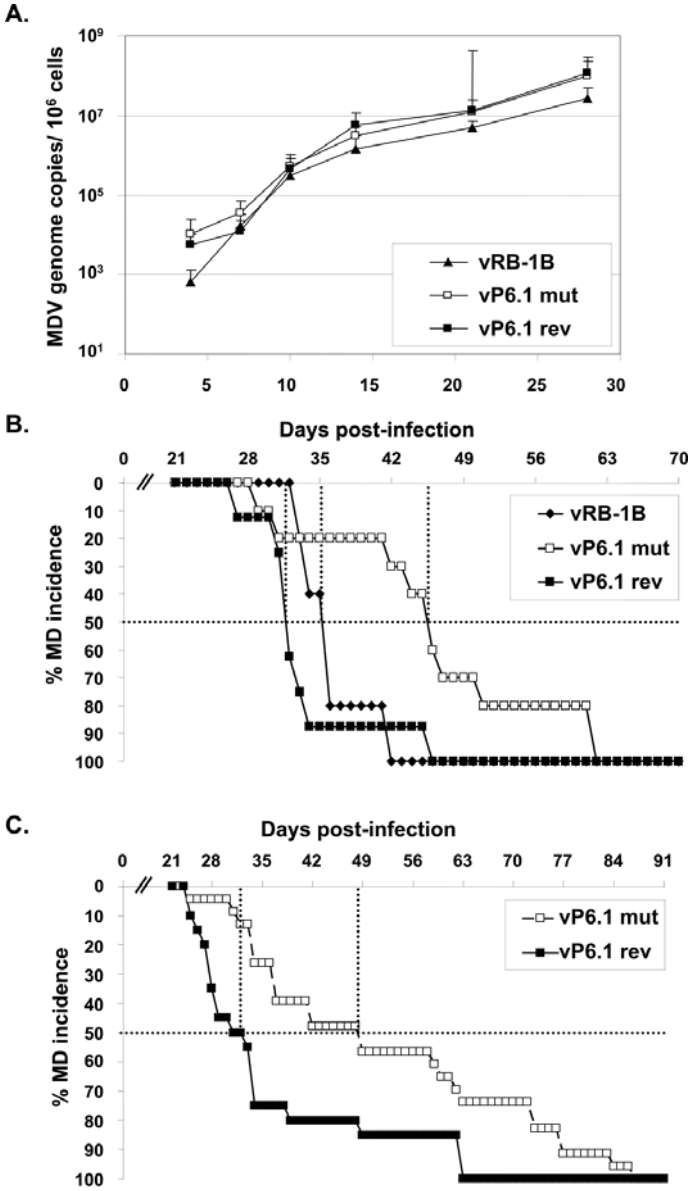


**Figure 4.4.** P6.1 stem-loop mutation does not affect lytic replication *in vivo*, but delays MD incidence. A) qPCR analysis of the viral *ICP4* gene and the host *iNOS* gene. Blood samples were taken at 4, 7, 10, 14, 21, and 28 dpi and total DNA was extracted. Mean MDV genome copies / $10^6$ blood cells of eight infected chickens per group as determined by qPCR analysis are shown with standard deviations (error bars). B) 1st animal experiment: MD incidence in percent in chickens infected with vRB-1B (n=5), vP6.1mut (n=10) and vP6.1rev (n=8) during the indicated time period C) 2nd animal experiment: MD incidence in percent of vP6.1mut (n=22) and vP6.1rev (n=20) during the indicated time period. The time to develop MD in 50% of the inoculated animals ($MD_{50}$) is indicated (dashed line) and was significantly increased in the P6.1mut group (p=0.0012).

mediated telomerase activity markedly delayed the onset of MD lymphomas (Fig 4.4B). We observed that the time until development of tumors and occurrence of MD in 50% of the infected animals ($MD_{50}$) was increased from 36 dpi in vRB-1B-infected chickens (n=5) and 32 dpi in vP6.1rev-infected animals (n=8) to 46 dpi in vP6.1mut-infected birds (n=10).

To eliminate subjectivity, in a second animal experiment, we used a double blinded approach to examine the onset of clinical signs. In agreement with the results of the first animal experiment, $MD_{50}$ was significantly delayed in vP6.1mut infected chickens (49 dpi, n=22) when compared to vP6.1rev expressing wt vTR (32 dpi, n=20) (p=0.0012). We hypothesize that the observed delay in the development of lymphomas is due to a curtailing of telomerase activity that is caused by the loss of enhanced telomere maintenance mediated by vTR. Such enhanced telomere maintenance, which was shown in MDV-infected animals (29) and is thought to play an important role for the survival of rapidly dividing MDV-transformed cells early in the transformation process, is probably mediated by vTR-chTERT interaction. In the absence of the P6.1 stem-loop, the interaction can no longer occur, and, therefore, the pool of transformed cancer stem cells surviving the initial crisis may be reduced.

It was notable, however, that, in contrast to viruses lacking vTR (32), all animals infected with v6.1mut succumbed to MD before termination of the experiment, indicating that vTR has functions independent of the formation of an active telomerase complex. From the results of the animal experiments we conclude that the rapid onset of MD observed in chickens infected with wt MDV (vRB-1B) or the vP6.1rev virus is clearly dependent on telomerase activity that involves vTR-chTERT interaction and telomerase activity. Importantly, lymphoma formation and fatal disease outcome is efficient even in the absence of enzymatically active telomerase.

**Tumor dissemination is increased in the absence of functional vTR-TERT interaction.** MDV-induced tumor formation and metastasis were previously shown be significantly reduced in the absence of vTR (32). In addition, our earlier findings of integrin αV up-regulation mediated by vTR alone suggested that malignant lymphoma dissemination may be a result of the action of vTR that is independent of vTR-TERT interaction (32). To address whether animals infected with the P6.1mut virus, in which vTR-TERT complex formation is absent and most likely more non-complexed vTR available, show an increase in dissemination, we enumerated the gross lesions in infected birds during necropsies on animals that had succumbed to infection. Consistent with our earlier results and the hypothesis that lymphomagenesis and metastasis could be largely determined by vTR action alone, disruption of the P6.1 stem-loop led to a significant increase in the number of solid lymphomas in chickens infected with the vP6.1mut virus when compared to vP6.1rev-infected chickens ($p=0.0016$). All vP6.1mut-infected animals developed gross tumors in at least three organs (Fig. 4.5A). Furthermore, the average number of organs with solid lymphomas was significantly increased from 3.1 in vP6.1rev to 4.0 in vP6.1mut ($p=0.0381$; Fig. 4.5B). We concluded, therefore, that the increase in tumor dissemination observed in vP6.1mut-infected animals supports a previous interpretation of vTR mediating integrin αV upregulation and increased metastasis (32).

**vTR and vTR P6.1 efficiently interact with RPL22.** As previously reported, transformation mediated by EBER-1 is dependent on its interaction with RPL22 (12). In order to determine if wild-type and/or mutant P6.1 vTR interact with RPL22, we performed biotin-RNA pull-down assays. vTR, vTR P6.1, chTR and EBER-1 were found to precipitate RPL22, while biotin-labeled β-actin control RNA did not (Fig. 4.5C). EBER-1 showed the strongest interaction, most likely because it contains

**Figure 4.5.** Disruption of vTR-TERT interaction leads to increased tumor dissemination and enhances interaction with RPL22. A) Dissemination pattern of vP6.1mut (22 chickens) and vP6.1rev (20 chickens) for *in vivo* experiment 2. Moribund chickens were euthanized, necropsied and evaluated for lymphoma dissemination. Results are shown as percentage of animals with 1-2, 3-4 or 5-6 organs containing lymphomatous lesions. B) Mean number of organs with gross tumors per animal with standard deviations. The mean number was significantly increased in the P6.1mut group indicated by the asterisk ($p=0.0381$). C) Biotin-RNA pull-down assay. Precipitated RPL22 (upper panel), unbound supernatant (middle panel), and RNA input control (lower panel) of indicated RNAs are shown. The figure is a representative of three independent experiments yielding similar results.

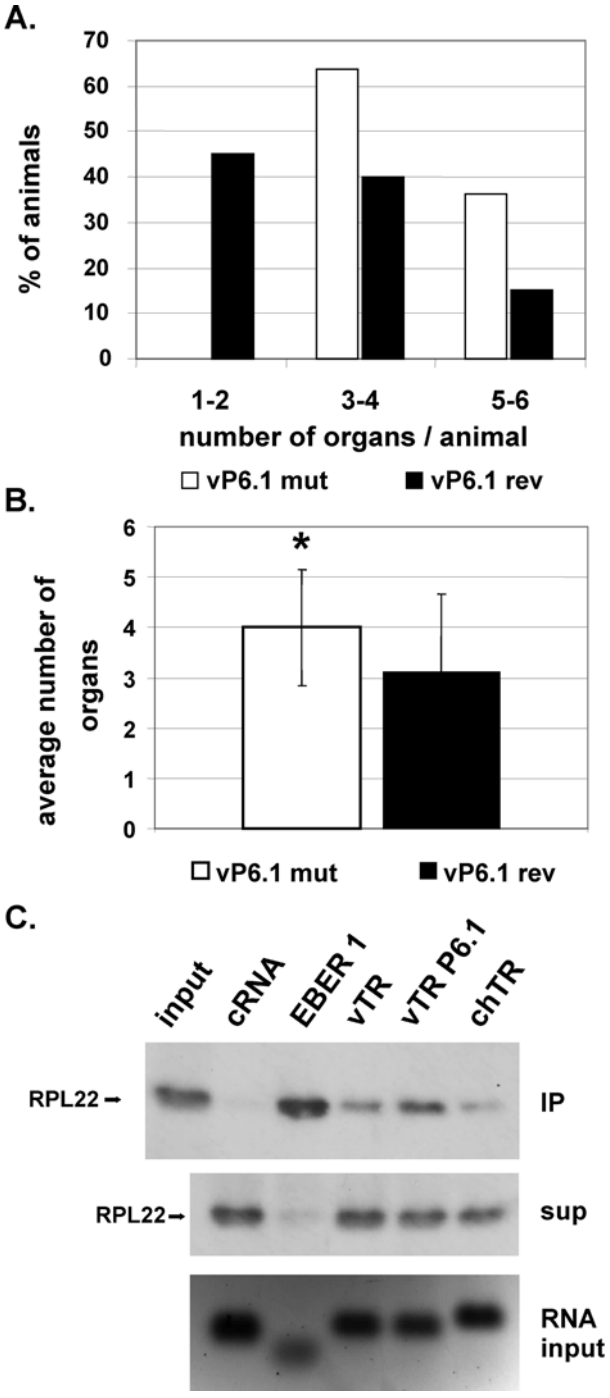
A.
70
60
50
40
30
20
10
0
% of animals
1-2
3-4
5-6
number of organs / animal
vP6.1 mut
vP6.1 rev
B.
6
5
4
3
2
1
0
*
average number of organs
vP6.1 mut
vP6.1 rev
C.
input
cRNA
EBER 1
vTR
vTR P6.1
chTR
RPL22
IP
RPL22
sup
RNA input

three independent RPL22 binding sites (8). Enhanced interaction of vTR P6.1 was observed when compared to wild-type vTR and chTR. This could be caused by the conformational change of the adjacent P6 stem–loop structure, that exhibits high similarity to the EBER-1 stem-loop 3 that is known to interact with RPL22 (unpublished data). In addition, the abrogation of vTR-TERT interaction could increase the amount of free vTR available for RPL22 interaction, thereby providing an explanation for the increased number of solid tumors found in vP6.1mut infected animals.

### 4.5. Overall Conclusion

In this report, we demonstrate that the herpesvirus telomerase RNA, vTR, has at least two functions in virus-induced lymphomagenesis. One of its functions is dependent on vTR-TERT interaction, while the other is independent of the formation of an active telomerase complex. The rapid onset of lymphoma formation seems dependent on vTR-mediated telomerase activity because a delay in the development of tumors was observed when vTR-TERT interaction was abrogated. The documented increase in telomerase activity mediated by the presence of vTR in complex with TERT when compared to the presence of cellular TR likely plays an important role in the initial establishment and maintenance of MDV-transformed cells. It may, therefore, facilitate the development of lymphomas by increasing the pool of candidate tumor stem cells. Functions of vTR that are independent of telomerase activity, however, are needed later in the process and influence homing of tumor cells to various organs, seeding and metastasis. These processes are likely a consequence of TR-mediated gene regulation shown by Le and coworkers (20). In addition, interaction of vTR with RPL22 suggests an alternative mechanism involved in transformation, as demonstrated for EBV EBER-1. In conclusion, this study demonstrates that TR is

directly involved in tumor formation *in vivo*, in a fashion that is independent of its function as an integral component of an active telomerase complex.

### 4.6. Material and Methods

**Cells and viruses.** CECs were prepared from specific-pathogen-free embryos and maintained as described previously (23). Recombinant viruses were reconstituted in CECs by $CaPO_4$ transfection of purified BAC DNA as described previously (14, 26). The lox-P-flanked mini-F sequences within the infectious clones were removed by cotransfection with a Cre recombinase expression vector (pCAGGS-NLS/Cre) (14). Removal of the mini-F sequences was ensured by analyzing recombinant virus stocks by analytic PCR as described previously (14). Virus propagation as well as determination of virus growth kinetics and plaque sizes were performed as described previously (27).

**Generation of mutant MDV**. pP6.1mut and pP6.1rev were generated by two-step Red-mediated recombination (14, 30). Primers used for the mutagenesis are given in Table 4.1.

***In vivo* experiments.** SPF P2a (MHC: $B^{19}B^{19}$) chickens were inoculated intra-abdominally with 500 to 2,000 plaque-forming units at day 1 of age and housed in isolation units. All experimental procedures were conducted in compliance with approved Institutional Animal Care and Use Committee (IACUC) protocols (internal approval number: 2002-0085). Chickens were evaluated for symptoms of MDV-induced disease on a daily basis and examined for gross tumors when clinical symptoms were evident.

**DNA extraction and qPCR assays.** DNA was extracted from whole blood and MDV genomic copies were determined by qPCR (13, 15). Briefly, MDV DNA copy

**Table 4.1.** Primers used for cloning and mutagenesis. Underlined sequences indicate restriction enzyme sites. Bold indicates mutated sequences.

| Construct name | | sequence (5' → 3') |
|---|---|---|
| pP6.1mut | for | CGCAGGCCGCGGTCGGCCGGCACCCGCCATTGCCGCCGCGA**TCTC**TTCG CCTCTGTCAGCCTCGTAGGGATAACAGGGTAATCGATTT |
| | rev | GCCGCATCTCCCGGGCGCCGCCGAGGCTGACAGAGGCGAA**GAGA**TCGCG GCGGCAATGGCGGGGCCAGTGTTACAACCAATTAACC |
| pP6.1rev | for | GCAGGCCGCGGTCGGCCGGCACCCGCCATTGCCGCCGCGA**AGAG**TTCGC CTCTGTCAGCCTCGTAGGGATAACAGGGTAATCGATTT |
| | rev | CCGCATCTCCCGGGCGCCGCCGAGGCTGACAGAGGCGAA**CTCT**TCGCGG CGGCAATGGCGGGGCCAGTGTTACAACCAATTAACC |
| puc119-vTR | for | CATGCCTGCAGTAATACGACTCACTATAGGGACACGTGGCGGGTGGAAGG |
| | rev | GATCCTCTAGATGCGCATGTGGGAGCGACGCC |
| puc119-vTR-P6.1 | for | **TC**TTCGCCTCTGTCAGCCTCG |
| | rev | **GA**TCGCGGCGGCAATGGC |
| puc119-vTR-AU5 | for | **TATAA**CGGAGGTATTGATGGTACTGTC |
| | rev | **TATATA**ACACAGCGGAGCCTTCCAC |
| pcDNA-chTERT-His | for | ACGCGTGGCGGGTGGAAG |
| | rev | GCGTGTGGGAGCGACGCC |
| pcDNA-chTR | for | ACGCGTGGCGGGTGGAAG |
| | rev | GCGTGTGGGAGCGACGCC |
| pcDNA-RPL22 | for | GCCGCCATGGCGCCCGT |
| | rev | GTCCTCCTCCTCCTCCTCCTCC |

numbers were detected using primers and probe specific for the *ICP4* locus and normalization was achieved using chicken inducible nitric oxide synthase (*iNOS*) genome copies.

**Cloning of vTR variants, chTERT, chTR and RPL22.**. vTR was amplified from pRB-1B and subsequently cloned into the *PstI* and *XbaI* sites of the pUC119 plasmid resulting in plasmid pUC119-vTR. The T7 promoter was inserted at the 5′ end of vTR via a 5′ overhang in the vTR-T7-for primer. Mutation of the template (AU5) and the P6.1 stem-loop was done based on pUC119-vTR by Phusion Site-Directed Mutagenesis (Finnzymes Inc.) according to the supplier's instructions and resulting in pUC119-vTR-AU5 and pUC119-vTR-P6.1, respectively. Chicken TERT (chTERT) was obtained as a synthetic, codon-optimized sequence from GenScript (Piscataway, NJ USA), PCR amplified including the Kozak sequence and inserted into pcDNA3.1/V5-His TOPO (Invitrogen) containing a 5′ T7 promoter, resulting in plasmid pcDNA-chTERT-His. Chicken TR (chTR) and RPL22 was amplified from chicken DNA and inserted into pcDNA3.1/V5-His TOPO, resulting in pcDNA-chTR and pcDNA-RPL22-His. Oligonucleotides used for amplification are given in Table 4.1.

***In vitro* transcription**. vTR variants, chTR, EBER-1, or β-actin were transcribed using the Maxiscript T7 kit (Ambion) following the manufacturer's instructions where the linearized plasmids pUC119-vTR, pUC119-vTR-AU5, pUC119-vTR-P6.1, cDNA-chTR, pSG5-EBER-1 (a kind gift of Dr. Rona Scott, Louisiana State University Health Science Center, Shreveport, LA) and pTRI-β-actin (Ambion) served as templates. Biotin-labeled RNAs were generated using the biotin RNA labeling mix (Roche). chTERT and RPL22 were transcribed via the mMESSAGE mMACHINE® T7 Kit (Ambion) according to the supplier's recommendation using linearized pcDNA-chTERT-His or pcDNA-RPL22 as templates. RNAs were purified via the

RNeasy Kit (Qiagen), analyzed on a 2% denaturing agarose-formaldehyde gel, and quantified with a NanoDrop 1000 (Thermo Scientific).

***In vitro* translation of chTERT.** *In vitro* transcribed chTERT-His or RPL22-His RNA was used for *in vitro* translation using the Rabbit Reticulocyte Lysate System (Promega) according to the manufacturer's protocol. chTERT-His and RPL22-His expression was analyzed by Western blotting, using a mouse anti-5xHis antibody (Qiagen).

**TRAP assay**. *In vitro*-transcribed vTR variants (1 μg) were incubated with 1 μL of *in vitro* translated chTERT, as shown in Figure 4.1C, for 1 h at 30 °C to reconstitute the telomerase complex. Telomerase activity was subsequently determined using the *TRAPeze* gel-based telomerase detection kit S7700 (Chemicon) following the manufacturer's instructions.

**Biotin-RNA pull-down assay.** Four μL in vitro translated RPL22-His was mixed with 3 nmol biotin labeled vTR, vTR P6.1, chTR, EBER-1 or β-actin control RNA and incubated in binding buffer (150 mM NaCl, 50 mM Tris pH 7.0, 0.1% Tween20, 1 μg of tRNA, 0.5 mM DTT, 0.5 mM PMSF) containing 10 μg tRNA for 1h at 37°C. 20 uL EZview Strepavidin beads (Sigma) were washed with binding buffer and added to the setup. After binding occurred for 1 h at RT, supernatant was collected and beads washed 7 times with binding buffer containing 1 μg tRNA. Precipitated and unbound protein was analyzed by Western blotting, using a mouse anti-5xHis antibody (Qiagen).

**Statistical analysis.** Significant differences in MD incidence were determined using the Wilcoxon rank-sum test (Fig. 4.4C). Significant differences in tumor distribution were determined using Chi-Square test (Fig. 4.5A). Significant differences in mean tumor incidences were determined using Student's *t* test (Fig. 4.5B).

## 4.7. Acknowledgments

We thank Kerstin Osterrieder for statistical advice. This study was supported by PHS grant 5R01CA127238 and an unrestricted grant from the Freie Universität Berlin to NO.

REFERENCES


1. **Anderson, S. J., J. P. Lauritsen, M. G. Hartman, A. M. Foushee, J. M. Lefebvre, S. A. Shinton, B. Gerhardt, R. R. Hardy, T. Oravecz, and D. L. Wiest**. 2007. Ablation of ribosomal protein L22 selectively impairs alphabeta T cell development by activation of a p53-dependent checkpoint. Immunity. **26**:759-772.

2. **Bellon, M. and C. Nicot**. 2008. Regulation of telomerase and telomeres: human tumor viruses take control. J Natl. Cancer Inst. **100**:98-108.

3. **Blasco, M. A.** 2002. Telomerase beyond telomeres. Nat. Rev. Cancer **2**:627-633.

4. **Blasco, M. A., H. W. Lee, M. P. Hande, E. Samper, P. M. Lansdorp, R. A. DePinho, and C. W. Greider**. 1997. Telomere shortening and tumor formation by mouse cells lacking telomerase RNA. Cell **91**:25-34.

5. **Blasco, M. A., M. Rizen, C. W. Greider, and D. Hanahan**. 1996. Differential regulation of telomerase activity and telomerase RNA during multi-stage tumorigenesis. Nat. Genet. **12**:200-204.

6. **Casillas, M. A., S. L. Brotherton, L. G. Andrews, J. M. Ruppert, and T. O. Tollefsbol**. 2003. Induction of endogenous telomerase (hTERT) by c-Myc in WI-38 fibroblasts transformed with specific genetic elements. Gene **316**:57-65.

7. **Chen, J. L., K. K. Opperman, and C. W. Greider**. 2002. A critical stem-loop structure in the CR4-CR5 domain of mammalian telomerase RNA. Nucleic Acids Res. **30**:592-597.

8. **Fok, V., R. M. Mitton-Fry, A. Grech, and J. A. Steitz**. 2006. Multiple domains of EBER 1, an Epstein-Barr virus noncoding RNA, recruit human ribosomal protein L22. RNA. **12**:872-882.

9. **Fragnet, L., M. A. Blasco, W. Klapper, and D. Rasschaert**. 2003. The RNA subunit of telomerase is encoded by Marek's disease virus. J Virol **77**:5985-5996.

10. **Fragnet, L., E. Kut, and D. Rasschaert**. 2005. Comparative functional study of the viral telomerase RNA based on natural mutations. J Biol. Chem. **280**:23502-23515.

11. **Greider, C. W. and E. H. Blackburn**. 1987. The telomere terminal transferase of Tetrahymena is a ribonucleoprotein enzyme with two kinds of primer specificity. Cell **51**:887-898.

12. **Houmani, J. L., C. I. Davis, and I. K. Ruf**. 2009. Growth-promoting properties of Epstein-Barr virus EBER-1 RNA correlate with ribosomal protein L22 binding. J Virol **83**:9844-9853.

13. **Jarosinski, K., L. Kattenhorn, B. Kaufer, H. Ploegh, and N. Osterrieder**. 2007. A herpesvirus ubiquitin-specific protease is critical for efficient T cell lymphoma formation. Proc. Natl. Acad. Sci. U. S. A **104**:20025-20030.

14. **Jarosinski, K. W., N. G. Margulis, J. P. Kamil, S. J. Spatz, V. K. Nair, and N. Osterrieder**. 2007. Horizontal transmission of Marek's disease virus requires US2, the UL13 protein kinase, and gC. J Virol **81**:10575-10587.

15. **Jarosinski, K. W., N. Osterrieder, V. K. Nair, and K. A. Schat**. 2005. Attenuation of Marek's disease virus by deletion of open reading frame RLORF4 but not RLORF5a. J Virol **79**:11647-11659.

16. **Kedde, M., C. le Sage, A. Duursma, E. Zlotorynski, B. van Leeuwen, W. Nijkamp, R. Beijersbergen, and R. Agami**. 2006. Telomerase-independent regulation of ATR by human telomerase RNA. J Biol. Chem. **281**:40503-40514.

17. **Kim, H., S. You, I. J. Kim, L. K. Foster, J. Farris, S. Ambady, F. A. Ponce de Leon, and D. N. Foster**. 2001. Alterations in p53 and E2F-1 function common to immortalized chicken embryo fibroblasts. Oncogene **20**:2671-2682.

18. **Kishi, M., G. Bradley, J. Jessip, A. Tanaka, and M. Nonoyama**. 1991. Inverted repeat regions of Marek's disease virus DNA possess a structure similar to that of the a sequence of herpes simplex virus DNA and contain host cell telomere sequences. J. Virol. **65**:2791-2797.

19. **Le, S., R. Sternglanz, and C. W. Greider**. 2000. Identification of two RNA-binding proteins associated with human telomerase RNA. Mol. Biol. Cell **11**:999-1010.

20. **Li, S., J. Crothers, C. M. Haqq, and E. H. Blackburn**. 2005. Cellular and gene expression responses involved in the rapid growth inhibition of human cancer cells by RNA interference-mediated depletion of telomerase RNA. J Biol. Chem. **280**:23709-23717.

21. **Maesawa, C., T. Inaba, H. Sato, S. Iijima, K. Ishida, M. Terashima, R. Sato, M. Suzuki, A. Yashima, S. Ogasawara, H. Oikawa, N. Sato, K. Saito, and T. Masuda**. 2003. A rapid biosensor chip assay for measuring of telomerase activity using surface plasmon resonance. Nucleic Acids Res. **31**:E4.

22. **Murre, C.** 2007. Ribosomal proteins and the control of alphabeta T lineage development. Immunity. **26**:751-752.

23. **Osterrieder, N.** 1999. Sequence and initial characterization of the U(L)10 (glycoprotein M) and U(L)11 homologous genes of serotype 1 Marek's Disease Virus. Arch. Virol. **144**:1853-1863.

24. **Osterrieder, N., J. P. Kamil, D. Schumacher, B. K. Tischer, and S. Trapp**. 2006. Marek's disease virus: from miasma to model. Nat. Rev. Microbiol. **4**:283-294.

25. **Petherbridge, L., A. C. Brown, S. J. Baigent, K. Howes, M. A. Sacco, N. Osterrieder, and V. K. Nair**. 2004. Oncogenicity of virulent Marek's disease virus cloned as bacterial artificial chromosomes. J. Virol. **78**:13376-13380.

26. **Schumacher, D., B. K. Tischer, W. Fuchs, and N. Osterrieder**. 2000. Reconstitution of Marek's disease virus serotype 1 (MDV-1) from DNA cloned as a bacterial artificial chromosome and characterization of a glycoprotein B-negative MDV-1 mutant. J. Virol. **74**:11088-11098.

27. **Schumacher, D., B. K. Tischer, S. Trapp, and N. Osterrieder**. 2005. The protein encoded by the US3 orthologue of Marek's disease virus is required for efficient de-envelopment of perinuclear virions and involved in actin stress fiber breakdown. J Virol **79**:3987-3997.

28. **Shay, J. W. and S. Bacchetti**. 1997. A survey of telomerase activity in human cancer. Eur. J Cancer **33**:787-791.

29. **Shkreli, M., G. Dambrine, D. Soubieux, E. Kut, and D. Rasschaert**. 2007. Involvement of the oncoprotein c-Myc in viral telomerase RNA gene regulation during Marek's disease virus-induced lymphomagenesis. J Virol **81**:4848-4857.

30. **Tischer, B. K., J. von Einem, B. Kaufer, and N. Osterrieder**. 2006. Two-step red-mediated recombination for versatile high-efficiency markerless DNA manipulation in Escherichia coli. Biotechniques **40**:191-197.

31. **Toczyski, D. P. and J. A. Steitz**. 1991. EAP, a highly conserved cellular protein associated with Epstein-Barr virus small RNAs (EBERs). EMBO J **10**:459-466.

32. **Trapp, S., M. S. Parcells, J. P. Kamil, D. Schumacher, B. K. Tischer, P. M. Kumar, V. K. Nair, and N. Osterrieder**. 2006. A virus-encoded telomerase RNA promotes malignant T cell lymphomagenesis. J. Exp. Med. **203**:1307-1317.

33. **Ueda, C. T. and R. W. Roberts**. 2004. Analysis of a long-range interaction between conserved domains of human telomerase RNA. RNA. **10**:139-147.

# CHAPTER FIVE

## Herpesvirus telomeres allow efficient integration into host chromosomes and mobilization of quiescent viral genomes

**Benedikt B. Kaufer, Keith Jarosinski, Nikolaus Osterrieder.** Herpesvirus telomeres allow efficient integration into host chromosomes and mobilization of quiescent viral genomes

Submitted to Cell 2010

## 5.1. Abstract

Several lymphotropic herpesviruses, including Epstein Barr virus (EBV), human herpesvirus 6 (HHV-6) and Marek's disease virus (MDV), are capable of integrating their genomes into host chromosomes. For the latter two viruses, integration of viral DNA is found at the distal end of host chromosomes, where telomeres consisting of telomeric repeat sequences and telomere associated proteins form structures that prevent chromosomal instability and degeneration. It is also known that HHV-6, MDV and other herpesviruses harbor telomeric repeats identical to host telomeric sequences at either end of the linear viral genomes, but the role of these genetic elements has remained enigmatic. Using MDV as a natural virus-host model, we show that herpesvirus telomeric repeats facilitate viral genome integration into host telomeres and that these repeat structures are crucial for efficient tumor formation and reactivation of latent virus from the quiescent state of infection. Our results, therefore, provide the first conclusive evidence that herpesvirus telomeric repeats mediate chromosomal integration. Finally, our data and the fact that telomeric repeats are present in many herpesvirus species suggest that telomere-mediated integration is a highly conserved mechanism, which ensures faithful virus genome maintenance in host cells during cell division and also allows efficient mobilization of dormant viral genomes. This mobilization mechanism, therefore, appears to endow herpesviruses with the ability to spread within a population of susceptible individuals and thus is necessary for continued virus evolution and survival.

## 5.2. Introduction

A number of DNA viruses and retroviruses are capable of integrating their genetic material into the host genome, which ensures viral genome maintenance and replication during cell division. Among the herpesviruses that are found in animals as diverse as crustaceans and humans, Epstein-Barr virus (EBV), human herpesvirus 6 (HHV-6), and Marek's disease virus (MDV) have been found in an integrated state during the latent, quiescent stage of the virus life cycle (6, 8, 9, 19). Other members of this group of viruses maintain their genomes exclusively as an episome during this phase of infection. Establishment of latency is a unifying and important principle for all herpesviruses that is utilized for prolonged, usually life-long, maintenance of the agents' genetic material in once infected hosts. From the latent state, virus is reactivated intermittently to allow virus spread from infected to uninfected individuals in a population (14). Latency is a poorly understood series of events, which will uniformly result in the expression of only very few viral genes with the sole purpose of genome maintenance whilst avoiding a fully lytic replicative cycle causing cellular death. Latency may only require genome maintenance when non proliferative cells such as neurons are infected. However, in other cell types, for example lymphocytes, faithful and continued replication of viral DNA during each mitosis must be ensured (29).

Herpesvirus integration is well-known for maintenance of viral DNA in rapidly dividing cells, but the mechanistic principles underlying this process have remained elusive. Previously, HHV-6 and MDV, two lymphotropic viruses that can cause lymphoma, have been found integrated at the distal ends of host chromosomes (1, 7, 18). A recent study suggested HHV-6 integrates at the proximal end of telomeres, protein-associated repeat sequences that protect chromosomes from damage and extensive shortening during DNA replication, and that integration in telomeres

facilitates vertical transmission of the virus (1). In addition HHV-6A and B, human herpesvirus 7 (HHV-7), MDV and several other herpesviruses harbor telomeric repeats (TMRs) identical to host telomere sequences $(TTAGGG)_n$ at either end of their linear genomes (15, 28). Based on the observations of the presence of telomeric repeats in viral genomes and their integration into host telomeres, we hypothesized that herpesviruses use these virus-specific telomeric repeat sequences to integrate their genetic information into host telomeres, thereby ensuring faithful replication and maintenance of the viral genome in rapidly dividing cells.

In the case of MDV, integration and efficient induction of the latent state of infection is considered the basis for tumor formation. The efficiency of establishing latency has been shown to correlate directly with the number of cells harboring latent genomes. Out of many latently infected and initially transformed cells, one outcompetes all others with the consequence that tumours within one animal are almost invariably monoclonal (6, 7). The establishment of MDV latency results in the expression of proteins and RNAs that play a crucial role in the maintenance of the quiescent stage, but also survival of the host cell. Arguably the most important latency- and tumor-associated MDV gene is *Meq*, which serves as a repressor of lytic viral gene products, but at the same time is a potent transcriptional activator of the proto-oncoprotein c-Jun and interacts with p53 as well as Rb. Meq thereby strongly enhances transformation and T cell proliferation, which leads to a rapid onset of tumor formation (2, 16, 17, 21) , making MDV an optimal natural virus-host model for studying herpesvirus integration and the effects on tumorigenesis.

Here we show that herpesvirus telomeric repeats facilitate directed integration into host telomeres, which is crucial for efficient tumor formation and virus reactivation from latency. In the absence of the viral telomeric repeats, herpesvirus integration is severely impaired and occurs at random, single sites within

chromosomes in the form of concatemers. Our observation that genome integration occurs even in the absence of telomere-mediated integration suggests that herpesvirus integration is a prerequisite for transformation and tumorigenesis as well as reactivation and spread to susceptible hosts.

### 5.3. Results and Discussion

**MDV integrates into host telomeres.** MDV is a highly oncogenic animal herpesvirus (21) that is able to integrate its genome at the distal ends of multiple chromosomes (7). To elucidate whether MDV integrates into host telomeres during the latent and tumor phase of infection, we performed pulsed field gel electrophoresis experiments. DNA from MDV-induced lymphoblastoid T cell lines (LCLs) was fragmented with *BclI*, a restriction enzyme frequently cutting in both the host and viral genome, but not in telomeric repeats (Fig. 5.1A). Southern blot analysis using probes specific for the terminal fragment of the $TR_S$ of the viral genome revealed that MDV is integrated into large fragments of up to 450 Kbp that were indigestible with *BclI*. The sizes of the reactive fragments were found to correlate well with that reported for chicken telomeres, which range in size between 10 and 2,000 kbp (Fig. 5.1B) (5). The presence of telomere sequences in fragments containing the viral genome was confirmed using a telomere specific probe (TMR), which demonstrated that fragments reactive with the short repeat region of the genome ($TR_S$, Fig. 5.2A) coincided with bands positive for telomeres (Fig. 5.1B). These results suggest that MDV integrates into or in very close proximity of the telomeres. To further define where exactly MDV integrates into the chromosome, we probed for sequences specific for the other terminal genome region, the terminal repeat long sequences ($TR_L$, Fig. 5.2A). Hybridization with $TR_L$ sequences resulted in very short reactive fragments, indicating that MDV indeed integrates into telomeric sequences, which are located at either

**Figure 5.1.** Identification of MDV integration sites. A) Schematic representation of potential integration sites of the MDV genome within the host chromosome. Fragments resulting from digestion with *BclI* are depicted and expected fragment sizes are given. Terminal MDV genome fragments (red bars), telomeres and *BclI* restriction sites are indicated. B) Pulsed field gel electrophoresis (PFGE) analysis of LCLs using *BclI*. PFGE patterns of three representative cell lines analyzed by Southern blot, probing for the left MDV terminus ($TR_L$), right MDV terminus ($TR_S$) or telomere sequences (TMR) are shown. The 22.4 and 27.0 kbp fragments correspond to uncleaved termini and internal repeat fragments of the viral DNA. Arrows indicate colocalization of fragments that contain the $TR_S$ and high molecular weight telomere sequences. Results are representative of three independent experiments giving identical results. The number of integration sites detected by FISH is given at the bottom of the blot images.

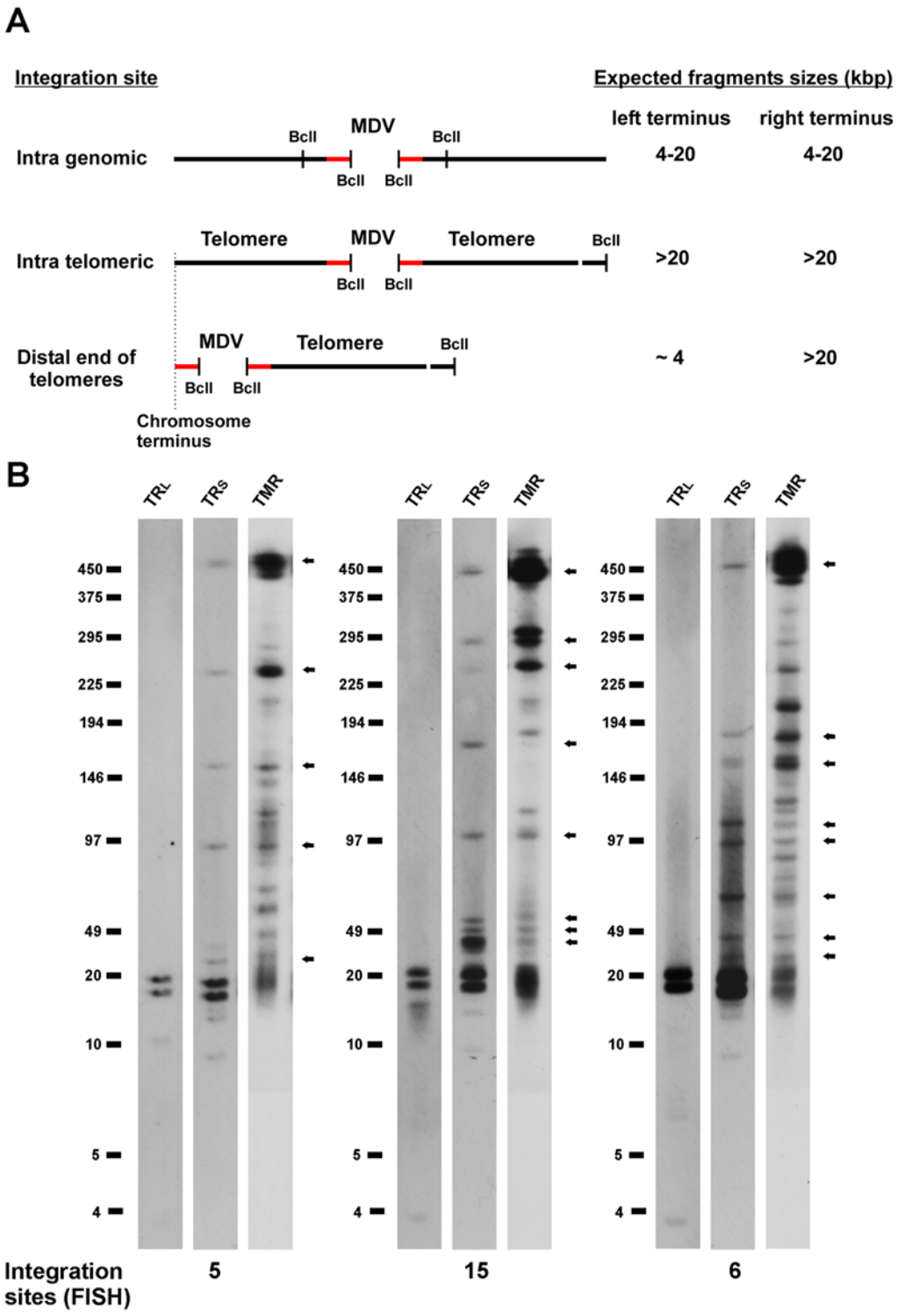
A
Integration site
Expected fragments sizes (kbp)
left terminus
right terminus
Intra genomic
BclI
MDV
BclI
BclI
BclI
4-20
4-20
Intra telomeric
Telomere
MDV
Telomere
BclI
BclI
BclI
>20
>20
Distal end of telomeres
MDV
Telomere
BclI
BclI
BclI
~ 4
>20
Chromosome terminus
B
TRL
TRS
TMR
450
375
295
225
194
146
97
49
20
10
5
4
Integration sites (FISH)
5
15
6

the proximal (subtelomeric) or distal end of the telomeres (Fig. 5.1B). Our results for lymphotropic MDV, therefore, are in agreement with a recent report showing that integration of a human lymphotropic herpesvirus, HHV-6, occurs at the internal end of the telomeres (1).

**Integrity of viral telomeric repeats is dispensable for virus growth *in vitro*.** MDV DNA replication results in the formation of four isomers, where its two unique regions ($U_L$ and $U_S$) can invert relative to the long or short inverted repeat sequences ($TR_L$ and $TR_S$). MDV DNA harbors an additional copy of telomeric repeats that ensures the presence of telomeres at all possible termini of the four DNA isomers (Fig. 5.2A). To address the question of whether the viral telomeric repeats mediate integration and if integration is important for establishment of latency and oncogenesis of MDV, we replaced the repeats present in pRB-1B, an infectious BAC clone of the highly oncogenic RB-1B MDV strain, with either structurally similar repeats harboring only two nucleotide exchanges (pTE1) relative to the telomere sequences or with completely scrambled repeats (pTE2) (Fig. 5.3). We replaced both the terminal and internal telomeric repeat regions that each contain multiple telomeric repeats (mTMR), with up to 100 copies of telomeric repeats, and short telomeric repeats (sTMR), which constantly specify 6 copies (Fig. 5.3). In an additional mutant, we deleted the multiple telomeric repeat region (pΔmTMR) to define the role of the longer repeats (Fig. 5.3). Based on the pTE1, pTE2 and pΔmTMR mutants, we also engineered revertant infectious clones in which the original telomere sequences were restored in both loci (pTE1rev, pTE2rev and pΔmTMRrev). All infectious clones were confirmed by PCR, DNA sequencing and multiple restriction fragment length polymorphism analyses (RFLP) to ensure the integrity of the genome and to exclude fortuitous mutations elsewhere in the genome. Southern blot analysis confirmed that the herpesvirus telomeric repeats and restored telomeres were as designed in the

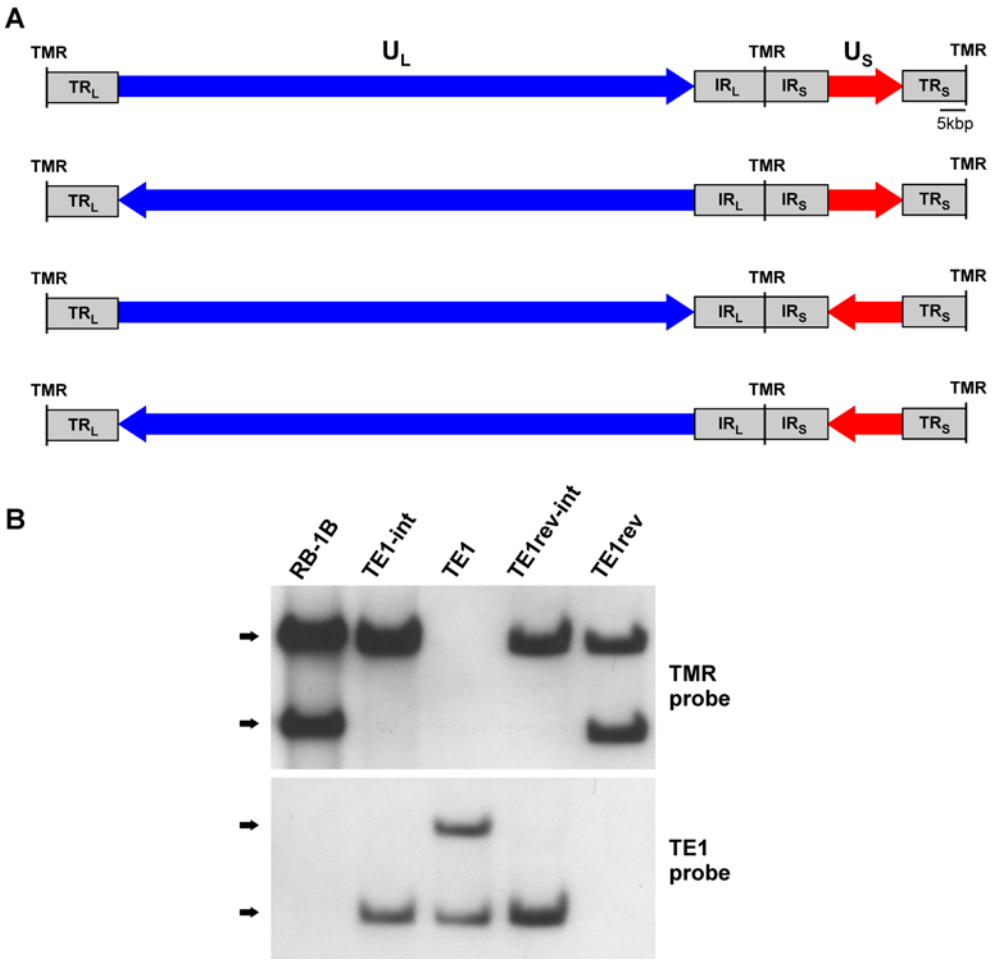


**Figure 5.2.** MDV genomic isomers. Schematic representation of the four isomeric forms of the MDV genome. A) Orientation of the unique-long ($U_L$) and unique-short ($U_S$) segments of the genome is shown relative to each other and the internal and terminal repeat regions of the long ($TR_L$, $IR_L$) and short segment ($IR_S$, $TR_S$). Telomeric repeats (TMR) within the genome are indicated. B) Southern blot analysis of the TE1 mutant viral genome and revertant genomes. Fragments containing telomeric repeats or the TE1 repeat were detected with specific oligonucleotide probes [TMR: $(TTAGGG)_7$ or TE1 $(TAAGGC)_7$] in parental pRB-1B, recombination intermediates and final mutant clones.

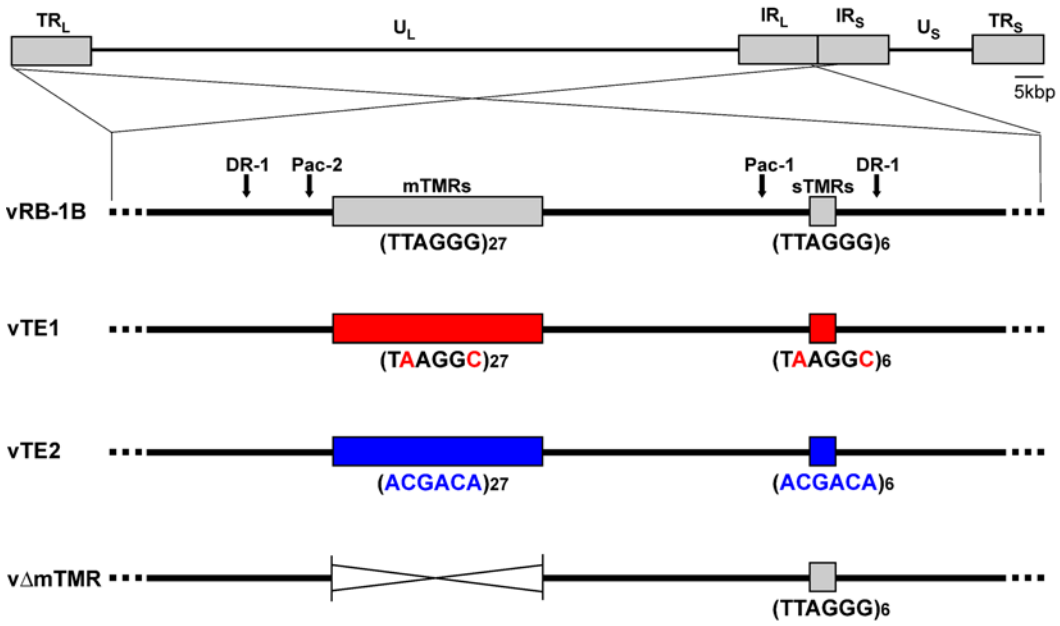


**Figure 5.3.** MDV telomeric repeat mutants. Schematic representation of the MDV genome with a focus on viral a-like sequences containing the multiple (mTMR) and short telomeric repeat region (sTMR) present in the MDV genome. Recombinant BAC constructs in which the telomeric repeats $(TTAGGG)_n$ were replaced by TE1 $(TAAGGC)_n$ or TE2 $(ACGACA)_n$ as well as a BAC construct in which the mTMR region was deleted are shown.

recombinant viral genomes (Fig. 5.2B). Recombinant viruses were reconstituted from BAC DNA in chicken embryo cells, and growth properties were evaluated using multi-step growth kinetics (data not shown) and plaque size assays. The viruses derived from pTE1 (vTE1), pTE2 (vTE2) and pΔmTMR (vΔmTMR) showed growth properties that were virtually indistinguishable from those of parental or revertant viruses (Fig. 5.4A-C), indicating that neither the telomeric repeat sequences nor the mTMRs are important for lytic replication *in vitro*.

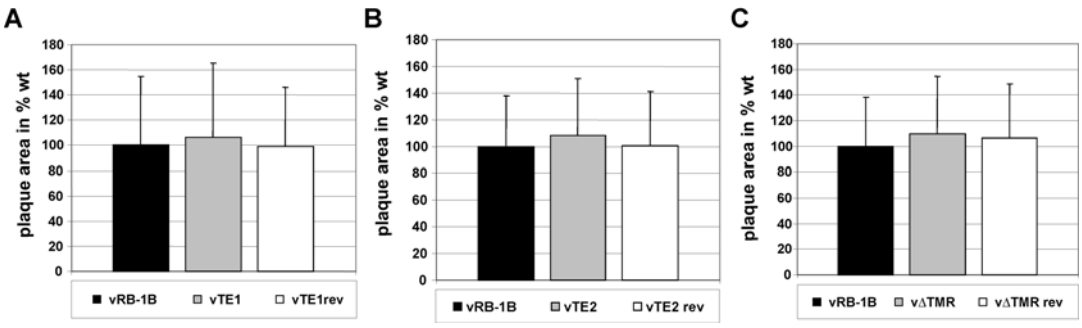


**Figure 5.4.** Mutation of herpesvirus telomeric repeats has no effect on virus replication *in vitro*. A-C), Plaque size assay of vRB-1B, vTE1 and vTE1rev (A), vTE2 and vTE2rev (B) and vΔmTMR and vΔmTMRrev (C). Plaque areas were determined for 50 randomly selected plaques of each virus. Results are shown as mean plaque areas in percent of the parental vRB-1B with standard deviations (error bars).

**Absence of herpesvirus telomeric repeats significantly reduces disease incidence and tumor development.** To address the role of the herpesvirus telomeric repeats in disease and tumor development *in vivo*, one-day old P2a chickens highly susceptibe to MDV infection were experimentally infected with parental vRB-1B, mutant vTE1, vTE2, or vΔTMR viruses, or the respective revertant viruses. After infection, we monitored viral levels in peripheral blood as well as disease and tumor development. Viral loads in the blood were only mildly affected in animals infected with vTE1, vTE2 or vΔmTMR (Fig. 5.5A-C), indicating that herpesvirus telomeric repeats do not play a prominent role in lytic replication *in vivo*, similar to the situation in cultured cells. In stark contrast, disease and tumor development were severely impaired in the telomere mutant viruses. Only 57.1%, 47.1% and 57.9% of chickens, infected with vTE1, vTE2 or vΔmTMR, respectively, developed clinical disease, while 95-100% of animals infected with either parental or revertant viruses presented with clinical disease (Fig. 5.5D-F). Tumor development was also significantly decreased in animals infected with vTE1 (65.7%, p=0.021), vTE2 (48.6%) and vΔmTMR (61.4%, $p=1.98x10^{-6}$) when compared to parental vRB-1B or repair viruses (95-100%) (Fig. 5.5G-I). Taken together, the average tumor incidence of all telomere mutants viruses (vMut) (60.0%) in 9 independent experiments was significantly reduced when compared to parental vRB-1B (97.5%; $p=1.26x10^{-8}$) or revertant viruses (vRev) (98%; $p=3.68x10^{-6}$).

In order to determine if mutation of the telomeric repeats affected spread to naïve hosts within a population, we housed infected and uninfected chickens together. While mutant viruses were fully able to spread to uninfected animals as evidenced by qPCR detection of viral DNA in chicken blood (data not shown), disease incidence in animals infected with vTE1 (11.1%), vTE2 (25.0%) or vΔmTMR (33.3%)

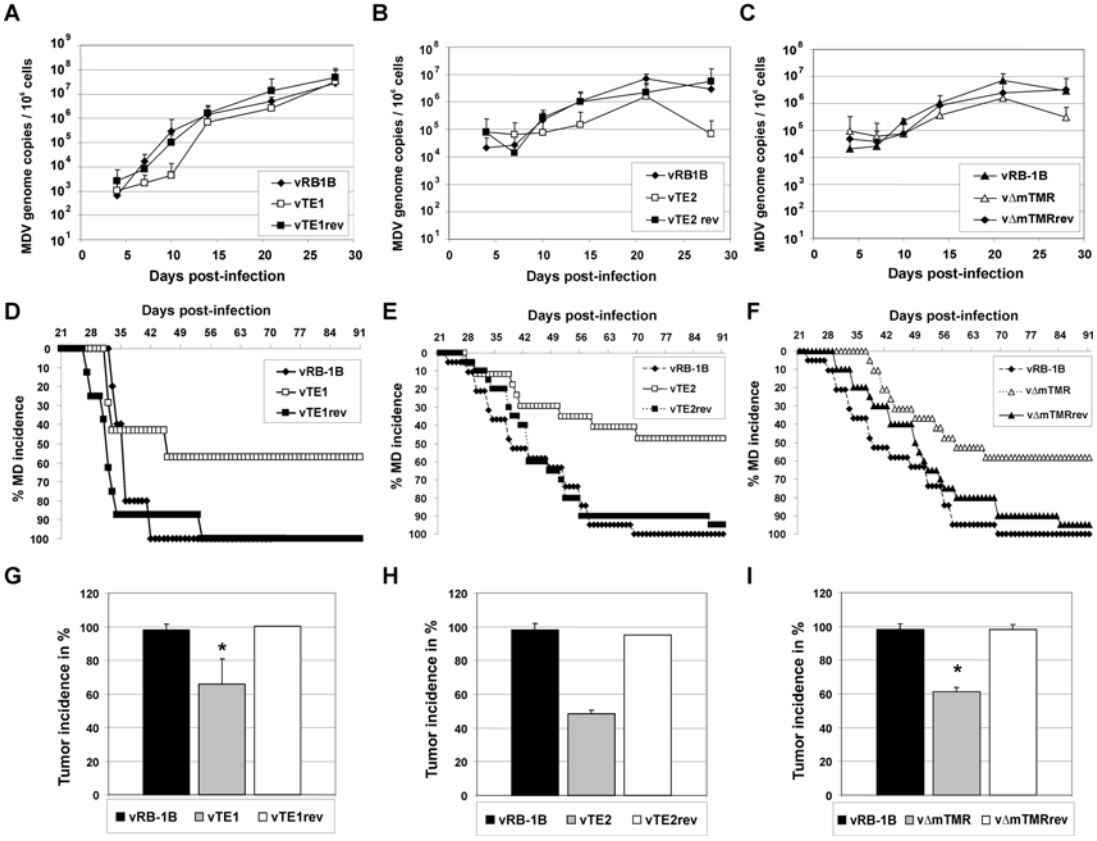


**Figure 5.5.** Mutation of herpesvirus telomeric repeats mildly affects lytic replication, but severely impairs disease and tumor development *in vivo*. A-C), qPCR analysis of the viral genome copies (*ICP4*) relative to host genome copoies (*iNOS*). Blood samples of animals infected with vRB-1B, vTE1 or vTE1rev (A), vTE2 or vTE2rev (B), and vΔmTMR or vΔmTMRrev (C) were taken at 4, 7, 10, 14, 21, and 28 dpi, and total DNA was extracted. Mean MDV genome copies per 1 x $10^6$ genome copies of eight infected chickens per group are shown with standard deviations (error bars). D-F), MD incidence in percent of chickens infected by the intra-abdominal route with vRB-1B (D, n=5; E, n=19; F, n=19), vTE1 (n=7) or vTE1rev (n=8) (D), vTE2 (n=17) or vTE2rev (n=20) (E), and vΔmTMR (n=19) or vΔmTMRrev (n=20) (F) was monitored during the indicated time period after infection. G-I), Tumor incidence in P2a chickens infected with parental vRB-1B or mutant viruses, (G) vTE1 and vTE1rev; (H) vTE2 and vTE2rev, and (I) vΔmTMR and vΔmTMRrev. Results are shown as mean tumor incidences for two (G), three (H) or four (I) independent experiments with standard deviations (error bars). The mean tumor incidences in chickens infected with vTE1 and vΔmTMR were significantly decreased compared to those infected with vRB-1B and are indicated by asterisks (G, p=0.021; I**,** p=1.98x $10^{-6}$). Each group contained between 5 and 20 animals with an average group size of n=13.6.

was dramatically diminished when compared to parental or revertant viruses (80-100%) (Fig. 5.6A-C). Tumor development was also significantly decreased in chickens infected with vTE1 (25.5%), vTE2 (25.0%) or vΔmTMR (27.8%, p=0.01) when compared to those infected with parental vRB-1B or repair viruses (83.8-100%) (Fig. 5.6D-F). Average tumor incidence was significantly reduced after infection with telomere mutant viruses (vMut) (26.3%) in 7 independent experiments when compared to parental vRB-1B (96.8%; $p=2.17x10^{-7}$) or revertant viruses (vRev) (86.6%; $p=7.72x10^{-5}$).

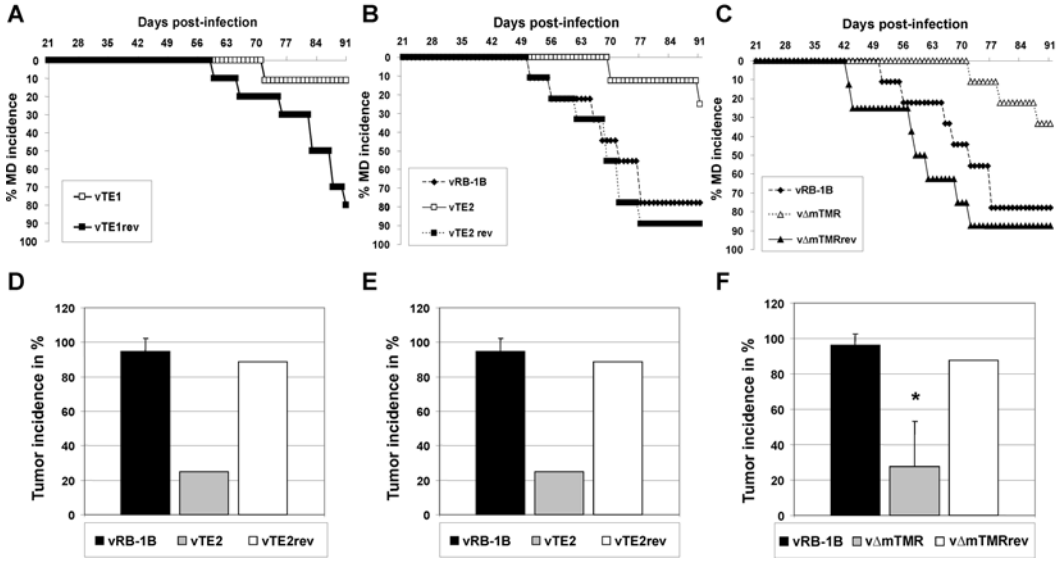


**Figure 5.6.** Disease and tumor development are severely impaired in absence of the viral telomeric repeats in animals infected via the natural route of infection. A-C), MD incidence in percent determined for in-contact animals housed with chickens infected with vRB-1B (n=9), vTE1 (n=10) or vTE1rev (n=10) (A), vTE2 (n=8) or vTE2rev (n=9) (B), and vΔmTMR (n=8) or vΔmTMRrev (n=8) (C). Chickens were monitored during the indicated time period and MD was recorded after necropsy and gross pathological examination. D-E), MD incidence in percent of contact animals housed with animals infected with vRB-1B or mutant viruses. (D) vTE1 and vTE1rev; (E) vTE2 and vTE2rev, and (F) vΔmTMR and vΔmTMRrev. Results are shown as mean tumor incidences of two (D, E) or three independent experiments (F) with standard deviations (error bars). The mean tumor incidences in chickens infected with vΔmTMR in F were significantly decreased compared to incidences in animals infected with vRB-1B and are indicated by asterisks (p=0.011). Each group contained between 2 and 10 animals with an average group size of n=6.7.

The results suggested an even more drastic defect in tumor development of vTE1, vTE2 and vΔmTMR in chickens exposed by the natural route of infection. To confirm that the defect in disease and tumor development was not only restricted to chickens that are highly susceptible to MDV, we also infected N2a chickens, which exhibit increased resistance to MDV infection. Similar to the situation in P2a animals, tumor incidences were drastically reduced after infection of N2a chickens with vTE1 (25.6%), vTE2 (15.8%) or vΔmTMR (15.8%) when compared to the incidence after infection with the corresponding revertant viruses (42.9 – 63.1%) (Fig. 5.7A-C).

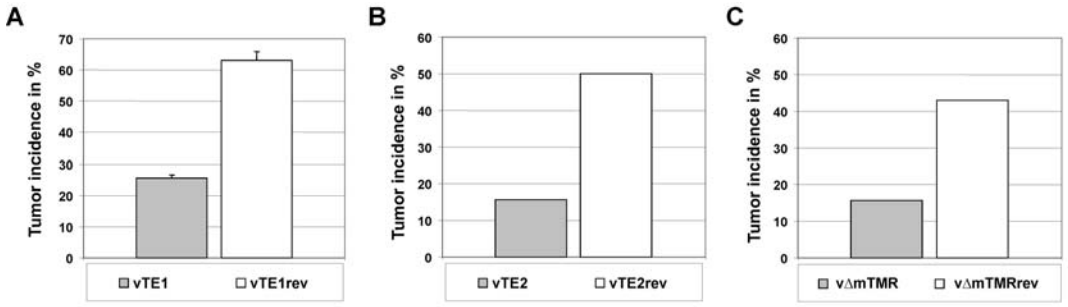


**Figure 5.7.** Tumor development is severely impaired in the absence of viral telomeric repeats in chickens with increased resistance to MDV infection. A-C), Tumor incidence in resistant N2a chickens infected with parental vRB-1B or mutant viruses, (A) vTE1 and vTE1rev; (B) vTE2 and vTE2rev, and (C) vΔmTMR and vΔmTMRrev. Results are shown as mean tumor incidences of one (B,C) or two (A) independent experiments with standard deviations (error bars). Each group contained between 18 and 21 animals with an average group size of n=19.5.

**Integration defects of viruses harboring mutant telomeric repeats.** We then asked whether the telomere mutant viruses were still able to integrate viral DNA into the host genome and performed metaphase fluorescent in situ hybridization (FISH). Analysis of LCLs derived from animals infected with parental vRB-1B, mutant or revertant viruses revealed that vTE1, vTE2 and vΔmTMR had severe integration defects. While integration of wild-type MDV DNA was identified in the telomeres of up to 15 different chromosomes in individual LCLs derived from chickens infected with vRB-1B or revertant viruses, vTE1, vTE2 and vΔmTMR DNA was found integrated invariably in only a single chromosomal locus of each cell line (Fig. 5.8A and B).

We then applied PFGE and Southern blot analyses to confirm whether integration of wild-type MDV DNA as detected by FISH truly represents integration or rather tethering of the viral episome to host chromosomes as was shown for EBV (27) and to investigate the status of viral DNA after integration of viruses with mutant telomeric repeats. Digestion with *SfiI*, a restriction enzyme that does not cut within the MDV genome, allowed the distinction between integrated and non-integrated/tethered MDV DNA (Fig. 5.9A). Extended proteinase K digestion of LCL DNA embedded in agarose was applied to exclude the possibility of tethering of the viral genome to the host chromosome by a proteinaceous structure. Consistent with the FISH results, multiple integration sites with varying sizes of reactive fragments were identified in DNA of LCLs from animals infected with vRB-1B or vTE1rev. In contrast, in the case of LCLs derived from vTE1-infected animals, integration was restricted to a single large DNA fragment of approximately 1.9 Mbp in size. To address whether the integration sites found in vTE1 LCLs also mapped to telomeres, we performed PFGE after *BclI* digestion. Southern blotting confirmed that vTE1 genomes were only detected in low molecular weight fragments of 4-20 kbp in size

A

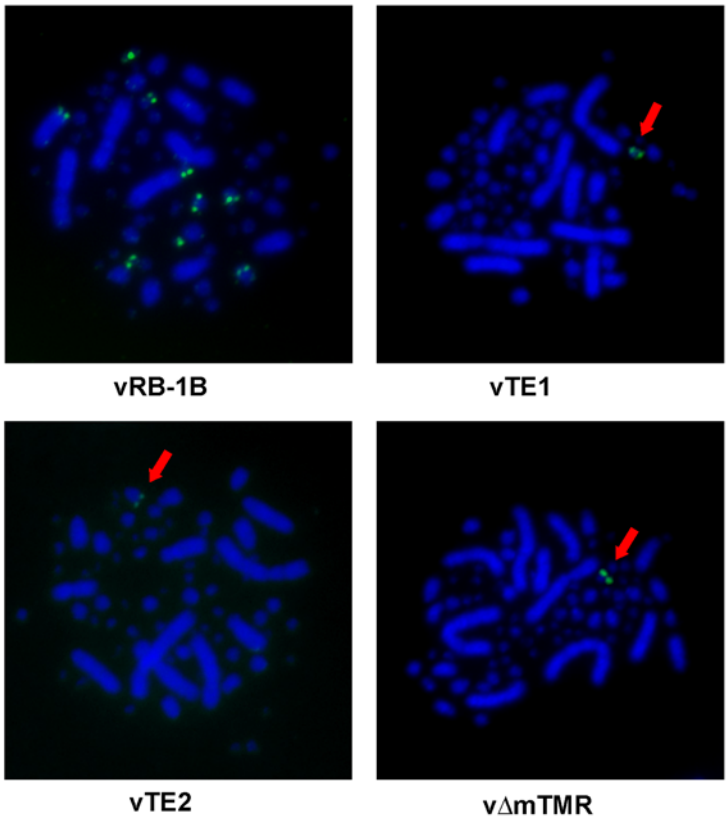


B

| Virus | Number of cell lines | Average number of integration sites | Range |
|---|---|---|---|
| vRB-1B | 10 | 5.55 | 1-15 |
| vTE1 | 5 | 1 | 1 |
| vTE1rev | 2 | 5.5 | 5-6 |
| vTE2 | 7 | 1 | 1 |
| vTE2rev | 2 | 3.5 | 3-4 |
| vΔmTMR | 4 | 1 | 1 |
| vΔmTMRrev | 8 | 2.75 | 1-6 |

**Figure 5.8.** Integration is severely impaired in absence of the viral telomeric repeats. A) Fluorescent in situ hybridization (FISH) analysis detecting MDV integration sites (anti-DIG FITC, green) in metaphase chromosomes (DAPI stain, blue) of representative cell lines of vRB-1B, vTE1, vTE2 and vΔmTMR. B) Average number of integration sites in vRB-1B, mutant and revertant cell lines. The number of analyzed cell lines and the frequencies of integration events are given.

with both the $TR_S$ and $TR_L$ probe. We did not detect, however, any colocalization with telomere-containing fragments (Fig. 5.9B, Fig. 5.10A-C). This data demonstrated that only minimal changes in MDV telomeric repeat sequences abrogated specific integration into host telomeres and suggests that mutant viral DNA integrates randomly into intrachromosomal sites.

In a following series of experiments we determined if MDV integrates as a single viral genome or as concatemers and analyzed MDV genome copy numbers in LCL's. Large genome fragments with high intensity of reactive bands (Fig. 5.9A) had already suggested that vTE1 might be integrated not as a single copy but as multiples in the form of head-to-head or head-to-tail concatemers. Viral copy numbers in LCLs were determined by Southern blot analysis using normalization to copies of host β2 microglobulin (B2M, Fig. 5.10A-D). Although integrated at only one site, MDV genome copy numbers in all vTE1 cell lines analyzed were comparable to those present in CU482, a cell line with 11 integration sites, clearly indicating that vTE1 genomes were integrated as concatemers (Fig. 5.9C, Fig. 5.10E). These findings were also confirmed by qPCR analysis of numbers of viral DNA copies individual LCLs (data not shown).

**Reactivation of viruses with mutant telomeric repeats is severely impaired.** Finally, we asked whether integration of viral genomes into telomeres had a measurable effect on virus fitness, more specifically we assessed reactivation of virus from the latent, quiescent state of infection. While genome maintenance during the latent phase of the virus life cycle is an important transitory phase, reactivation and spread to new hosts are essential for continued virus survival. Since integration into host telomeres could allow virus genome mobilization through homologous recombination between virus and host telomeres, we analyzed the efficiency of virus reactivation from LCLs. Reactivation assays that rely on induction of the lytic

**Figure 5.9.** Integration occurs randomly in the absence of viral telomeric repeats. A) Schematic representation and corresponding PFGE and Southern blot analysis of LCL DNA digested with *SfiI*. Fragment sizes generated by *SfiI* digestion of integrated and non-integrated MDV genomes are depicted and sizes are given. The size of the linear MDV genome observed during lytic replication is indicated by an arrow. Results are representative of three independent Southern blot analyses. B) Southern blot of DNA of LCLs derived from animals infected with vTE1 and digested with *BclI*. Potential intragenomic and telomeric integration sites are indicated. Results are representative of three independent Southern blot analyses. C) Quantification of MDV copies in tumor cells. Results are shown as mean herpesvirus genome copies detected by the $TR_L$ probe relative to B2M in three independent experiments. The data are shown relative to LCL CU482 derived from a vRB-1B-infected chicken with standard deviations (error bars).

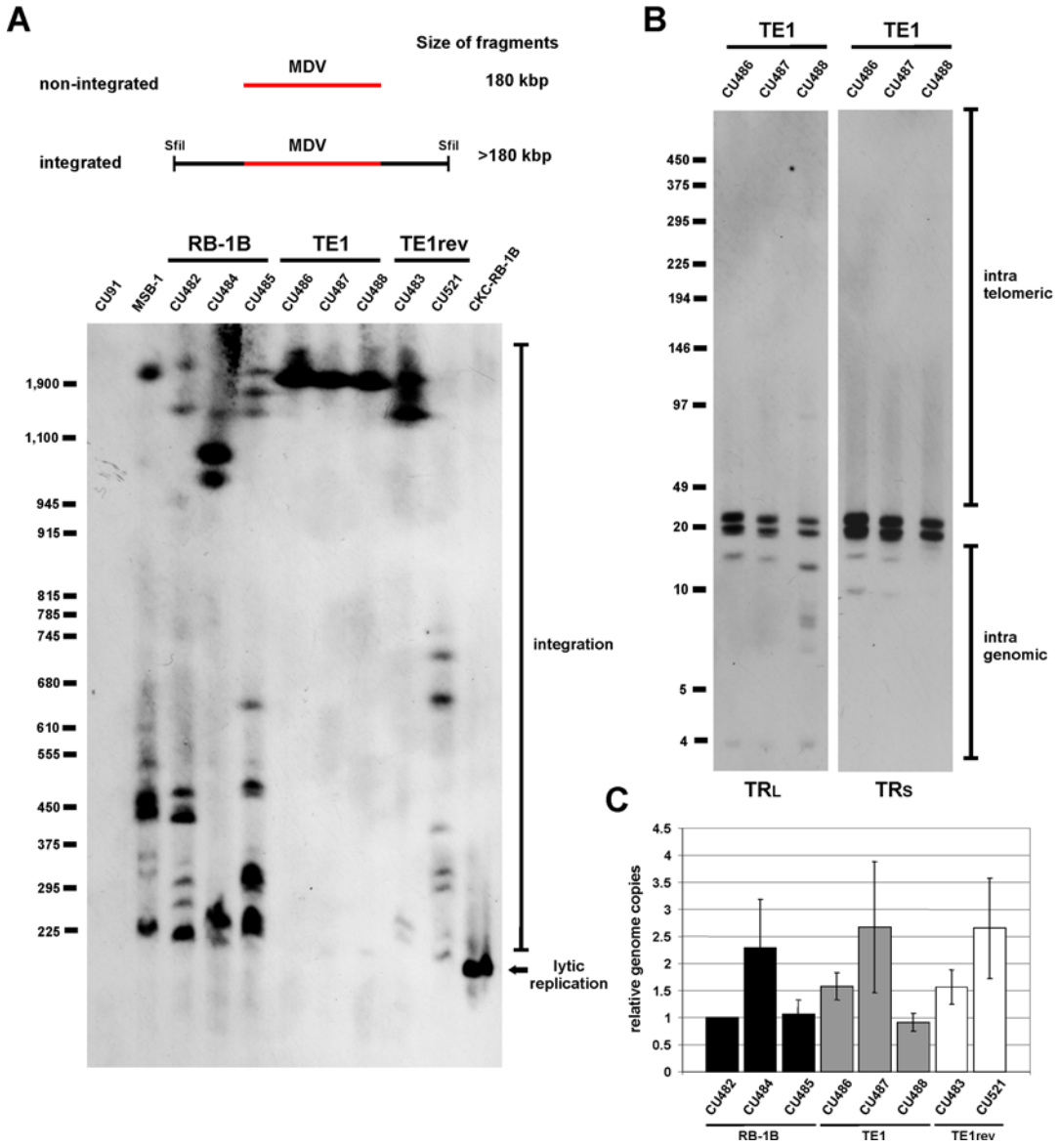
A
Size of fragments
non-integrated
MDV
180 kbp
integrated
SfiI
MDV
SfiI
>180 kbp
RB-1B
TE1
TE1rev
CU91
MSB-1
CU482
CU484
CU485
CU486
CU487
CU488
CU483
CU521
CKC-RB-1B
1,900
1,100
945
915
815
785
745
680
610
555
450
375
295
225
integration
lytic replication
B
TE1
TE1
CU486
CU487
CU488
CU486
CU487
CU488
450
375
295
225
194
146
97
49
20
10
5
4
intra telomeric
intra genomic
TRL
TRS
C
relative genome copies
4.5
4
3.5
3
2.5
2
1.5
1
0.5
0
CU482
CU484
CU485
CU486
CU487
CU488
CU483
CU521
RB-1B
TE1
TE1rev

**Figure 5.10.** Herpesvirus telomere mutants integrate as concatemers into chromosomes. A-D) Pulsed field gel electrophoresis (PFGE) and Southern blot analysis of DNA of LCLs derived from chickens infected with vRB-1B, vTE1 or vTE1rev. DNA was digested with *BclI* and fragments containing the left terminus ($TR_L$, A), right terminus ($TR_S$ ,B), telomere sequences (TMR, C) or β2 microglobulin (B2M, D) were detected using sequence-specific DIG-labeled probes. Results are representative for three independent experiments. E) Quantification of MDV copies in tumor cells. Results are shown as mean herpesvirus genome copies detected by the $TR_S$ probe relative to B2M in three independent experiments. The data are shown relative to LCL CU482 derived from a vRB-1B-infected chicken with standard deviations (error bars).

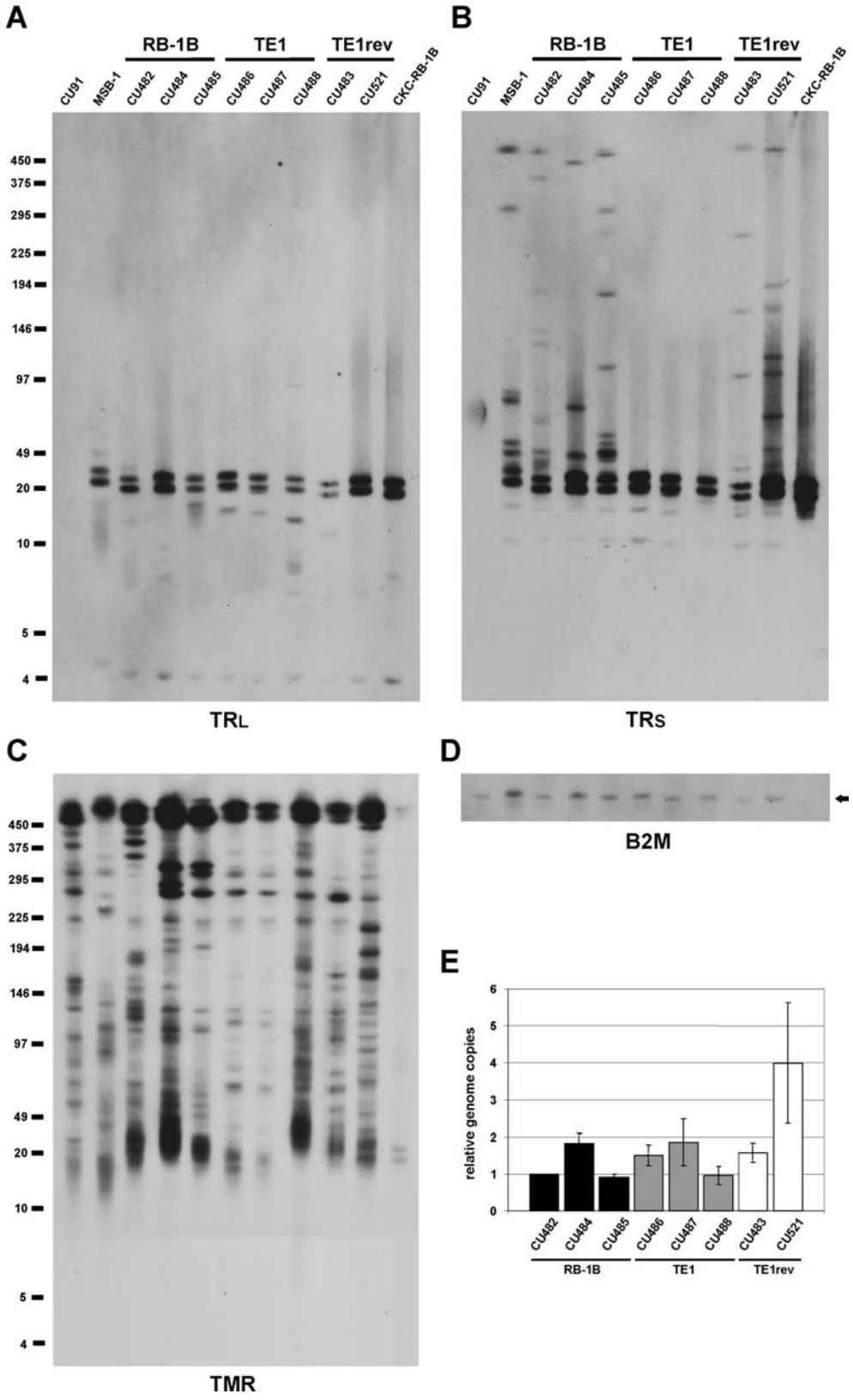
A
RB-1B
TE1
TE1rev
CU91
MSB-1
CU482
CU484
CU485
CU486
CU487
CU488
CU483
CU521
CKC-RB-1B
450
375
295
225
194
146
97
49
20
10
5
4
TRL
B
TRS
C
TMR
D
B2M
E
relative genome copies
6
5
4
3
2
1
0

replication cycle from latent genomes revealed that vTE1, vTE2 and vΔmTMR were severely impaired with respect to their efficiency of genome mobilization and reactivation from latently infected cells (Fig. 5.11A-C). The average number of plaques induced on CEC's per $1x10^6$ tumor cells was significantly (5- to 39-fold) decreased in the case of cell lines derived from birds infected with vTE1 ($1.13 \times 10^4$), vTE2 ($7.06 \times 10^4$) and vΔmTMR ($0.91 \times 10^4$) when compared to those from birds infected with parental vRB-1B ($3.53 \times 10^5$) (Fig. 5.11A-C). We concluded that integration of MDV DNA into host telomeres serves a purpose beyond genome maintenance during latency by allowing efficient and rapid mobilization of virus genomes in response to external cues for initiation of the lytic phase of infection.

In summary, we conclude from our results that telomere-mediated integration plays a critical role in the establishment of the latent state and tumorigenesis of MDV on the one hand, and mobilization of latent genomes required for virus reactivation and spread to other individuals in a population on the other hand (Fig. 5.12). Therefore, our data proves that integration of herpesvirus DNA is not, as had been speculated earlier, a dead-end, but an integral part of the virus' life cycle.

## 5.4. Material and Methods

**Cells and viruses.** Chicken embryo cells (CEC) were prepared from specific-pathogen-free (SPF) embryos and maintained as described previously (20). Recombinant viruses were reconstituted in CEC by $CaPO_4$ transfection of purified bacterial artificial chromosome (BAC) DNA as described previously (12, 25). The mini-F sequences flanked by loxP sites within the infectious clones were removed by co-transfection with a Cre recombinase expression vector (pCAGGS-NLS/Cre) (12). Removal of mini-F sequences was ensured by analyzing recombinant virus stocks via PCR as described previously (12). Virus propagation as well as determination of virus

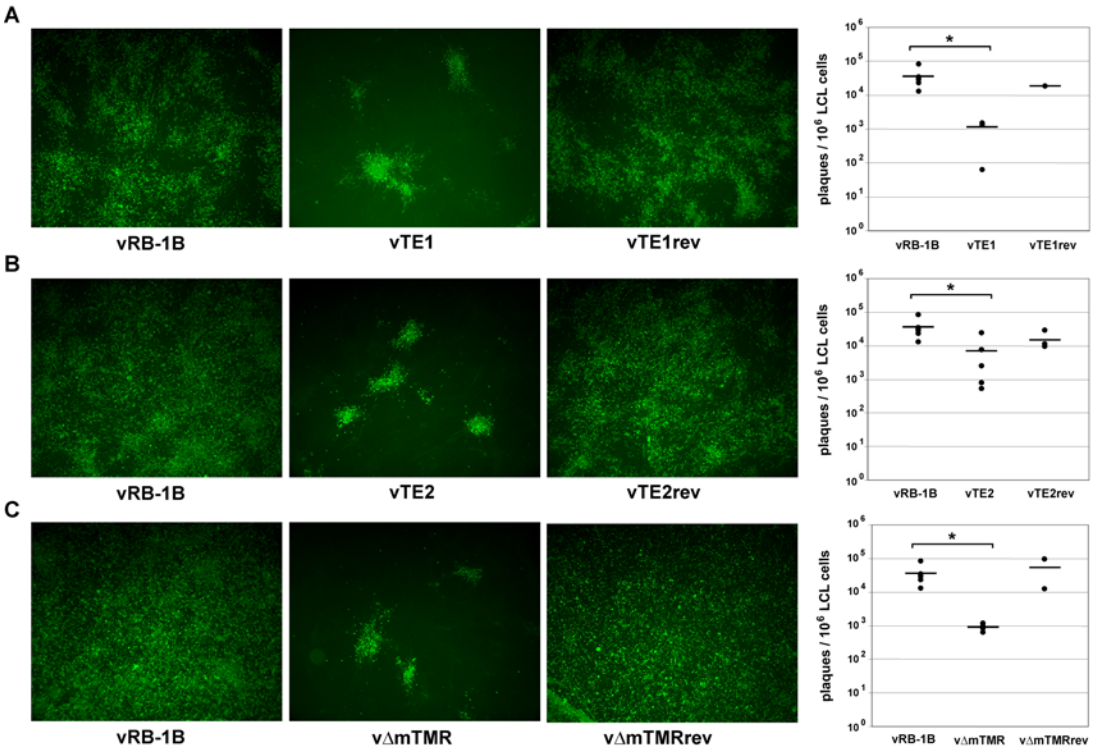


**Figure 5.11.** Reactivation is significantly impaired in the absence of viral telomeric repeats. A-C) Reactivation assay using LCL's derived from animals infected with vRB-1B, vTE1 or vTE1rev (A), vTE2 or vTE2rev (B), or vΔmTMR or vΔmTMRrev (C). Representative images of virus reactivation in chicken embryo cells are shown. Quantification of reactivation assays is shown as average number of plaques per 1 x $10^6$ tumor cells for each individual cell line (A-C, right panel), performed in triplicate for each of three independent experiments. Reactivation of lytic virus from vTE1, vTE2 and vΔmTMR-derived LCLs was significantly reduced compared to that from vRB-1B-derived LCLs as indicated by the asterisks (A, p=0.013; B, p=0.039; C, p=0.025).

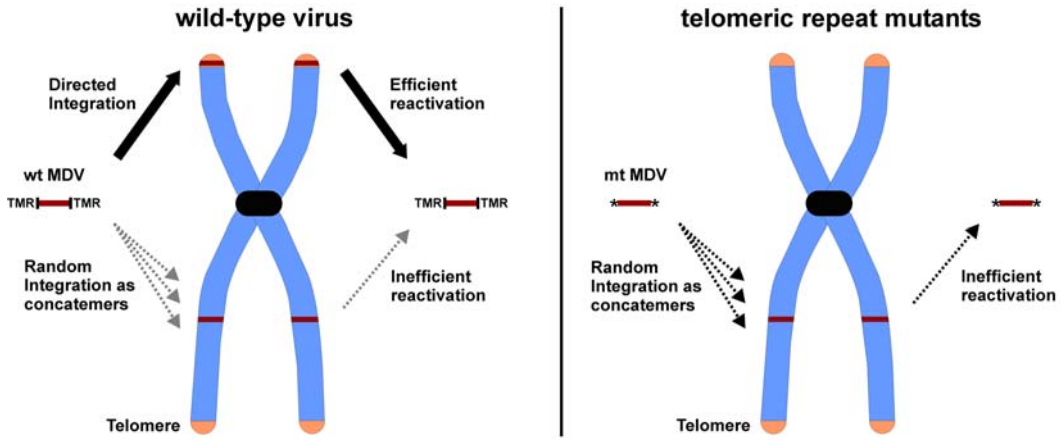


**Figure 5.12.** Model of herpesvirus genome integration and mobilization in presence and absence of viral telomeric repeats. Integration of wild type virus into host telomeres is efficiently mediated by the herpesvirus telomeric repeats. It allows efficient tumorigenesis and reactivation from latency, while random integration events are rare. Telomere mutant viruses (vTE1, vTE2 and vΔmTMR) are not able to integrate into telomeres, but integrate at random sites within chromosomes in form of concatemers. This integration process is inefficient and results in significantly reduced tumorigenicity and reactivation of the virus. Reactivation from latency occurs very efficient in the presence and is severely impaired in the absence of the herpesvirus telomeric repeats.

growth kinetics and plaque sizes were performed as described previously (26).

**Generation of mutant MDV**. The MDV telomere region (Fig. 5.3) was amplified from pRB-1B and cloned into the pCR2.1 Topo vector (Invitrogen) resulting in pTMR. Plasmids containing a synthetic telomere region in which viral telomeric repeats $(TTAGGG)_n$ were replaced by telomere exchange repeats 1 $(TAAGGC)_n$ or telomere exchange repeats 2 $(ACGACA)_n$ were obtained from Celtec and Genscript, respectively, and designated pTE1 and pTE2. Transfer plasmids for mutagenesis were generated as described previously (30). Briefly, the *aphAI*-I-*Sce*I cassette was amplified from pEPkan-SII and inserted into pTMR, pTE1 or pTE2 using a unique *SacI* or *NheI* restriction site within the viral telomere region resulting in plasmids pTMR-transfer, pTE1-transfer and pTE2-transfer, respectively. Corresponding transfer plasmids and oligonucleotides (Table 5.1) were used for mutagenesis as described previously (30). All clones were confirmed by PCR, DNA sequencing, Southern blot analysis and multiple restriction fragment length polymorphism analyses (RFLP) to ensure integrity of the genomes and to exclude fortuitous mutations elsewhere in the genome (data not shown). Primers used for transfer plasmids and mutagenesis are given in Table 5.1.

***In vivo* experiments.** SPF P2a (MHC haplotype $B^{19}B^{19}$) or N2a (MHC haplotype $B^{21}B^{21}$) chickens were experimentally infected by intra-abdominal inoculation with 500 to 2,000 plaque-forming units at day 1 of age or via the natural route of infection by co-housing of uninfected with infected animals. All experimental procedures were conducted in compliance with approved Institutional Animal Care and Use Committee (IACUC) protocols under the internal approval number 2002-0085. Chickens were evaluated for symptoms of MDV-induced disease on a daily basis and examined for tumorous lesions when clinical symptoms were evident or at termination of the experiments.

**Table 5.1.** Oligonucleotides used for cloning, Southern blot probes and BAC mutagenesis.

| Construct name | | sequence (5' → 3') |
|---|---|---|
| **pTMR** | for | CGGATGCTGGAGCTGCC |
| | rev | CTGCGAGATGCGGGCTG |
| **pTMR-transfer** | for | GCTTTGAGCTCGGGATCGAGACTAGGTTCACGGTAGGGATAACAGGGTAATCGATTT |
| | rev | ATCCCGAGCTCAAAGCACGGAAATCCACACTGGAACCGCCAGTGTTACAACCAATTAACC |
| **pTE1-transfer** | for | CTAAGGCTAGCGCTAAGGGTTCAGGCCTAGGCTAAGTAGGGATAACAGGGTAATCGATTT |
| | rev | TAGCGCTAGCCTTAGCCTTAGGCCAGTGTTACAACCAATTAACC |
| **pTE2-transfer** | for | GCTTTGAGCTCGGGATCGAGACTAGGTTCACGGTAGGGATAACAGGGTAATCGATTT |
| | rev | ATCCCGAGCTCAAAGCACGGAAATCCACACTGGAACCGCCAGTGTTACAACCAATTAACC |
| **TE1, TE2 & Rev** | for | CGCGCCCTCTAACCCTCTCGCGGCCACACACTGTATAAAAAAAAATTTCGTCGAACC |
| | rev | GGAGCAGGGATGTGGTCTACGAACCGGATGTAGTAGTGCAGGCAGGTGTACAACTGC |
| **ΔmTMR** | for | GTATAAAAAAAAATTTCGTCGAACCCCTAGCGGCCAACCGATCCCCCCAAATTTTCACCC |
| | rev | GGAGCAGGGATGTGGTCTACGAACCGGATGTAGTAGTGCAGGCAGGTGTACAACTGC |
| **TR$_L$ probe** | for | TCCCTTCCCCTTTTACTTTGTTTG |
| | rev | TGCCGCCCCAACTGCTCAT |
| **TRs probe** | for | CCCGCCGATGCTGCCCTAAAC |
| | rev | TCCGCCAGACACCTACTCAAG |
| **B2M probe** | for | TGCGGCTCCTTCAGCGTCTCGTG |
| | rev | GAAGGCGGCGGCGGTGGTG |

**DNA extraction and qPCR analysis.** DNA was extracted from whole chicken blood using the EZ 96 blood DNA kit (Omega Bio-Tek) and MDV genomic copies were determined by qPCR (11, 13). MDV DNA copy numbers were detected using primers and probe specific for the *ICP4* locus and normalization was achieved by determining copies of the chicken inducible nitric oxide synthase (*iNOS*) gene (12).

**Lymphoblastoid cell lines (LCLs).** LCLs were generated as described previously (3, 4). Tumor tissue from MDV-infected animals was harvested and sieved through a cell strainer before lymphocytes were isolated using Histopaque 1119 (Sigma) density gradient centrifugation. Purified cells were cultivated in Leibovitz-McCoy medium as

modified by Hahn (Cellgro) supplemented with 10% FBS and 5% chicken serum at 41°C under a 5% $CO_2$ atmosphere.

**Fluorescence in situ hybridization (FISH).** Metaphase chromosome preparations and FISH analysis were performed as described previously (23). A digoxigenin (DIG)-labeled MDV whole genome probe was generated via the DIG High Prime kit (Roche) and used to detect MDV integration sites that were visualized using a FITC-conjugated anti-DIG antibody (Sigma). Metaphase FISH preparations were analyzed using the Axio Imager M1 system and the Axiovision software (Zeiss).

**Pulsed field gel electrophoresis (PFGE) analysis.** PFGE analysis was performed as described previously (10). LCLs (1 x $10^7$/ml) were embedded in 1% agarose and digested at 50ºC for 48 h hours in lysis buffer (0.5 M EDTA, 1% (w/v) N-laurylsarcosine) containing 1 mg/ml Proteinase K. Proteinase K was inactivated with 0.01 mM phenylmethanesulfonyl fluoride and agarose plugs digested with either *SfiI* or *BclI* (New England Biolabs) overnight according to manufacturer's instructions. DNA fragments were resolved by PFGE using the CHEF-DR III system (Bio Rad). *SfiI* fragments were resolved with 50-100 s and *BclI* fragments with 1-25 s switch time gradients at 6V/cm, 14ºC, a 120º angle and run times of 36 h and 24 h, respectively.

**Southern blot analysis.** Southern blots were performed after DNA transfer onto a positively charged nylon membrane (Whatman) (24). Fragments containing the $TR_L$ or $TR_S$ termini of the MDV genome were identified with specific probes generated via the PCR DIG Probe Synthesis kit (Roche). Telomeric repeats or mutant repeats were detected using DIG-labeled oligonucleotide probes (MWG Eurofins, Table 5.1).

**Reactivation assay**. Established LCLs were purified via Histopaque 1119 gradient centrifugation (Sigma) (22), washed with PBS, and serial 10-fold dilutions (1 x $10^3$, 1 x $10^4$, 1 x $10^5$ or 1 x $10^6$) LCLs were seeded on fresh CEC cultures. MDV reactivation was stimulated by co-cultivation of LCLs with CEC at low serum

concentrations (0.1% FBS) and a temperature shift to 37º C as described previously (4). LCLs were completely removed 24 h after seeding through extensive washing. Four days after infection, CEC cultures were fixed, stained and analyzed by immunofluorescence using a chicken anti-MDV antiserum and visualized by an Alexa 488 conjugated anti-chicken antibody.

**Statistical analysis.** Significant differences in means of tumor incidences (Fig. 5.5F and H; Fig. 5.6F) and LCL reactivation assays (Fig. 5.11A-C) were determined using Student's *t* test.

## 5.5. Acknowledgments

We thank Kerstin Osterrieder for help with the statistical calculations and advice. We thank Annemarie Egerer for her technical assistance. We thank Joel Baines and Colin Parrish for editing the manuscript. This study was supported by PHS grant 5R01CA127238 and an unrestricted grant from the Freie Universität Berlin to NO.

REFERENCES


1. **Arbuckle, J. H., M. M. Medveczky, J. Luka, S. H. Hadley, A. Luegmayr, D. Ablashi, T. C. Lund, J. Tolar, K. De Meirleir, J. G. Montoya, A. L. Komaroff, P. F. Ambros, and P. G. Medveczky**. 2010. The latent human herpesvirus-6A genome specifically integrates in telomeres of human chromosomes in vivo and in vitro. Proc. Natl. Acad. Sci. U. S. A **107**:5563-5568.

2. **Brown, A. C., S. J. Baigent, L. P. Smith, J. P. Chattoo, L. J. Petherbridge, P. Hawes, M. J. Allday, and V. Nair**. 2006. Interaction of MEQ protein and C-terminal-binding protein is critical for induction of lymphomas by Marek's disease virus. Proc. Natl. Acad. Sci. U. S. A **103**:1687-1692.

3. **Calnek, B. W., K. K. Murthy, and K. A. Schat**. 1978. Establishment of Marek's disease lymphoblastoid cell lines from transplantable versus primary lymphomas. Int. J Cancer **21**:100-107.

4. **Calnek, B. W., W. R. Shek, and K. A. Schat**. 1981. Spontaneous and induced herpesvirus genome expression in Marek's disease tumor cell lines. Infect. Immun. **34**:483-491.

5. **Delany, M. E., L. M. Daniels, S. E. Swanberg, and H. A. Taylor**. 2003. Telomeres in the chicken: genome stability and chromosome ends. Poult. Sci. **82**:917-926.

6. **Delecluse, H. J. and W. Hammerschmidt**. 1993. Status of Marek's disease virus in established lymphoma cell lines: herpesvirus integration is common. J. Virol. **67**:82-92.

7. **Delecluse, H. J., S. Schuller, and W. Hammerschmidt**. 1993. Latent Marek's disease virus can be activated from its chromosomally integrated state in herpesvirus-transformed lymphoma cells. EMBO J. **12**:3277-3286.

8. **Gulley, M. L., M. Raphael, C. T. Lutz, D. W. Ross, and N. Raab-Traub**. 1992. Epstein-Barr virus integration in human lymphomas and lymphoid cell lines. Cancer **70**:185-191.

9. **Hall, C. B., M. T. Caserta, K. Schnabel, L. M. Shelley, A. S. Marino, J. A. Carnahan, C. Yoo, G. K. Lofthus, and M. P. McDermott**. 2008. Chromosomal integration of human herpesvirus 6 is the major mode of congenital human herpesvirus 6 infection. Pediatrics **122**:513-520.

10. **Herschleb, J., G. Ananiev, and D. C. Schwartz**. 2007. Pulsed-field gel electrophoresis. Nat. Protoc. **2**:677-684.

11. **Jarosinski, K., L. Kattenhorn, B. Kaufer, H. Ploegh, and N. Osterrieder**. 2007. A herpesvirus ubiquitin-specific protease is critical for efficient T cell lymphoma formation. Proc. Natl. Acad. Sci. U. S. A **104**:20025-20030.

12. **Jarosinski, K. W., N. G. Margulis, J. P. Kamil, S. J. Spatz, V. K. Nair, and N. Osterrieder**. 2007. Horizontal transmission of Marek's disease virus requires US2, the UL13 protein kinase, and gC. J Virol **81**:10575-10587.

13. **Jarosinski, K. W., N. Osterrieder, V. K. Nair, and K. A. Schat**. 2005. Attenuation of Marek's disease virus by deletion of open reading frame RLORF4 but not RLORF5a. J Virol **79**:11647-11659.

14. **Jones, C.** 1998. Alphaherpesvirus latency: its role in disease and survival of the virus in nature. Adv. Virus Res. **51**:81-133.

15. **Kishi, M., H. Harada, M. Takahashi, A. Tanaka, M. Hayashi, M. Nonoyama, S. F. Josephs, A. Buchbinder, F. Schachter, D. V. Ablashi, and .** 1988. A repeat sequence, GGGTTA, is shared by DNA of human herpesvirus 6 and Marek's disease virus. J Virol **62**:4824-4827.

16. **Liu, J. L. and H. J. Kung**. 2000. Marek's disease herpesvirus transforming protein MEQ: a c-Jun analogue with an alternative life style. Virus Genes **21**:51-64.

17. **Lupiani, B., L. F. Lee, X. Cui, I. Gimeno, A. Anderson, R. W. Morgan, R. F. Silva, R. L. Witter, H. J. Kung, and S. M. Reddy**. 2004. Marek's disease virus-encoded Meq gene is involved in transformation of lymphocytes but is dispensable for replication. Proc. Natl. Acad. Sci. U. S. A **101**:11815-11820.

18. **Luppi, M., P. Barozzi, R. Marasca, and G. Torelli**. 1994. Integration of human herpesvirus-6 (HHV-6) genome in chromosome 17 in two lymphoma patients. Leukemia **8 Suppl 1**:S41-S45.

19. **Luppi, M., R. Marasca, P. Barozzi, S. Ferrari, L. Ceccherini-Nelli, G. Batoni, E. Merelli, and G. Torelli**. 1993. Three cases of human herpesvirus-6 latent infection: integration of viral genome in peripheral blood mononuclear cell DNA. J. Med. Virol. **40**:44-52.

20. **Osterrieder, N.** 1999. Sequence and initial characterization of the U(L)10 (glycoprotein M) and U(L)11 homologous genes of serotype 1 Marek's Disease Virus. Arch. Virol. **144**:1853-1863.

21. **Osterrieder, N., J. P. Kamil, D. Schumacher, B. K. Tischer, and S. Trapp**. 2006. Marek's disease virus: from miasma to model. Nat. Rev. Microbiol. **4**:283-294.

22. **Parcells, M. S., R. L. Dienglewicz, A. S. Anderson, and R. W. Morgan**. 1999. Recombinant Marek's disease virus (MDV)-derived lymphoblastoid cell lines: regulation of a marker gene within the context of the MDV genome. J. Virol. **73**:1362-1373.

23. **Rens, W., B. Fu, P. C. O'Brien, and M. Ferguson-Smith**. 2006. Cross-species chromosome painting. Nat. Protoc. **1**:783-790.

24. **Sambrook, J. and D.F.Fritsch and T.Maniatis**. 1989. Molecular cloning: a laboratory manual. Cold Spring Harbor, N.Y..

25. **Schumacher, D., B. K. Tischer, W. Fuchs, and N. Osterrieder**. 2000. Reconstitution of Marek's disease virus serotype 1 (MDV-1) from DNA cloned as a bacterial artificial chromosome and characterization of a glycoprotein B-negative MDV-1 mutant. J. Virol. **74**:11088-11098.

26. **Schumacher, D., B. K. Tischer, S. Trapp, and N. Osterrieder**. 2005. The protein encoded by the US3 orthologue of Marek's disease virus is required for efficient de-envelopment of perinuclear virions and involved in actin stress fiber breakdown. J Virol **79**:3987-3997.

27. **Sears, J., M. Ujihara, S. Wong, C. Ott, J. Middeldorp, and A. Aiyar**. 2004. The amino terminus of Epstein-Barr Virus (EBV) nuclear antigen 1 contains AT hooks that facilitate the replication and partitioning of latent EBV genomes by tethering them to cellular chromosomes. J Virol **78**:11487-11505.

28. **Secchiero, P., J. Nicholas, H. Deng, T. Xiaopeng, N. van Loon, V. R. Ruvolo, Z. N. Berneman, M. S. Reitz, Jr., and S. Dewhurst**. 1995. Identification of human telomeric repeat motifs at the genome termini of human herpesvirus 7: structural analysis and heterogeneity. J Virol **69**:8041-8045.

29. **Stevens, J. G.** 1989. Human herpesviruses: a consideration of the latent state. Microbiol. Rev. **53**:318-332.

30. **Tischer, B. K., J. von Einem, B. Kaufer, and N. Osterrieder**. 2006. Two-step red-mediated recombination for versatile high-efficiency markerless DNA manipulation in Escherichia coli. Biotechniques **40**:191-197.

# CHAPTER SIX

## Summary and Conclusions

## 5.1. VZV P-Oka BAC – generation of a novel tool for VZV research

Generation of recombinant varicella-zoster viruses (VZV) harboring targeted mutations has been one of the major challenges in VZV research. Mutagenesis approaches using homologuous recombination in mammalian cells is very inefficient and requires plaque purification, which is extremely difficult due to the slow replication and highly cell-associated nature of VZV. In Chapter 2 I describe the establishment of a full-length bacterial artificial chromosome (BAC) system for strain P-Oka strain based on previously established overlapping cosmid clones (1). The BAC system (pP-Oka) allowed efficient generation of VZV mutants in *E.coli* and is now widely used by VZV researchers. Transfection of pP-Oka in human melanoma cells (MeWo) resulted in the reconstitution of the virus. Replication of BAC- derived virus was indistinguishable from wild type P-Oka. Since most applications, such as vaccine development, require the removal of foreign bacterial sequences that facilitate replication in *E.coli* (mini-F sequence), we developed a strategy that accomplished the elimination of all foreign nucleotides. Hereby, an inversely oriented sequence duplication between the positive selection marker (antibiotic resistance gene) and the bacterial replicon allowed the removal of the mini-F sequences in mammalian cells, while the sequences are maintained in *E. coli* through antibiotic selection.

In addition, we previously established a two-step Red-mediated mutagenesis technique which allowed a highly efficient and reliable modification of the newly established VZV BAC (13). Using these two newly established tools, we investigated the role of the major tegument protein encoded by *ORF9,* a homologue of herpes simplex virus 1 (HSV-1) UL49 (VP22) in VZV replication. We mutated the *ORF9* start codon in pP-Oka, which abrogated ORF9 expression, and generated revertant viruses in which the start codon was restored. In the absence of the *ORF9* gene product, virus replication was severely impaired, while wild type and revertant viruses

had comparable growth kinetics. Delivery of *ORF9* in *trans* via baculovirus-mediated gene transfer partially restored virus replication of *ORF9*-deficient viruses, confirming that the growth defect is attributed to *ORF9* gene function.

Our data clearly demonstrates that *ORF9* gene function is essential for VZV replication and is in agreement with previous reports on the *ORF9* homologue in Marek's disease virus (MDV) UL49 that is crucial for MDV replication *in vitro*. In contrast to VZV and MDV that are highly cell-associated *in vitro* and *in vivo*, the products of the *ORF9* homologues in other alphaherpesviruses that produce extracellular, cell-free virus, such as HSV-1 and bovine herpesvirus 1 (BHV-1), are not essential *in vitro* (5, 9, 12). Intriguingly, cell-to-cell spread is significantly reduced in BHV-1 (8), suggesting an important role of the *ORF9* protein and at least some of its homologues in cell-to-cell spread. Recent reports also showed that HSV-1 pUL49 is required for efficient viral spread *in vivo*, underlining the importance of this group of tegument proteins in herpesvirus replication and pathogenesis (4).

### 5.2. ORFS/L – implications on UL inversions

In addition to that, we used the pP-Oka system to investigate the role of *ORFS/L* (*ORF0*), which is one of the VZV genes with no known function and no direct orthologue in other alphaherpesviruses (7). *ORFS/L* is located at the extreme terminus of $U_L$, directly adjacent to the a-like sequences, which are known to be involved in cleavage and packaging of viral DNA. In Chapter 2, we demonstrate that the *ORFS/L* protein localizes to the Golgi network in infected and transfected cells, suggesting that it is a functional orthologue of HSV-2 *UL56*, which has the identical subcellular localization and was previously suggested to be the *UL56* homologue due to its close proximity to *ORF3*, the homologue of *UL55*. In addition, we could prove that the *ORFS/L* gene product is important for efficient VZV replication *in vitro*. We

also identified a 5′ region of *ORFS/L* that is essential for replication and plays a role in cleavage and packaging of viral DNA, previously suggested by Davison and colleagues (2). Since this essential region has no homology to the opposite end of $U_L$, it could provide an explanation for the almost exclusive packaging in VZV virions of two viral DNA isomers with an invariable $U_L$ orientation.

### 5.3. vTR – functions of the virally encoded telomerase RNA that are independent of the telomerase activity

Marek's disease virus (MDV), a highly oncogenic alphaherpesvirus, is genetically closely related to VZV discussed in Chapter 2 and 3. Early stages of MDV infection resembles primary VZV infection with characteristic skin lesions known as chicken pox, however, late stages of infection, specifically latency, are quite distinct (11). While VZV establishes latency in long lived neuronal cells and remains quiescent until a reactivation event occurs, MDV mainly targets B and CD4+ T-cells, which have generally a limited life span. Therefore, MDV evolved several mechanisms that promote the survival of CD4+ T cells, likely with a Treg phenotype, and allow the maintenance of its genetic information in latently infected cells. In Chapter 4 and 5 we shed light on two major factors, viral telomerase RNA (vTR) and the viral telomeric repeats, involved in establishment of and reactivation from latency as well as tumorigenesis.

One factor that significantly contributes to MDV-induced lymphomagenesis is vTR, a homologue of host telomerase RNA (TR) (14). In the telomerase complex, vTR as well as cellular TR interacts with the catalytic subunit, telomerase reverse transcriptase (TERT), and provides the template for the maintenance of telomeres. Hereby, interaction of the main components vTR and TERT, which are sufficient for telomerase activity, is an essential prerequisite for telomerase activity. As recent

studies have suggested that TRs possess telomerase-independent functions, we investigated whether the tumor-promoting capacity of vTR is dependent on formation of a functional telomerase complex. In Chapter 4 we demonstrate that vTR, the MDV-encoded telomerase RNA, serves two distinct functions in MDV-induced tumor formation. The first is dependent on increased telomerase activity, which is crucial for rapid onset of lymphoma formation in infected animals. vTR becomes part of the telomerase complex and contributes to the survival of rapidly dividing transformed cells. The second function of vTR is independent of telomerase action and is crucial for tumor formation and metastasis. This latter function is likely a consequence of vTR-mediated gene regulation that is at least in part controlled by interaction of vTR with RPL22, a cellular factor involved in T-cell development and virus-induced transformation. Taken together, our study demonstrates that telomerase RNA encoded by a herpesvirus is directly involved in tumor formation *in vivo*, in a fashion that is largely independent of its function within an active telomerase complex.

### 5.4. Telomeric repeats – means of entry into and exit out of host chromosomes

Herpesvirus integration into the host chromosome, as identified for several lymphotropic herpesviruses, including Epstein Barr virus (EBV), human herpesvirus 6 (HHV-6) and MDV, was long thought to be an unintended consequence of viral replication (3, 6, 10). In Chapter 5, we identified a directed integration mechanism, which ensures faithful virus genome maintenance in host cells during cell division and also allows efficient mobilization of dormant viral genomes using MDV as a natural virus-host model.

We demonstrated that directed integration into the host genome is facilitated by herpesvirus telomeric repeats, which are present in several herpesviruses including HHV-6 and MDV. Our results, therefore, provide the first conclusive evidence that

herpesvirus telomeric repeats not only mediate chromosomal integration but that these repeat structures are crucial for efficient tumor formation and reactivation of latent virus from the quiescent state of infection. In the absence of viral telomeric repeats, herpesvirus integration is severely impaired and occurs at random, single sites within chromosomes. In this latter case, MDV genomes are integrated as concatemers. Our observation that integration occurs even in the absence of telomere-mediated integration suggests that herpesvirus integration into the host genome is not simply a consequence of virus replication, but rather is a critical prerequisite for transformation and tumorigenesis as well as for reactivation and spread to new susceptible hosts.

REFERENCES


1. **Cohen, J. I. and K. E. Seidel**. 1993. Generation of varicella-zoster virus (VZV) and viral mutants from cosmid DNAs: VZV thymidylate synthetase is not essential for replication in vitro. Proc. Natl. Acad. Sci. U. S. A **90**:7376-7380.

2. **Davison, A. J.** 1984. Structure of the genome termini of varicella-zoster virus. J Gen Virol **65 ( Pt 11)**:1969-1977.

3. **Delecluse, H. J. and W. Hammerschmidt**. 1993. Status of Marek's disease virus in established lymphoma cell lines: herpesvirus integration is common. J. Virol. **67**:82-92.

4. **Duffy, C., J. H. LaVail, A. N. Tauscher, E. G. Wills, J. A. Blaho, and J. D. Baines**. 2006. Characterization of a UL49-null mutant: VP22 of herpes simplex virus type 1 facilitates viral spread in cultured cells and the mouse cornea. J Virol **80**:8664-8675.

5. **Elliott, G., W. Hafezi, A. Whiteley, and E. Bernard**. 2005. Deletion of the herpes simplex virus VP22-encoding gene (UL49) alters the expression, localization, and virion incorporation of ICP0. J. Virol. **79**:9735-9745.

6. **Hall, C. B., M. T. Caserta, K. Schnabel, L. M. Shelley, A. S. Marino, J. A. Carnahan, C. Yoo, G. K. Lofthus, and M. P. McDermott**. 2008. Chromosomal integration of human herpesvirus 6 is the major mode of congenital human herpesvirus 6 infection. Pediatrics **122**:513-520.

7. **Jeffrey I.Cohen, Stephen E.Straus, and Ann M.Arvin**. 2007. **Fields Virology**, p. 2276-2278. *In* D. M. K. P. M. H. e. al. 5. Ed. B.N.Fields (ed.). Lippincott-Raven Publishers, Philadelphia.

8. **Kalthoff, D., H. Granzow, S. Trapp, and M. Beer**. 2008. The UL49 gene product of BoHV-1: a major factor in efficient cell-to-cell spread. J Gen Virol **89**:2269-2274.

9. **Liang, X., B. Chow, Y. Li, C. Raggo, D. Yoo, S. ttah-Poku, and L. A. Babiuk**. 1995. Characterization of bovine herpesvirus 1 UL49 homolog gene and product: bovine herpesvirus 1 UL49 homolog is dispensable for virus growth. J. Virol. **69**:3863-3867.

10. **Luppi, M., R. Marasca, P. Barozzi, S. Ferrari, L. Ceccherini-Nelli, G. Batoni, E. Merelli, and G. Torelli**. 1993. Three cases of human herpesvirus-6 latent infection: integration of viral genome in peripheral blood mononuclear cell DNA. J. Med. Virol. **40**:44-52.

11. **Osterrieder, N., J. P. Kamil, D. Schumacher, B. K. Tischer, and S. Trapp**. 2006. Marek's disease virus: from miasma to model. Nat. Rev. Microbiol. **4**:283-294.

12. **Ren, X., J. S. Harms, and G. A. Splitter**. 2001. Bovine herpesvirus 1 tegument protein VP22 interacts with histones, and the carboxyl terminus of VP22 is required for nuclear localization. J. Virol. **75**:8251-8258.

13. **Tischer, B. K., J. von Einem, B. Kaufer, and N. Osterrieder**. 2006. Two-step red-mediated recombination for versatile high-efficiency markerless DNA manipulation in Escherichia coli. Biotechniques **40**:191-197.

14. **Trapp, S., M. S. Parcells, J. P. Kamil, D. Schumacher, B. K. Tischer, P. M. Kumar, V. K. Nair, and N. Osterrieder**. 2006. A virus-encoded telomerase RNA promotes malignant T cell lymphomagenesis. J. Exp. Med. **203**:1307-1317.